

**ASSESSMENT REPORT
SPANISH MOUNTAIN GOLD PROPERTY**

Dighem Survey, October 2006

Tenure Number **345884**
Juan A Claims
Cariboo Mining Division

N.T.S Map Area 93A-11

Latitude 52⁰ 25' 30" north; Longitude 121⁰ 26' 30" west

For:

FREEPORT RESOURCES INC.
8711 Elsmore Road
Richmond, B.C. V7C 2A4

By:

Zdenek D. Hora, M.Sc., P.Geo.
June 20, 2007

TABLE OF CONTENTS

| | <i>Page</i> |
|---------------------------------|-------------|
| 1.0 Introduction | 1 |
| 2.0 History | 3 |
| 3.0 Geology | |
| 4.0 Geophysics | 4 |
| 5.0 Conclusions | 6 |
| 6.0 References | 7 |
| 7.0 Statement of qualifications | 8 |

Figures

| | |
|--|---|
| 1. Location Map | 1 |
| 2. Claim Location Map | 2 |
| 3. Flight Line Locations, with Magnetic Anomalies | 4 |
| 4. Airborne Resistivity Map, Spanish Mountain Area | 5 |

Appendices

| | |
|---|-------------------------|
| A | Itemized Cost Statement |
| B | DIGHEM Survey, 2006 |

1.0 INTRODUCTION

This report documents the airborne geophysical survey flown in 2006 over the majority of Freeport Resources Inc.'s (Freeport's) Spanish Mountain Gold property, Licence Number 345884 (Juan A claims).



Figure 1. Location Map, Spanish Mountain Gold Property

The Juan A claim block is located near Likely in the Cariboo region of central British Columbia. It is accessible by road. Importantly, it is adjacent to claims on Spanish Mountain, where Skygold Ventures Ltd. and Wildrose Resources Ltd. identified a large gold mineralization system, so far only partially tested by diamond drilling. Mineralized zones occur in elongated lenses, sub-parallel to dip-slope. Geological structures which host gold mineralization on Skygold/Wildrose claims continue onto Freeport's claim block.

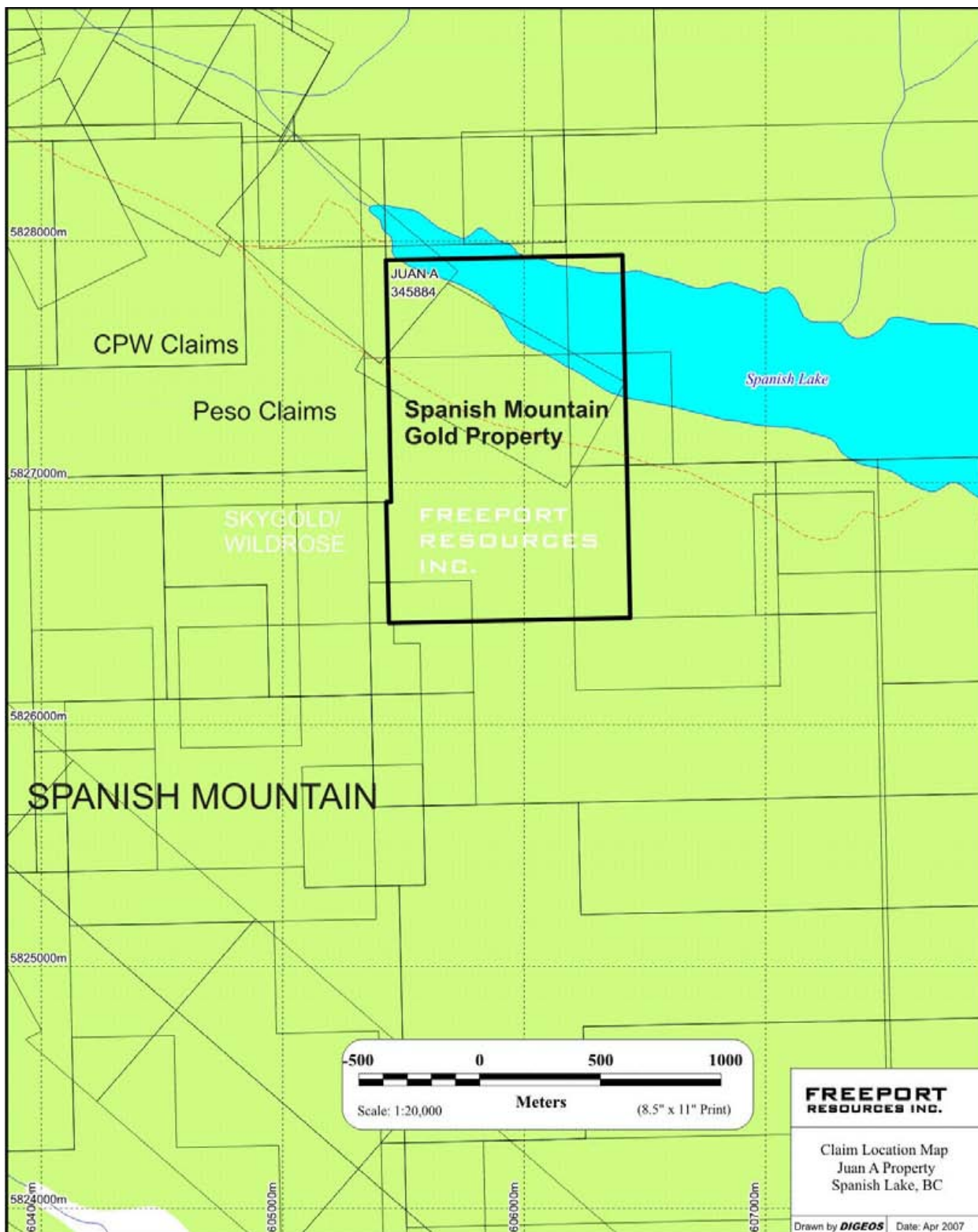


Figure 2. Claim Location Map

2.0 HISTORY

Spanish Mountain has been known as a rich placer mining area, with gold mined from nearby creeks and gravels since 1870's, including the famed Bullion Pit, which was mined until 1942. Quartz veins with gold were first discovered in 1933 west of the Spanish Mountain Gold property, on what is now known as the CPW claims. Sporadic exploration was carried out until 1947, with systematic exploration on Spanish Mountain by several companies commencing in 1970.

Comprehensive work is presently being conducted by Skygold Ventures Ltd. and Wildrose Resources Ltd., including a planned 60,000 metre drill program in 2007. Freeport's claims are less than half a mile (or 800 metres) east of the mineralized zone, which is reportedly open towards the Freeport ground.

3.0 GEOLOGY

The region is underlain by Upper Triassic metasedimentary rocks with some intercalated volcanics of the basal part of the Nicola Group. The metasedimentary rock consist of slaty to phyllitic, dark grey to black shale and siltstone, grey limestone and up the stratigraphy some banded tuff, volcanic breccia and pillow lavas. Gold mineralization on Spanish Mountain as reported by Skygold Ventures Ltd. is of two types. The main zone consists of quartz veins/stockworks with gold, galena, sphalerite, chalcopyrite, tetrahedrite and pyrite.

The second type of gold mineralization is a lower grade, bulk tonnage ore represented by auriferous pyrite in a graphitic silty shale along a contact between argillites and greywackes. It is this type that is expected to extend onto Freeport's Spanish Mountain Gold property.

GEOPHYSICS

As a part of airborne geophysical survey on Spanish Mountain, a major part of the Freeport claims was covered as well. The flown resistivity and magnetic survey results are attached to this report.

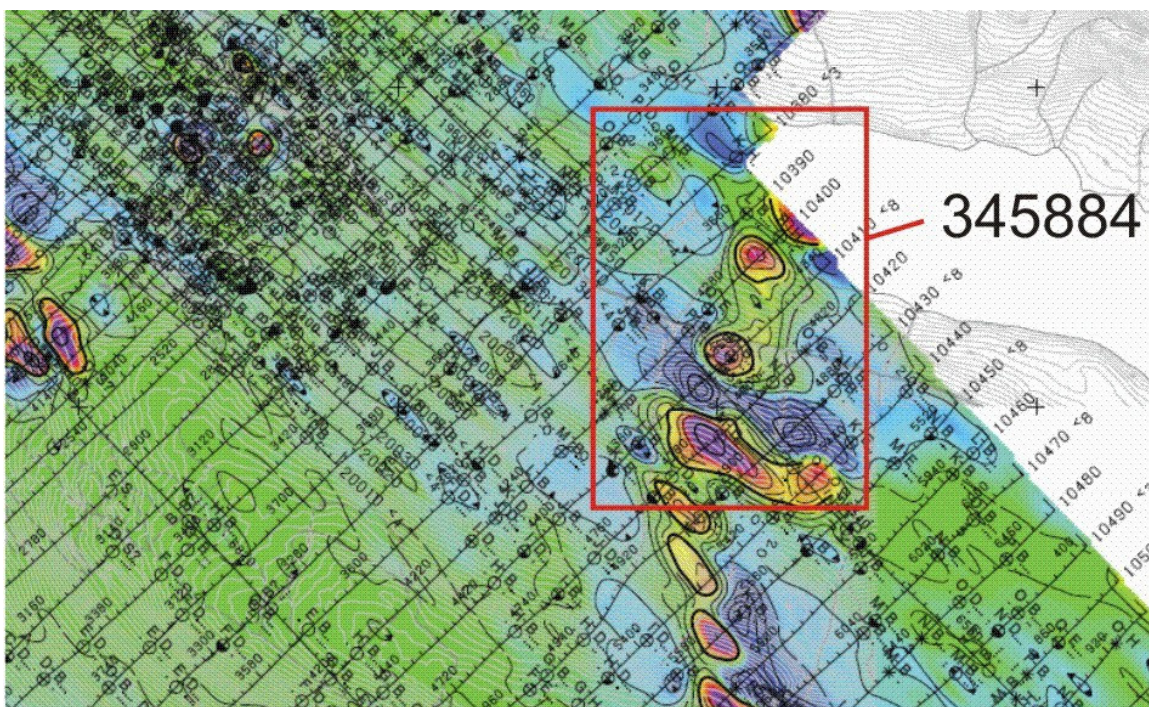


Figure 3. Flight Line locations, with magnetic anomalies

A DIGHEM electromagnetic/resistivity/magnetic survey was flown for Wildrose Resources Ltd. and Skygold Ventures Ltd., from October 14 to 16, 2006. Survey coverage consisted in total of approximately 306 line-kilometres, including 7.4 line-kilometres over claims held by Freeport Resources Inc.

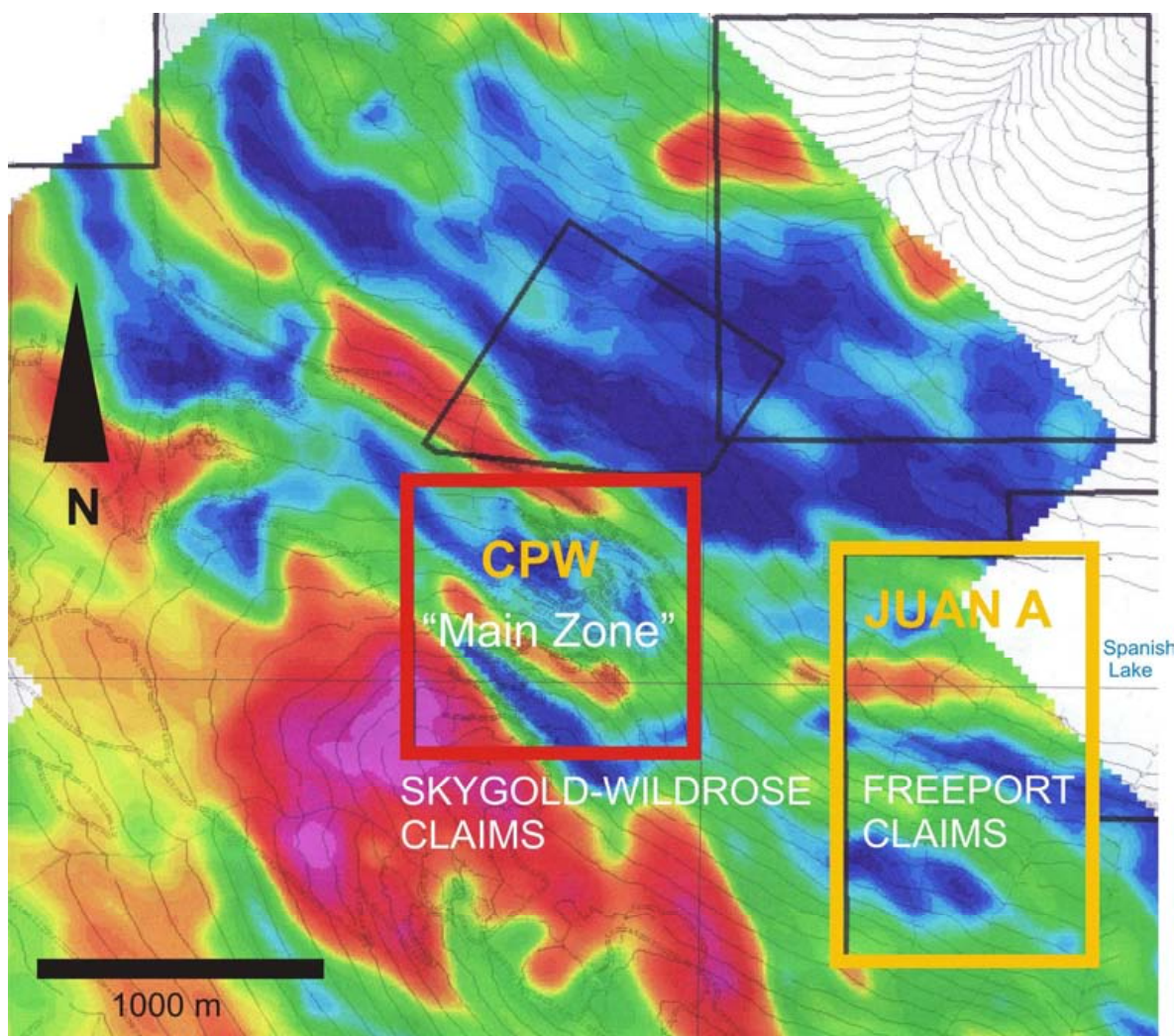


Figure 4. Airborne Resistivity map, Spanish Mountain area

The survey employed the DIGHEM electromagnetic system. Ancillary equipment consisted of a magnetometer, radar and barometric altimeters, a digital video camera, a digital recorder, and an electronic navigation system. The instrumentation was installed in an AS350B2 turbine helicopter (Registration C-FZTA) that was provided by Questral Helicopters Ltd. The helicopter flew at an average airspeed of 100 km/h with an EM sensor height of approximately 30 metres. The results are documented in maps attached to this report.

According to information provided by Wildrose Resources Ltd, the low resistivity areas are generally correlative with shale and argillite. This is the potentially mineralized lithology. The magnetic anomalies are supposed to indicate the intrusive rocks. Since there are some inconsistencies in this interpretation between the two maps, the Ecole Polytechnique in Montreal has been engaged to provide an independent interpretation.


4.0 CONCLUSIONS

Exploration on Spanish Mountain property by Skygold/Wildrose outlined a mineralized zone extending approximately 1.2 kilometres by 0.8 kilometre which remains open in all directions (press release of May 17, 2007).

The 2006 completed airborne resistivity geophysical survey suggests that favourable, lower-grade, bulk tonnage gold mineralization indicated by low resistivity may continue onto the Freeport's block of claims.

It is therefore recommended, that Freeport follow up on this hypothesis after independent re-interpretation of geophysics confirms information provided by Wildrose Resources Ltd.

Respectfully submitted,


Z.D. Hora, M.Sc., P.Geo.
3657 Doncaster Drive
Victoria, B.C.
June 18, 2007



6.0 REFERENCES

Ball, C.W.: *Stryker Resources Inc.*, Revised Geological Report, Juan A Claim Group, Spanish Mountain, January 21, 1980

Morton, J.W.: *Wildrose Resources Ltd.*, Letter of February 16, 2007

Perkins, D.A.: *Stryker Resources Inc.*, Juan A Mineral Claims, Assessment Report, November 1993

Smith, P.A.: Dighem Survey for Wildrose Resources Ltd./Skygold Ventures Ltd., Spanish Mountain Project, Likely, B.C., *Fugro Airborne Surveys Corp.*, December 8, 2006

No author: Spanish Mountain, MINFILE 093A 043, *BC Ministry of Energy and Mines*

Bullion Pit, MINFILE 093A 025, *BC Ministry of Energy and Mines*

Spanish Mountain Project, *Wildrose Resources Ltd.*, 2006, SEDAR overview

Skygold Ventures Ltd., Press release August 23, 2004, July 12, 2006, September 5, 2006, March 1, 2007, March 20 2007, April 16, 2007, May 17, 2007

7.0 Statement of qualifications

I, Zdenek D. Hora, M.Sc., P.Geo., of Victoria, British Columbia, do hereby certify that:

I am a Consulting Geologist and since 1975, a Registered Professional Geoscientist in British Columbia and previously in Alberta, residing at 3657 Doncaster Drive, Victoria, B.C., V8P 3W8.

I graduated from Charles University of Prague, Czechoslovakia with a M.Sc. Degree in geology in 1958. Since graduation, I have been continuously practicing my profession in Europe and overseas, and since 1971 in Canada, namely in Quebec, Alberta, the N.W.T. and British Columbia. My work has largely been focussed on the geology, exploration and evaluation of industrial minerals deposits. From 1978 to 1984, I was the Industrial Minerals Specialist for the British Columbia Ministry of Energy, Mines and Petroleum Resources. From 1984 to 1999, I acted as the Program Manager for industrial minerals inventory and market studies in the province. Since my retirement in 1999, I am consulting in the field of industrial minerals – property assessment and evaluation, tenure aspect of industrial minerals in B.C. and its historical development, aggregate prospecting and deposit models for a wide range of industrial minerals. My professional activities included teaching industrial minerals courses (i.e. University of Victoria -- Economic Geology; B.C. Ministry of Energy, Mines and Petroleum Resources, B.C. and Yukon Chamber of Mines, and Geological Association of Canada – Courses for Prospectors). I have previously served as Chairman of the Industrial Minerals Division of the Canadian Institute of Mining, Metallurgy and Petroleum (CIM), and was the organizer and Co-Chairman of the 27th FORUM on Geology of Industrial Minerals and several other symposiums dealing with industrial minerals. From 1995 to 2000, I was part of the CIM Standing Committee on Reserve Definitions representing the CIM Industrial Minerals Division. I am presently a Consulting Geologist and have been so since June, 1999. As a result of my experience and qualifications, I am a Qualified Person as defined in N.P. 43-101.

This report is based review of published and unpublished reports, press releases and information provided to me by Freeport Resources Inc.

I have not received, nor do I expect to receive any interest, directly or indirectly, in the properties or securities of Freeport Resources Inc. or any affiliate. I am independent of Freeport Resources Inc. in accordance with the application of Section 1.5 of National Instrument 43-101. I consent to use of this report by the company in submissions for any Regulatory requirements and development opportunities. I am not aware of any material fact or material change which is not reflected in this report. I have read National Instrument 43-101, Form 43-101F1 and this report has been prepared in compliance with NI 43-101 and Form 43-101F1.

Dated in Victoria, B.C., June 20th, 2007.

Z.D. Hora, M.Sc., P.Geo.



APPENDIX A

ITEMIZED COST STATEMENT

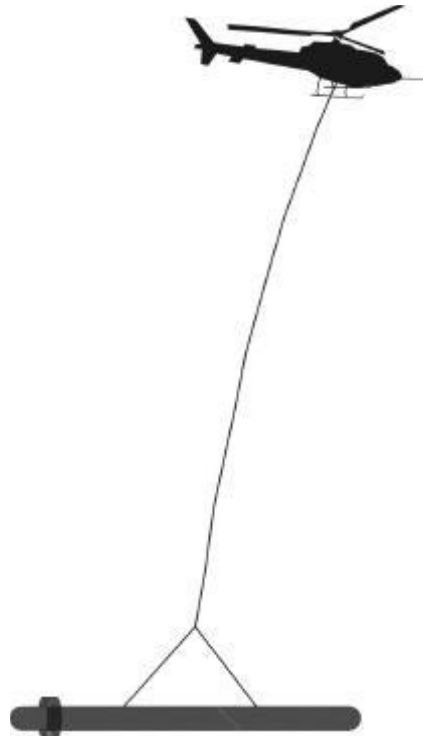
APPENDIX B

Dighem Survey, October 2006

Report #06075

**DIGHEM SURVEY
FOR
WILDROSE RESOURCES LTD./SKYGOLD VENTURES LTD.
SPANISH MOUNTAIN PROJECT
LIKELY, BRITISH COLUMBIA**

NTS: 93A/11



Fugro Airborne Surveys Corp.
Mississauga, Ontario

Paul A. Smith
Geophysicist

December 8, 2006

SUMMARY

This report describes the logistics, data acquisition, processing and presentation of results of a DIGHEM^V airborne geophysical survey carried out for Wildrose Resources Ltd. and Skygold Ventures, over a property located near Likely, B.C. Total coverage of the survey block amounted to 306 km, including infill lines and one detailed (75 m) block. The survey was flown from October 14 to October 16, 2006.

The purpose of the survey was to detect zones of conductive mineralization and to provide information that could be used to map the geology and structure of the survey area. This was accomplished by using a DIGHEM^V multi-coil, multi-frequency electromagnetic system, supplemented by a high sensitivity cesium magnetometer. The information from these sensors was processed to produce maps that display the magnetic and conductive properties of the survey area. A GPS electronic navigation system ensured accurate positioning of the geophysical data with respect to the base maps.

The survey data were processed and compiled in the Fugro Airborne Surveys Toronto office. Map products and digital data were provided in accordance with the scales and formats specified in the Survey Agreement.

The survey property contains several anomalous features, many of which are considered to be of moderate to high priority as exploration targets. Most of the inferred bedrock conductors appear to warrant further investigation using appropriate surface exploration

techniques. Areas of interest may be assigned priorities on the basis of supporting geophysical, geochemical and/or geological information. After initial investigations have been carried out, it may be necessary to re-evaluate the remaining anomalies based on information acquired from the follow-up program.

CONTENTS

| | | |
|----|--|------|
| 1. | INTRODUCTION | 1.1 |
| 2. | SURVEY OPERATIONS..... | 2.1 |
| 3. | SURVEY EQUIPMENT | 3.1 |
| | Electromagnetic System | 3.1 |
| | In-Flight EM System Calibration | 3.2 |
| | Airborne Magnetometer | 3.4 |
| | Magnetic Base Station..... | 3.4 |
| | Navigation (Global Positioning System) | 3.5 |
| | Radar Altimeter..... | 3.8 |
| | Barometric Pressure and Temperature Sensors | 3.9 |
| | Digital Data Acquisition System..... | 3.9 |
| | Video Flight Path Recording System | 3.10 |
| 4. | QUALITY CONTROL AND IN-FIELD PROCESSING..... | 4.1 |
| 5. | DATA PROCESSING | 5.1 |
| | Flight Path Recovery | 5.1 |
| | Electromagnetic Data | 5.1 |
| | Apparent Resistivity | 5.2 |
| | Dielectric Permittivity and Magnetic Permeability Corrections..... | 5.4 |
| | Resistivity-depth Sections (optional) | 5.5 |
| | Total Magnetic Field | 5.6 |
| | Calculated Vertical Magnetic Gradient | 5.7 |
| | EM Magnetite (optional) | 5.7 |
| | Magnetic Derivatives (optional) | 5.7 |
| | Digital Elevation (optional)..... | 5.8 |
| | Contour, Colour and Shadow Map Displays..... | 5.9 |
| | Multi-channel Stacked Profiles | 5.10 |
| 6. | PRODUCTS | 6.1 |
| | Base Maps..... | 6.1 |
| | Final Products..... | 6.2 |
| 7. | SURVEY RESULTS | 7.1 |
| | General Discussion | 7.1 |

| | |
|---|---------|
| Magnetics | 7.4 |
| Apparent Resistivity | 7.5 |
| Electromagnetic Anomalies..... | 7.6 |
| Potential Targets in the Survey Area..... | 7.8 |
| 8. CONCLUSIONS AND RECOMMENDATIONS..... | 8.1 |

APPENDICES

- A. List of Personnel
- B. Data Processing Flowcharts
- C. Background Information
- D. Data Archive Description
- E. EM Anomaly List
- F. Glossary

1. INTRODUCTION

A DIGHEM^V electromagnetic/resistivity/magnetic survey was flown for Wildrose Resources Ltd. and Skygold Ventures Ltd., from October 14 to October 16, 2006, over a survey block located southeast of Likely, British Columbia. The survey area can be located on NTS map sheet 93A/11 (Figure 2).

Survey coverage consisted of approximately 306 line-km, including one detailed block and one infill area. Flight lines were flown in an azimuthal direction of 045° with a line separation of 150 metres for the main block, and 75 m for the infill block. The detailed area comprised 17 lines that were flown 312° with a line separation of 75 m. Tie lines were flown orthogonal to the main traverse lines with a line separation of 1.5 km.

The survey employed the DIGHEM^V electromagnetic system. Ancillary equipment consisted of a magnetometer, radar and barometric altimeters, a digital video camera, a digital recorder, and an electronic navigation system. The instrumentation was installed in an AS350B2 turbine helicopter (Registration C-FZTA) that was provided by Questral Helicopters Ltd. The helicopter flew at an average airspeed of 100 km/h with an EM sensor height of approximately 30 metres.

Due to the presence of cultural features in the survey area, any interpreted conductors that occur in close proximity to cultural sources, should be confirmed as bedrock conductors prior to drilling.



Figure 1: Fugro Airborne Surveys DIGHEM EM bird with AS350-B2

2. SURVEY OPERATIONS

The base of operations for the survey was established at Likely, British Columbia.

The survey area can be located on NTS map sheet 93A/11 (Figure 2).

Table 2-1 lists the corner coordinates of the three survey blocks in NAD83, UTM Zone 10, central meridian 123°W.

Table 2-1

**Nad83 Utm
Zone 10**

| Block | Corners | X-UTM (E) | Y-UTM (N) |
|----------------|---------------|-----------|-----------|
| 06075-1 | 1 | 601677 | 5828439 |
| | 2 | 604098 | 5830753 |
| | 3 | 606534 | 5828352 |
| | 4 | 605930 | 5827775 |
| | 5 | 607656 | 5825870 |
| | 6 | 607454 | 5825678 |
| | 7 | 607879 | 5825235 |
| | 8 | 604121 | 5821643 |
| | 9 | 602831 | 5822921 |
| | 10 | 603686 | 5823739 |
| | 11 | 601931 | 5825363 |
| | 12 | 602655 | 5826055 |
| | 13 | 601862 | 5826771 |
| | 14 | 602642 | 5827516 |
| 06075-2 | 1 | 603985 | 5829203 |
| | Detail | 605605 | 5827743 |
| | Area | 604731 | 5826886 |
| | 4 | 603095 | 5828341 |
| | | | |

- 2.2 -

| | | | |
|----------------|---|--------|---------|
| 06075-3 | 1 | 602161 | 5826501 |
| infills | 2 | 605335 | 5829533 |
| | 3 | 606027 | 5828851 |
| | 4 | 602162 | 5825149 |
| | 5 | 601931 | 5825363 |
| | 6 | 602655 | 5826055 |

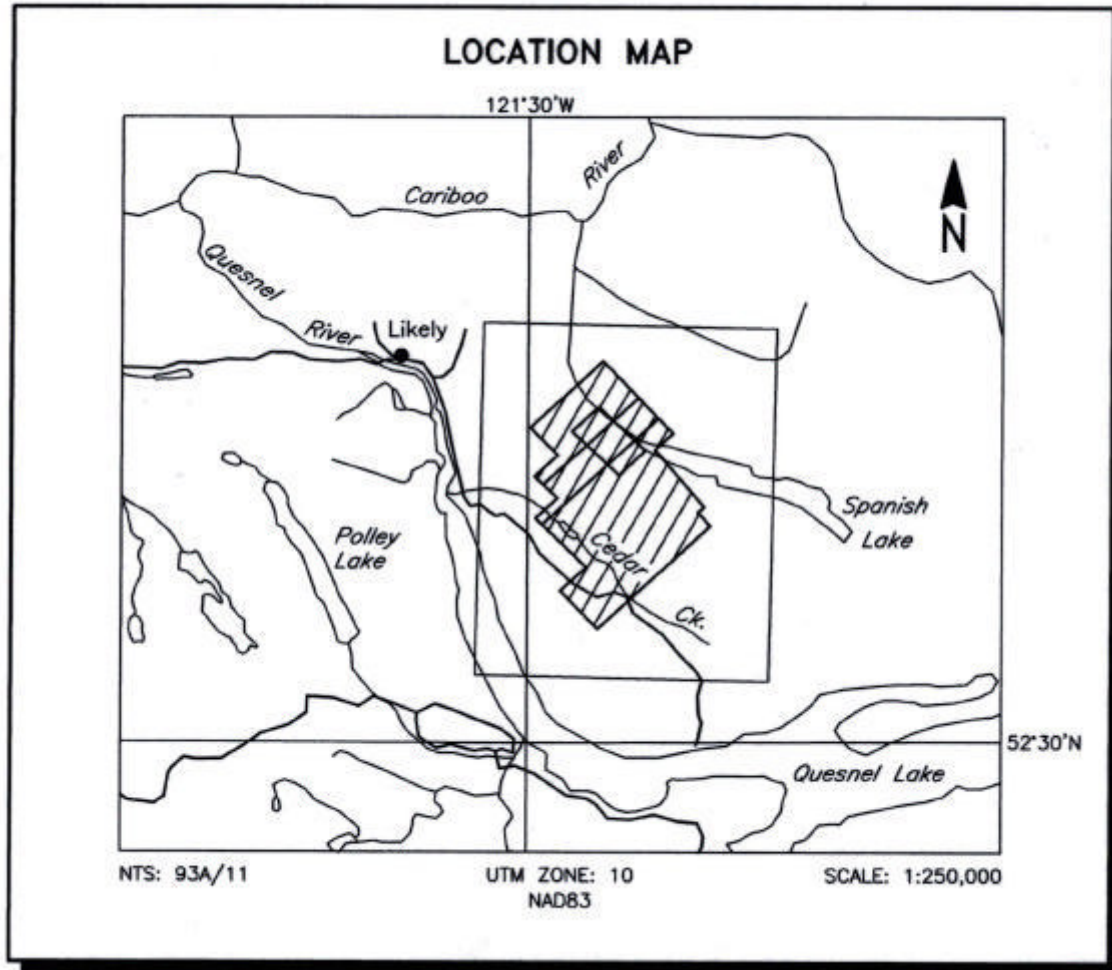


Figure 2
Location Map and Sheet Layout
Spanish Mountain Survey Area
Job # 06075

The survey specifications were as follows:

| Parameter | Specifications |
|---|-------------------------|
| Traverse line direction (Main Block/Infill) | 045°/045° |
| Traverse line spacing (Main Block/Infill) | 150 m/150 m |
| Tie line direction | 312° |
| Tie line spacing | 1.5 km |
| Traverse line direction (Detailed Block) | 312° |
| Traverse line spacing (Detailed Block) | 75 m |
| Sample interval | 10 Hz, 3.3 m @ 120 km/h |
| Aircraft mean terrain clearance | 58 m |
| EM sensor mean terrain clearance | 30 m |
| Mag sensor mean terrain clearance | 30 m |
| Average speed | 120 km/h |
| Navigation (guidance) | ±5 m, Real-time GPS |
| Post-survey flight path | ±2 m, Differential GPS |

3. SURVEY EQUIPMENT

This section provides a brief description of the geophysical instruments used to acquire the survey data and the calibration procedures employed. The geophysical equipment was installed in an AS350B2 helicopter. This aircraft provides a safe and efficient platform for surveys of this type.

Electromagnetic System

Model: DIGHEM^V BKS51

Type: Towed bird, symmetric dipole configuration operated at a nominal survey altitude of 30 metres. Coil separation is 8 metres for 900 Hz, 1000 Hz, 5500 Hz and 7200 Hz, and 6.3 metres for the 56,000 Hz coil-pair.

| Coil orientations, frequencies and dipole moments | <u>Atm²</u> | <u>orientation</u> | <u>nominal</u> | <u>actual</u> |
|--|------------------------|--------------------|----------------|---------------|
| | 211 | coaxial / | 1000 Hz | 1113 Hz |
| | 211 | coplanar / | 900 Hz | 881 Hz |
| | 67 | coaxial / | 5500 Hz | 5871 Hz |
| | 56 | coplanar / | 7200 Hz | 7031 Hz |
| | 15 | coplanar / | 56,000 Hz | 55,540 Hz |

Channels recorded: 5 in-phase channels
5 quadrature channels
2 monitor channels

Sensitivity: 0.06 ppm at 1000 Hz Cx
0.12 ppm at 900 Hz Cp
0.12 ppm at 5,500 Hz Cx
0.24 ppm at 7,200 Hz Cp
0.60 ppm at 56,000 Hz Cp

Sample rate: 10 per second, equivalent to 1 sample every 3.3 m,
at a survey speed of 120 km/h.

The electromagnetic system utilizes a multi-coil coaxial/coplanar technique to energize conductors in different directions. The coaxial coils are vertical with their axes in the flight direction. The coplanar coils are horizontal. The secondary fields are sensed simultaneously by means of receiver coils that are maximum coupled to their respective transmitter coils. The system yields an in-phase and a quadrature channel from each transmitter-receiver coil-pair.

In-Flight EM System Calibration

Calibration of the system during the survey uses the Fugro AutoCal automatic, internal calibration process. At the beginning and end of each flight, and at intervals during the flight, the system is flown up to high altitude to remove it from any “ground effect” (response from the earth). Any remaining signal from the receiver coils (base level) is measured as the zero level, and is removed from the data collected until the time of the next calibration. Following the zero level setting, internal calibration coils, for which the response phase and amplitude have been determined at the factory, are automatically triggered – one for each frequency. The on-time of the coils is sufficient to determine an accurate response through any ambient noise. The receiver response to each calibration coil “event” is compared to the expected response (from the factory calibration) for both phase angle and amplitude, and any phase and gain corrections are automatically applied to bring the data to the correct value.

In addition, the outputs of the transmitter coils are continuously monitored during the survey, and the gains are adjusted to correct for any change in transmitter output.

Because the internal calibration coils are calibrated at the factory (on a resistive halfspace) ground calibrations using external calibration coils on-site are not necessary for system calibration. A check calibration may be carried out on-site to ensure all systems are working correctly. All system calibrations will be carried out in the air, at sufficient altitude that there will be no measurable response from the ground.

The internal calibration coils are rigidly positioned and mounted in the system relative to the transmitter and receiver coils. In addition, when the internal calibration coils are calibrated at the factory, a rigid jig is employed to ensure accurate response from the external coils.

Using real time Fast Fourier Transforms and the calibration procedures outlined above, the data are processed in real time, from measured total field at a high sampling rate, to in-phase and quadrature values at 10 samples per second.

Airborne Magnetometer

| | | |
|--------------|--------------------------------|-------------------------------------|
| Model: | CS2 sensor | Fugro D1344 processor with Scintrex |
| Type: | Optically pumped cesium vapour | |
| Sensitivity: | 0.01 nT | |
| Sample rate: | 10 per second | |

The magnetometer sensor is housed in the EM bird, 28 m below the helicopter.

Magnetic Base Station

Primary

| | | |
|-------------------------|---|---|
| Model: | Fugro CF1 base station with timing provided by integrated GPS | |
| Sensor type: | Geometrics G822 | |
| Counter specifications: | Accuracy: | ± 0.1 nT |
| | Resolution: | 0.01 nT |
| | Sample rate | 1 Hz |
| GPS specifications: | Model: | Marconi Allstar |
| | Type: | Code and carrier tracking of L1 band, 12-channel, C/A code at 1575.42 MHz |
| | Sensitivity: | -90 dBm, 1.0 second update |
| | Accuracy: | Manufacturer's stated accuracy for differential corrected GPS is 2 metres |
| Environmental | | |
| Monitor specifications: | Temperature: | |
| | • Accuracy: | $\pm 1.5^{\circ}\text{C}$ max |

- Resolution: 0.0305°C
- Sample rate: 1 Hz
- Range: -40°C to +75°C

Barometric pressure:

- Model: Motorola MPXA4115A
- Accuracy: $\pm 3.0^\circ$ kPa max (-20°C to 105°C temp. ranges)
- Resolution: 0.013 kPa
- Sample rate: 1 Hz
- Range: 55 kPa to 108 kPa

A digital recorder is operated in conjunction with the base station magnetometer to record the diurnal variations of the earth's magnetic field. The clock of the base station is synchronized with that of the airborne system, using GPS time, to permit subsequent removal of diurnal drift. The Fugro CF1 was the primary magnetic base station. It was located at the Likely Airstrip at WGS84 Lat. 52°36'51.47020"N, Long. 121°30'47.97633"W, at an ellipsoidal elevation of 955.51 m.

Navigation (Global Positioning System)

Airborne Receiver for Real-time Navigation & Guidance

| | |
|--------------|--|
| Model: | Novatel OEM4 with PNAV 2100 interface |
| Type: | SPS (L1 band), 24-channel, C/A code at 1575.42 MHz, S code at 0.5625 MHz, Real-time differential, WAAS enabled. |
| Sensitivity: | -132 dBm, 0.5 second update |
| Accuracy: | Manufacturer's stated accuracy is better than 5 metres real-time |

- 3.6 -

Antenna:

Aero AT2775

Primary Base Station for Post-Survey Differential Correction

| | |
|--------------|--|
| Model: | Novatel Millennium. |
| Type: | Code and carrier tracking of L1-C/A code at 1575.42 MHz and L2-P code at 1227.0 MHz. Dual frequency, 24-channel. |
| Sample rate: | 10 Hz update. |
| Accuracy: | Better than 1 metre in differential mode. |
| Antenna: | Aero AT1675 |

Secondary GPS Base Station

| | |
|--------------|--|
| Model: | Marconi Allstar OEM, CMT-1200 |
| Type: | Code and carrier tracking of L1 band, 12-channel, C/A code at 1575.42 MHz |
| Sensitivity: | -90 dBm, 1.0 second update |
| Accuracy: | Manufacturer's stated accuracy for differential corrected GPS is 2 metres. |

The Novatel OEM4 is a line of sight, satellite navigation system that utilizes time-coded signals from at least four of forty-eight available satellites to calculate the position and to provide real time guidance to the helicopter. A Novatel Millennium system was used as the primary base station receiver. The mobile and base station raw XYZ data were recorded, thereby permitting post-survey differential corrections for theoretical accuracies of better than 2 metres. A Marconi Allstar GPS unit, part of the CF-1, was used as a secondary (back-up) base station.

Each base station receiver is able to calculate its own latitude and longitude. For this survey, the primary GPS station was located at Northern Lights Lodge at latitude 52°36'52.07174"N, longitude 121°30'49.17240"W at an elevation of 956.83 metres above the ellipsoid. The secondary GPS unit was located at the Likely Airstrip at latitude 52°36'51.47020"N, longitude 121°30'47.97633"W at an ellipsoidal elevation of 955.51 metres. The GPS records data relative to the WGS84 ellipsoid, which is the basis of the revised North American Datum (NAD83). Conversion software is used to transform the WGS84 coordinates to the Zone 10 UTM system displayed on the maps.

Radar Altimeter

| | |
|---------------|---------------------------------|
| Manufacturer: | Honeywell/Sperry |
| Model: | AA 330 |
| Type: | Short pulse modulation, 4.3 GHz |
| Sensitivity: | 0.3 m |
| Sample rate: | 2 per second |

The radar altimeter measures the vertical distance between the helicopter and the ground.

This information is used in the processing algorithm that determines conductor depth.

Barometric Pressure and Temperature Sensors

| | |
|--------------|--|
| Model: | DIGHEM D 1300 |
| Type: | Motorola MPX4115AP analog pressure sensor AD592AN high-impedance remote temperature sensors |
| Sensitivity: | Pressure: 150 mV/kPa Temperature: 100 mV/°C or 10 mV/°C (selectable) |
| Sample rate: | 10 per second |

The D1300 circuit is used in conjunction with one barometric sensor and up to three temperature sensors. Two sensors (baro and temp) are installed in the EM console in the aircraft, to monitor pressure (1KPA) and internal operating temperatures (2TDC).

Digital Data Acquisition System

| | |
|---------------|--------------------------------------|
| Manufacturer: | Fugro |
| Model: | HeliDAS |
| Recorder: | San Disk compact flash card (PCMCIA) |

The stored data are downloaded to the field workstation PC at the survey base, for verification, backup and preparation of in-field products.

Video Flight Path Recording System

| | |
|-----------|---|
| Type: | Panasonic WVCL322 Colour Video Camera |
| Recorder: | HeliDAS (A-D conversion with Axis Image Server) |
| Format: | JPEG |

Fiducial numbers are recorded continuously and are displayed on the margin of each image. This procedure ensures accurate correlation of data with respect to visible features on the ground.

4. QUALITY CONTROL AND IN-FIELD PROCESSING

Digital data for each flight were transferred to the field workstation, in order to verify data quality and completeness. A database was created and updated using Geosoft Oasis Montaj and proprietary Fugro Atlas software. This allowed the field personnel to calculate, display and verify both the positional (flight path) and geophysical data on a screen or printer. Records were examined as a preliminary assessment of the data acquired for each flight.

In-field processing of Fugro survey data consists of differential corrections to the airborne GPS data, verification of EM calibrations, drift correction of the raw airborne EM data, spike rejection and filtering of all geophysical and ancillary data, verification of flight path, calculation of preliminary resistivity data, diurnal correction, and preliminary leveling of magnetic data.

All data, including base station records, were checked on a daily basis, to ensure compliance with the survey contract specifications. Reflights were required if any of the following specifications were not met.

Navigation - Positional (x,y) accuracy of better than 10 m, with a CEP (circular error of probability) of 95%.

- 4.2 -

- Flight Path - No lines to exceed $\pm 25\%$ departure from nominal line spacing over a continuous distance of more than 1 km, except for reasons of safety.
- Clearance - Mean terrain sensor clearance of 30 m, ± 10 m, except where precluded by safety considerations, e.g., restricted or populated areas, severe topography, obstructions, tree canopy, aerodynamic limitations, etc.
- Airborne Mag - The non-normalized 4th difference will not exceed 1.6 nT over a distance of more than 1 km.
- Base Mag - Diurnal variations not to exceed 10 nT over a straight line time chord of 1 minute.
- EM - Spheric pulses may occur having strong peaks but narrow widths. The EM data area considered acceptable when their occurrence is less than 10 spheric events exceeding the stated noise specification for a given frequency per 100 samples continuously over a distance of 2,000 metres.

| Frequency | Coil Orientation | Peak to Peak Noise Envelope (ppm) |
|-----------|---------------------|-----------------------------------|
| 1000 Hz | Vertical coaxial | 5.0 |
| 900 Hz | horizontal coplanar | 10.0 |
| 5500 Hz | vertical coaxial | 10.0 |
| 7200 Hz | horizontal coplanar | 20.0 |
| 56,000 Hz | horizontal coplanar | 40.0 |

5. DATA PROCESSING

Flight Path Recovery

The raw range data from at least four satellites are simultaneously recorded by both the base and mobile GPS units. The geographic positions of both units, relative to the model ellipsoid, are calculated from this information. Differential corrections, which are obtained from the base station, are applied to the mobile unit data to provide a post-flight track of the aircraft, accurate to within 2 m. Speed checks of the flight path are also carried out to determine if there are any spikes or gaps in the data.

The corrected WGS84 latitude/longitude coordinates are transformed to the UTM coordinate system used on the final maps. Images or plots are then created to provide a visual check of the flight path.

Electromagnetic Data

EM data are processed at the recorded sample rate of 10 samples/second. Spheric rejection median and Hanning filters are then applied to reduce noise to acceptable levels. EM test profiles are then created to allow the interpreter to select the most appropriate EM anomaly picking controls for a given survey area. The EM picking parameters depend on several factors but are primarily based on the dynamic range of the resistivities within the

survey area, and the types and expected geophysical responses of the targets being sought.

Anomalous electromagnetic responses are selected and analysed by computer to provide a preliminary electromagnetic anomaly map. The automatic selection algorithm is intentionally oversensitive to assure that no meaningful responses are missed. Using the preliminary map in conjunction with the multi-parameter stacked profiles, the interpreter then classifies the anomalies according to their source and eliminates those that are not substantiated by the data. The final interpreted EM anomaly map includes bedrock, surficial and cultural conductors. A map containing only bedrock conductors can be generated, if desired.

Apparent Resistivity

The apparent resistivities in ohm-m are generated from the in-phase and quadrature EM components for all of the coplanar frequencies, using a pseudo-layer half-space model. The inputs to the resistivity algorithm are the in-phase and quadrature amplitudes of the secondary field. The algorithm calculates the apparent resistivity in ohm-m, and the apparent height of the bird above the conductive source. Any difference between the apparent height and the true height, as measured by the radar altimeter, is called the pseudo-layer and reflects the difference between the real geology and a homogeneous halfspace. This difference is often attributed to the presence of a highly resistive upper layer. Any errors in the altimeter reading, caused by heavy tree cover, are included in the

pseudo-layer and do not affect the resistivity calculation. The apparent depth estimates, however, will reflect the altimeter errors. Apparent resistivities calculated in this manner may differ from those calculated using other models.

In areas where the effects of magnetic permeability or dielectric permittivity have suppressed the in-phase responses, the calculated resistivities will be erroneously high. Various algorithms and inversion techniques can be used to partially correct for the effects of permeability and permittivity.

Apparent resistivity maps portray all of the information for a given frequency over the entire survey area. This full coverage contrasts with the electromagnetic anomaly map, which provides information only over interpreted conductors. The large dynamic range afforded by the multiple frequencies makes the apparent resistivity parameter an excellent mapping tool.

The preliminary apparent resistivity maps and images are carefully inspected to identify any lines or line segments that might require base level adjustments. Subtle changes between in-flight calibrations of the system can result in line-to-line differences that are more recognizable in resistive (low signal amplitude) areas. If required, manual level adjustments are carried out to eliminate or minimize resistivity differences that can be attributed, in part, to changes in operating temperatures. These leveling adjustments are usually very subtle, and do not result in the degradation of discrete anomalies.

After the manual leveling process is complete, revised resistivity grids are created. The resulting grids can be subjected to a microleveling technique in order to smooth the data for contouring. The coplanar resistivity parameter has a broad 'footprint' that requires very little filtering.

The calculated resistivities for the three coplanar frequencies are included in the XYZ and grid archives. Values are in ohm-metres on all final products.

Dielectric Permittivity and Magnetic Permeability Corrections¹

In resistive areas having magnetic rocks, the magnetic and dielectric effects will both generally be present in high-frequency EM data, whereas only the magnetic effect will exist in low-frequency data.

The magnetic permeability is first obtained from the EM data at the lowest frequency, because the ratio of the magnetic response to conductive response is maximized and because displacement currents are negligible. The homogeneous half-space model is used. The computed magnetic permeability is then used along with the in-phase and quadrature response at the highest frequency to obtain the relative dielectric permittivity, again using the homogeneous half-space model. The highest frequency is used because the ratio of dielectric response to conductive response is maximized. The resistivity can

then be determined from the measured in-phase and quadrature components of each frequency, given the relative magnetic permeability and relative dielectric permittivity.

Resistivity-depth Sections (optional)

The apparent resistivities for all frequencies can be displayed simultaneously as coloured resistivity-depth sections. Usually, only the coplanar data are displayed as the close frequency separation between the coplanar and adjacent coaxial data tends to distort the section. The sections can be plotted using the topographic elevation profile as the surface. The digital terrain values, in metres a.m.s.l., can be calculated from the GPS Z-value or barometric altimeter, minus the aircraft radar altimeter.

Resistivity-depth sections can be generated in three formats:

- (1) Sengpiel resistivity sections, where the apparent resistivity for each frequency is plotted at the depth of the centroid of the in-phase current flow²; and,
- (2) Differential resistivity sections, where the differential resistivity is plotted at the differential depth³.

¹ Huang, H. and Fraser, D.C., 2001 Mapping of the Resistivity, Susceptibility, and Permittivity of the Earth Using a Helicopter-borne Electromagnetic System: Geophysics 106 pg 148-157.

² Sengpiel, K.P., 1988, Approximate Inversion of Airborne EM Data from Multilayered Ground: Geophysical Prospecting 36, 446-459.

³ Huang, H. and Fraser, D.C., 1993, Differential Resistivity Method for Multi-frequency Airborne EM Sounding: presented at Intern. Airb. EM Workshop, Tucson, Ariz.

(3) Occam⁴ or Multi-layer⁵ inversion.

Both the Sengpiel and differential methods are derived from the pseudo-layer half-space model. Both yield a coloured resistivity-depth section that attempts to portray a smoothed approximation of the true resistivity distribution with depth. Resistivity-depth sections are most useful in conductive layered situations, but may be unreliable in areas of moderate to high resistivity where signal amplitudes are weak. In areas where in-phase responses have been suppressed by the effects of magnetite, or adversely affected by cultural features, the computed resistivities shown on the sections may be unreliable.

Both the Occam and multi-layer inversions compute the layered earth resistivity model that would best match the measured EM data. The Occam inversion uses a series of thin, fixed layers (usually 20 x 5m and 10 x 10m layers) and computes resistivities to fit the EM data. The multi-layer inversion computes the resistivity and thickness for each of a defined number of layers (typically 3-5 layers) to best fit the data.

Total Magnetic Field

A fourth difference editing routine was applied to the magnetic data to remove any spikes.

The aeromagnetic data were corrected for diurnal variation using the magnetic base station data. The results were then leveled using tie and traverse line intercepts. Manual

⁴ Constable et al, 1987, Occam's inversion: a practical algorithm for generating smooth models from electromagnetic sounding data: *Geophysics*, 52, 289-300.

⁵ Huang H., and Palacky, G.J., 1991, Damped least-squares inversion of time domain airborne EM data based on singular value decomposition: *Geophysical Prospecting*, 39, 827-844.

adjustments were applied to any lines that required leveling, as indicated by shadowed images of the gridded magnetic data. The manually leveled data were then subjected to a microleveling filter.

Calculated Vertical Magnetic Gradient

The diurnally-corrected total magnetic field data were subjected to a processing algorithm that enhances the response of magnetic bodies in the upper 500 m and attenuates the response of deeper bodies. The resulting vertical gradient map provides better definition and resolution of near-surface magnetic units. It also identifies weak magnetic features that may not be evident on the total field map. However, regional magnetic variations and changes in lithology may be better defined on the total magnetic field map.

EM Magnetite (optional)

The apparent percent magnetite by weight is computed wherever magnetite produces a negative in-phase EM response. This calculation is more meaningful in resistive areas.

Magnetic Derivatives (optional)

The total magnetic field data can be subjected to a variety of filtering techniques to yield maps or images of the following:

enhanced magnetics

second vertical derivative

reduction to the pole/equator

magnetic susceptibility with reduction to the pole

upward/downward continuations

analytic signal

All of these filtering techniques improve the recognition of near-surface magnetic bodies, with the exception of upward continuation. Any of these parameters can be produced on request.

Digital Elevation (optional)

The radar altimeter values (ALTR – aircraft to ground clearance) are subtracted from the differentially corrected and de-spiked GPS-Z values to produce profiles of the height above the ellipsoid along the survey lines. These values are gridded to produce contour maps showing approximate elevations within the survey area. The calculated digital terrain data are then tie-line leveled and adjusted to mean sea level. Any remaining subtle line-to-line discrepancies are manually removed. After the manual corrections are applied, the digital terrain data are filtered with a microleveling algorithm.

The accuracy of the elevation calculation is directly dependent on the accuracy of the two input parameters, ALTR and GPS-Z. The ALTR value may be erroneous in areas of heavy tree cover, where the altimeter reflects the distance to the tree canopy rather than the ground. The GPS-Z value is primarily dependent on the number of available satellites.

Although post-processing of GPS data will yield X and Y accuracies in the order of 1-2 metres, the accuracy of the Z value is usually much less, sometimes in the ± 10 metre range. Further inaccuracies may be introduced during the interpolation and gridding process.

Because of the inherent inaccuracies of this method, no guarantee is made or implied that the information displayed is a true representation of the height above sea level. Although this product may be of some use as a general reference, THIS PRODUCT MUST NOT BE USED FOR NAVIGATION PURPOSES.

Contour, Colour and Shadow Map Displays

The geophysical data are interpolated onto a regular grid using a modified Akima spline technique. The resulting grid is suitable for image processing and generation of contour maps. The grid cell size is 20% of the line interval.

Colour maps are produced by interpolating the grid down to the pixel size. The parameter is then incremented with respect to specific amplitude ranges to provide colour "contour" maps.

Monochromatic shadow maps or images are generated by employing an artificial sun to cast shadows on a surface defined by the geophysical grid. There are many variations in the shadowing technique. These techniques can be applied to total field or enhanced magnetic data, magnetic derivatives, resistivity, etc. The shadowing technique is also used as a quality control method to detect subtle changes between lines.

Multi-channel Stacked Profiles

Distance-based profiles of the digitally recorded geophysical data are generated and plotted at an appropriate scale. These profiles also contain the calculated parameters that are used in the interpretation process. These are produced as worksheets prior to interpretation, and are also presented in the final corrected form after interpretation. The profiles display electromagnetic anomalies with their respective interpretive symbols. Table 5-1 shows the parameters and scales for the multi-channel stacked profiles.

In Table 5-1, the log resistivity scale of 0.06 decade/mm means that the resistivity changes by an order of magnitude in 16.6 mm. The resistivities at 0, 33 and 67 mm up from the bottom of the digital profile are respectively 1, 100 and 10,000 ohm-m.

Table 5-1. Multi-channel Stacked Profiles

| Channel Name (Freq) | Observed Parameters | Scale Units/mm |
|---------------------|--|----------------|
| MAG5 | total magnetic field (fine) | 5 nT |
| MAG50 | total magnetic field (coarse) | 50 nT |
| ALTBIRD | EM sensor height above ground | 6 m |
| CXI1000 | vertical coaxial coil-pair in-phase (1000 Hz) | 5 ppm |
| CXQ1000 | vertical coaxial coil-pair quadrature (1000 Hz) | 5 ppm |
| CPI900 | horizontal coplanar coil-pair in-phase (900 Hz) | 10 ppm |
| CPQ900 | horizontal coplanar coil-pair quadrature (900 Hz) | 10 ppm |
| CXI5500 | vertical coaxial coil-pair in-phase (5500 Hz) | 10 ppm |
| CXQ5500 | vertical coaxial coil-pair quadrature (5500 Hz) | 10 ppm |
| CPI7200 | horizontal coplanar coil-pair in-phase (7200 Hz) | 20 ppm |
| CPQ7200 | horizontal coplanar coil-pair quadrature (7200 Hz) | 20 ppm |
| CPI56K | horizontal coplanar coil-pair in-phase (56,000 Hz) | 20 ppm |
| CPQ56K | horizontal coplanar coil-pair quadrature (56,000 Hz) | 20 ppm |
| CXSP | coaxial spherics monitor | |
| CXPL | coaxial powerline monitor | |
| CPPL | coplanar powerline monitor | |
| CPSP | coplanar spherics monitor | |
| | | |
| | Computed Parameters | |
| DIFI (mid freq.) | difference function in-phase from CXI and CPI | 10 ppm |
| DIFQ (mid freq.) | difference function quadrature from CXQ and CPQ | 10 ppm |
| RES900 | log resistivity | .06 decade |
| RES7200 | log resistivity | .06 decade |
| RES56K | log resistivity | .06 decade |
| DEP900 | apparent depth | 6 m |
| DEP7200 | apparent depth | 6 m |
| DEP56K | apparent depth | 6 m |
| CDT | conductance | 1 grade |

6. PRODUCTS

This section lists the final maps and products that have been provided under the terms of the survey agreement. Other products can be prepared from the existing dataset, if requested. These include magnetic enhancements or derivatives, percent magnetite, resistivities corrected for magnetic permeability and/or dielectric permittivity, digital terrain, resistivity-depth sections, inversions, and overburden thickness. Most parameters can be displayed as contours, profiles, or in colour.

Base Maps

Base maps of the survey area were produced by using digital topography (.dwg files) provided by Skygold Ventures Ltd. This process provides a relatively accurate, distortion-free base that facilitates correlation of the navigation data to the map coordinate system. The topographic files were combined with geophysical data for plotting the final maps. All maps were created using the following parameters:

Projection Description:

| | |
|----------------------------|-----------------------------|
| Datum: | NAD83 (WGS84) |
| Ellipsoid: | GRS 1980 |
| Projection: | UTM (Zone: 10) |
| Central Meridian: | 123°W |
| False Northing: | 0 |
| False Easting: | 500000 |
| Scale Factor: | 0.9996 |
| WGS84 to Local Conversion: | Molodensky |
| Datum Shifts: | DX: 0 DY: 0 DZ: 0 |

The following parameters are presented on a single map sheet, at a scale of 1:20,000. All maps include flight lines and topography, unless otherwise indicated. Preliminary products are not listed.

Final Products

| | No. of Map Sets | | |
|---------------------------------------|-----------------|-----------|--------|
| | Mylar | Blackline | Colour |
| EM Anomalies | | 2 | |
| Total Magnetic Field | | | 2 |
| Calculated Vertical Magnetic Gradient | | | 2 |
| Apparent Resistivity 7200 Hz | | | 2 |
| Apparent Resistivity 56,000 Hz | | | 2 |

Additional Products

| | |
|---|-----------|
| Digital Archive (see Archive Description) | 1 CD-ROM |
| Survey Report | 2 copies |
| Multi-channel Stacked Profiles | All lines |
| Digital Video (.BIN/.BDX format) | 1 DVD |

7. SURVEY RESULTS

General Discussion

Table 7-1 summarizes the EM responses in the survey area, with respect to conductance grade and interpretation. The apparent conductance and depth values shown in the EM Anomaly list appended to this report have been calculated from "local" in-phase and quadrature amplitudes of the Coaxial 5500 Hz frequency. The picking and interpretation procedure relies on several parameters and calculated functions. For this survey, the Coaxial 5500 Hz responses and the mid-frequency difference channels were used as two of the main picking criteria. The 7200 Hz coplanar results were also weighted to provide picks over wider or flat-dipping sources. The quadrature channels provided picks in areas where the in-phase responses might have been suppressed by magnetite.

The anomalies shown on the electromagnetic anomaly maps are based on a near-vertical, half plane model. This model best reflects "discrete" bedrock conductors. Wide bedrock conductors or flat-lying conductive units, whether from surficial or bedrock sources, may give rise to very broad anomalous responses on the EM profiles. These may not appear on the electromagnetic anomaly map if they have a regional character rather than a locally anomalous character.

TABLE 7-1 EM ANOMALY STATISTICS
SPANISH MOUNTAIN PROJECT AREA

| CONDUCTOR GRADE | CONDUCTANCE RANGE SIEMENS (MHOS) | NUMBER OF RESPONSES |
|--------------------|-------------------------------------|------------------------|
| 7 | >100 | 30 |
| 6 | 50 - 100 | 25 |
| 5 | 20 - 50 | 109 |
| 4 | 10 - 20 | 142 |
| 3 | 5 - 10 | 165 |
| 2 | 1 - 5 | 214 |
| 1 | <1 | 54 |
| * | INDETERMINATE | 44 |
| TOTAL | | 783 |

| CONDUCTOR MODEL | MOST LIKELY SOURCE | NUMBER OF RESPONSES |
|--------------------|----------------------------|------------------------|
| D | DISCRETE BEDROCK CONDUCTOR | 156 |
| B | DISCRETE BEDROCK CONDUCTOR | 456 |
| S | CONDUCTIVE COVER | 47 |
| H | ROCK UNIT OR THICK COVER | 97 |
| E | EDGE OF WIDE CONDUCTOR | 31 |
| L | CULTURE | 0 |
| TOTAL | | 783 |

(SEE EM MAP LEGEND FOR EXPLANATIONS)

These broad conductors, which more closely approximate a half-space model, will be maximum coupled to the horizontal (coplanar) coil-pair and should be more evident on the resistivity parameter. Resistivity maps, therefore, may be more valuable than the electromagnetic anomaly maps, in areas where broad or flat-lying conductors are considered to be of importance. Contoured resistivity maps, based on the 7200 Hz and 56,000 Hz coplanar data are included with this report.

Excellent resolution and discrimination of conductors was accomplished by using a fast sampling rate of 0.1 sec and by employing a “common” frequency (5500/7200 Hz) on two orthogonal coil-pairs (coaxial and coplanar). The resulting difference channel parameters often permit differentiation of bedrock and surficial conductors, even though they may exhibit similar conductance values.

Anomalies that occur near the ends of the survey lines (i.e., outside the survey area), should be viewed with caution. Some of the weaker anomalies could be due to aerodynamic noise, i.e., bird bending, which is created by abnormal stresses to which the bird is subjected during the climb and turn of the aircraft between lines. Such aerodynamic noise is usually manifested by an anomaly on the coaxial in-phase channel only, although severe stresses can affect the coplanar in-phase channels as well.

Magnetics

A Fugro CF-1 cesium vapour magnetometer was operated at the survey base to record diurnal variations of the earth's magnetic field. The clock of the base station was synchronized with that of the airborne system to permit subsequent removal of diurnal drift.

The total magnetic field data have been presented as contours on the base map using a contour interval of 5 nT where gradients permit. The map shows the magnetic properties of the rock units underlying the survey area.

The total magnetic field data have been subjected to a processing algorithm to produce maps of the calculated vertical gradient. This procedure enhances near-surface magnetic units and suppresses regional gradients. It also provides better definition and resolution of magnetic units and displays weak magnetic features that may not be clearly evident on the total field maps.

There is weak evidence on the magnetic maps that suggests that the survey area has been subjected to deformation and/or alteration. These structural complexities are evident on the contour maps as variations in magnetic intensity, irregular patterns, and as offsets or changes in strike direction.

If a specific magnetic intensity can be assigned to the rock type that is believed to host the target mineralization, it may be possible to select areas of higher priority on the basis of the total field magnetic data. This is based on the assumption that the magnetite content of the host rocks will give rise to a limited range of contour values that will permit differentiation of various lithological units.

The magnetic results, in conjunction with the other geophysical parameters, have provided valuable information that can be used to help map the geology and structure in the survey area.

Apparent Resistivity

Apparent resistivity maps, which display the conductive properties of the survey area, were produced from the 7200 Hz and 56,000 Hz coplanar data. The maximum resistivity values, which are calculated for each frequency, are 8,000 and 20,000 ohm-m respectively. These cutoffs eliminate the erratic higher resistivities that would result from unstable ratios of very small EM amplitudes.

In general, the resistivity patterns show moderately poor agreement with the magnetic trends. This suggests that many of the resistivity lows are contained within sedimentary units with very little magnetic expression. There are also a few areas where contour

patterns appear to be influenced by conductive surficial material that is associated with creeks and lakes in the survey area.

There are several very strong resistivity lows in the area. Some of these are quite extensive and often reflect "formational" conductors that may be of minor interest as direct exploration targets unless they are known to host auriferous mineralization. However, attention may be focused on areas where these zones appear to be faulted or folded or where anomaly characteristics differ along strike.

Electromagnetic Anomalies

The EM anomalies resulting from this survey appear to fall within one of three general categories. The first type consists of discrete, well-defined anomalies that yield marked inflections on the difference channels. These anomalies are usually attributed to conductive sulphides or graphite and are generally given a "B", "T" or "D" interpretive symbol, denoting a bedrock source.

The second class of anomalies comprises moderately broad responses that exhibit the characteristics of a half-space and do not yield well-defined inflections on the difference channels. Anomalies in this category are usually given an "S" or "H" interpretive symbol. The lack of a difference channel response usually implies a broad or flat-lying conductive source such as overburden. Some of these anomalies could reflect conductive rock units

at surface or at depth, zones of deep weathering, or alteration zones, all of which can yield "non-discrete" signatures.

The effects of conductive overburden are evident over portions of the survey area. Although the difference channels (DIFI and DIFQ) are extremely valuable in detecting bedrock conductors that are partially masked by conductive overburden, sharp undulations in the bedrock/overburden interface can yield anomalies in the difference channels which may be interpreted as possible bedrock conductors. Such anomalies usually fall into the "S?" or "B?" classification but may also be given an "E" interpretive symbol, denoting a resistivity contrast at the edge of a conductive unit.

The "?" symbol does not question the validity of an anomaly, but instead indicates some degree of uncertainty as to which is the most appropriate EM source model. This ambiguity results from the combination of effects from two or more conductive sources, such as overburden and bedrock, gradational changes, or moderately shallow dips. The presence of a conductive upper layer has a tendency to mask or alter the characteristics of bedrock conductors, making interpretation difficult. This problem is further exacerbated in the presence of magnetite.

In areas where EM responses are evident primarily on the quadrature components, zones of poor conductivity are indicated. Where these responses are coincident with magnetic anomalies, it is possible that the in-phase component amplitudes have been suppressed by the effects of magnetite. Poorly-conductive magnetic features can give rise to resistivity

anomalies that are only slightly below or slightly above background. If it is expected that poorly-conductive economic mineralization could be associated with magnetite-rich units, most of these weakly anomalous features will be of interest. In any areas where magnetite causes the in-phase components to become negative, the apparent conductance and depth of EM anomalies will be unreliable. Magnetite effects usually give rise to overstated (higher) resistivity values and understated (shallow) depth calculations.

The third class consists of cultural anomalies which are usually given the symbol "L" or "L?". Anomalies in this category can include telephone or power lines, pipelines, mining equipment, fences, metal bridges or culverts, buildings and other metallic structures.

As potential targets within the area may be associated with graphitic units containing weakly disseminated sulphides, and which are likely to be non-magnetic, it is impractical to assess the relative merits of EM anomalies on the basis of conductance or magnetic association. It is recommended that an attempt be made to compile a suite of geophysical "signatures" over any known areas of interest. Anomaly characteristics are clearly defined on the multi-parameter geophysical data profiles that are supplied as one of the survey products.

Potential Targets in the Survey Area

The electromagnetic anomaly map shows the anomaly locations with the interpreted conductor type, dip, conductance and depth being indicated by symbols. Direct magnetic correlation is also shown if it exists. The strike direction and length of the conductors are indicated only where anomalies can be correlated from line to line with a reasonable degree of confidence.

In areas where several conductors or conductive trends appear to be related to a common geological unit, these appear as lows on the resistivity maps. These broad lows often host multiple conductors, rather than a single source.

Magnetic relief is approximately 230 nT, ranging from a low of about 56,430 nT in the northwest corner to a high of more than 56,660 nT in the south, on line 10550. There are three main magnetic units that strike southeast in the southern half of the property, in addition to one segmented dyke-like feature that strikes south, from the eastern end of line 10340 to fiducial 2955 on line 10580.

The vertical gradient map shows that the three main magnetic zones in the south host several parallel bands that strike southeast. However, there are a few linear magnetic trends that strike east-southeast, intersecting the local geology at a shallow angle.

There are also several smaller, more isolated magnetic highs. A few of the smaller, sharp anomalies are due to metallic structures or mining equipment, although there are other strong plug-like features that have attributed to bedrock sources. Two of these plug-like

magnetic highs are evident on line 10040 at fiducial 4625 and on line 10210 at fiducial 877. The very short wavelength of the cultural anomalies sets them apart from the broader bedrock units.

There is very little direct correlation between magnetic and resistivity trends, although most of the conductive zones appear to be associated with units of lower magnetic susceptibility. The differences in contour patterns tend to suggest that at least some of the resistivity lows are related to near-surface conductivity such as overburden, while the magnetic results are seeing the deeper basement units. It is also apparent that most of the stronger bedrock conductors are non-magnetic and that they are contained within non-magnetic host rocks.

Resistivity lows on the property often yield values of less than 1 ohm-m. The most common causes of values in this range include massive sulphides, graphite, salt water, and some marine clays. Of these, massive sulphides containing pyrrhotite would be the most likely to yield a magnetic signature. In the absence of magnetic correlation, graphitic argillites or shales are considered to be the most likely causes of these highly conductive zones.

If it can be determined that auriferous mineralization in the area is associated with graphitic units, all of these conductors will become potential targets. However, in order to focus follow-up work on the more favourable areas, it will be necessary to devise a method to screen out the least attractive conductors. Any conductive zones that have been subjected to faulting or structural deformation may prove to be of greater interest.

Due to the vast number of anomalous responses in the area and their proximity to each other, it is often difficult to correlate conductor axes from line to line. This problem is exacerbated by the lack of magnetic correlation and the apparent changes in conductivity along strike. In many areas, the true conductor strikes and lengths could be quite different from those shown on the EM map.

It is beyond the scope of this report to attempt to describe the numerous conductors on the Spanish Mountain property. The following table lists only a few of the anomalous sections that are typical of the multi-conductor zones identified by the airborne survey.

| Anomaly | Type | Comments |
|--|-----------------------|--|
| 10180D 10180K 10180N 10180P 10180Q | E B H D H | Anomaly 10180D defines the western edge of the broad conductive unit that dominates the eastern half of the block. At least six separate conductors are evident in the 440 m interval between 10180D and 10180I. Most of these appear to reflect thin sources, evident on the coaxial channels, but which combine to form a broad resistivity low on the 900 Hz frequency at depth. A second resistivity low, from 10180K to 10180M suggests three thicker sources that yield values of less than 1 ohm-m. Anomalies 10180N and 10180Q reflect flat-lying conductive units at depths of approximately 30 m and 90 m respectively. The latter is seen only on the deeper 900 Hz and the higher frequencies identify a more resistive hill that overlies the buried unit. There are lateral inhomogeneities within this unit as evidenced by 10180P, which indicates a thin source. A subtle magnetic anomaly occurs east of the road, near fiducial 4040. |
| 10210D 10210E 10210F 10210H 10210J | B B B B B | With the exception of 10210K, these anomalies reflect moderately thick sources. All yield resistivity lows of less than 2 ohm-m. The sharp magnetic anomaly at 10210F is attributed to culture (building, vehicles and construction equipment). Although culture may have also affected the EM responses, |

| Anomaly | Type | Comments |
|--|---|--|
| 10210K | D | the three conductors observed in this area extend well beyond the area of cultural interference. The conductor axes shown on the map strike SSE. However, it is possible that the conductors through 10210D,E and F, could actually strike ESE. These three anomalies are very close to surface, while 10210H is at an estimated depth of 12 m. |
| 10290A 10290B 10290C 10290E 10290H 10290J 10290L | B B D B B B E | Line 10290 is one of the lines within the detailed survey block. Anomaly 10290A marks the beginning of a SE-trending conductive zone that is located on the southwestern slope of Spanish Mountain. This is not part of the broad, highly conductive unit that dominates the area northeast of tie line 19030. There is a very weak magnetic anomaly on the northeastern flank of 10290A, and a second stronger magnetic high at fiducial 3574, about 600 m to the northeast. No visible culture was evident on the video at either of these locations so they have been attributed to bedrock sources. The conductive zone at 10290A parallels the topographic elevation contours, and extends beyond the southern survey boundary, with a strike length of more than 4.5 km. Two magnetic units coincide with the southern portion of this conductive trend, near 10440D and 10510D. Anomaly 10290B is at the western edge of the broad multi-conductor zone on the northeast face of Spanish Mountain. The response at 10290C, about 140 m to the northeast, reflects a thin source with a probable NE dip. The very strong responses at 10290E, 10290H and 10290J all yield resistivities of less than 1 ohm-m. The latter anomaly is at an estimated depth of about 20 m. A resistive cap (hill?) overlies the deeper eastern end of the conductor, east of 10290L. |
| 10310A 10310B 10310D 10310F 10310G 10310H 10310J 10310M 10310N 10310P 10310Q | S? D B? B D D D B D B D | The conductors on this line are very similar to those on line 10290. Anomaly A has been attributed to a weakly conductive, poorly defined source, near surface. This 250 m-long conductor occurs near a magnetic contact and yields weak magnetic correlation, suggesting a possible bedrock source, rather than overburden. Anomalies 10310B and C appear to be due to two thin sources separated by 80 m. Anomaly 10310D is an extremely weak, thin conductor, but it correlates with a double-peaked magnetic anomaly that is not related to culture. Thin conductors are evident at 10310E,G,H,J,M,N and Q, while thicker, stronger conductors are seen at 10310F,I,K,L and P. Anomaly 10310J is located near a road. There is a construction site or camp at fiducial 3853 with several buildings and vehicles. The small magnetic high at 3853 is likely due to culture. However, the flanking conductors at 10310I and |

| Anomaly | Type | Comments |
|---------|------|---|
| | | 210310J have both been attributed to bedrock sources. |
| 10370C | E | Anomaly 10370C defines the western edge of the western conductive unit on this line. Anomalies 10370D,E and F reflect three thin NE-dipping sources within this conductive zone that is flanked by a moderately magnetic unit on the southwest. Anomalies 10370G through 10370Q are all contained within the eastern conductive zone. Thin sources are indicated at 10370G,H,K,L and N. The strong anomaly at 10370I-10370J could be due to one thick source, rather than two thin, closely-spaced conductors. These anomalies, in addition to 10370O and 10370P, give rise to resistivities of less than 1 ohm-m. The moderately strong magnetic anomaly between 10370P and 10370O is part of the inferred segmented dyke that strikes south, through fiducial 2954 on line 10580. |
| 10370D | B | |
| 10370E | D | |
| 10370F | D | |
| 10370G | B | |
| 10370H | D | |
| 10370I | B | |
| 10370J | B | |
| 10370N | B | |
| 10370Q | B | |
| 10440A | D | Anomaly 10440A is an isolated response that reflects a short, thin response near the eastern contact of a moderately strong magnetic unit. This is one of the very few anomalies on the property that suggests a probable dip towards the southwest. There is a small road in a cleared area at fiducial 5300, but there is no evidence of cultural objects near this short, but interesting conductor. Anomaly 10440B is a weak, poorly-defined thin source that also reflects an isolated conductor associated with a weak magnetic trough. Conductors 10440E and F are separated by about 130 m and are contained within the western conductive zone. A second resistivity low at 10440H hosts three thin conductors within a SSE-trending limb of conductive material along the opposite (NE) slope of Spanish Mountain. This conductive limb strikes SSE from 10380H, as an offshoot of the main conductive unit in the NE part of the property. Anomaly 10440J is a thicker source, located in a magnetic trough on the eastern flank of the inferred dyke. This highly conductive zone yields resistivities of less than 1 ohm-m. Anomaly 10440L is located on a road, but has been attributed to a prominent bedrock conductive trend that strikes ESE from 10370I, beyond the eastern property boundary. |
| 10440B | B? | |
| 10440E | B | |
| 10440F | B | |
| 10440G | D | |
| 10440H | D | |
| 10440J | B | |
| 10440L | B | |
| 10490A | S | Anomalies 10490A and B have both been attributed to surficial conductivity. The first is associated with a very small lake; the second is located in Cedar Creek. These are not considered to be attractive targets but they occur near the flanks of the strong magnetic unit in the SW portion of the property. Anomalies 10490C and D reflect two thin sources separated by 100 m. The two conductors flank a very weak magnetic high. A |
| 10490B | S | |
| 10490C | D | |
| 10490D | D | |
| 10490E | B | |
| 10490F | D | |
| 10490G | B | |

| Anomaly | Type | Comments |
|--|-----------------------------|--|
| 10490H 10490I 10490J 10490L 10490N 10490O | B B B B D B | stronger conductor occurs on the northwestern contact of a stronger magnetic anomaly, at 10490E. Anomaly 10490F reflects a thin NE-dipping conductor about 200 m to the northeast. The extremely high amplitude responses at 10490G and 10490I indicate the presence of up to four strong conductors that are close to surface. Anomaly 10490L, on the NE shoulder of 10490K, yields a low resistivity of less than 1 ohm-m at an estimated depth of about 30 m. Anomaly 10490O indicates a thin conductor near the apparent eastern limit of the main conductive zone, as defined by the higher frequencies. However, it is evident from the 900 Hz, that the conductive zone extends NE, to a depth of more than 85 m,. The topography suggests that this is a down-dip extension, rather than an increased thickness of resistive cover due to topography. Although there is a main road at fiducial 583 and several other bush roads, there is no visible culture on this line. |
| 10570A 10570B 10510C 10570F 10570H 10570I | D B? D B B H | Anomaly 10570A is part of a thin conductor near Cedar Creek that probably continues SE, beyond the limits of the survey, This thin source is located near the eastern flank of a moderate magnetic anomaly. Anomaly 10570B is extremely weak, and could be due to a spheric noise spike. However, it is associated with another magnetic high centered near fiducial 2705. Anomaly 10570C is a strong, thin, NE-dipping source with a second conductor about 100 m to the NE. Anomaly 10570F yields its strongest response on the 900 Hz, indicating an increase in conductivity at depth. The depth channel suggests the top of this conductor is at a depth of about 30 m. However, in the presence of a heavy tree canopy, depth estimates may be inaccurate. The most conductive portion of this line is at 10570H, where values of less than 1 ohm-m are evident. This zone is very close to surface, near the crest of a very weak magnetic anomaly on its northern flank. The magnetic high is associated with a small clearing, but there is no visible culture. Anomaly 10570I has a shoulder on its northeastern flank on the 900 Hz, suggesting that this conductor continues at depth. |
| 20080A 20080E 20080K | B B B | Line 20080 is one of the lines that were flown NW-SE over the detailed area at a line separation of 75 m, but orthogonal to the traverse lines in the main block. At least three, strong conductive zones are evident in this block. Because the general strike of these zones is NW-SE, parallel to the line direction, the poor coupling precluded distinct anomalies on |

| Anomaly | Type | Comments |
|---------|------|---|
| | | <p>the coaxial channels. Resistivity trends from the coplanar channels, however, are not affected. The orthogonal line direction should help to identify any conductors in the detailed area that exhibit folded structures or changes in strike direction towards the NE. Line 20080 has been chosen because there are at least three areas that exhibit NE-SW components. Anomaly 20080A is part of an ENE-WSW resistivity low between the north ends of lines 20030 and 20080. The zone is non-magnetic. The sharp magnetic high at 20040A is due to culture (mining equipment). Anomaly 20080E, at the centre of the block, also suggests an E-W component that intersects the central SE-trending conductor. Like the previous anomaly, 20080E also yields resistivities of less than 1 ohm-m. Anomaly 20080K is associated with a pod of conductive material that appears to be connected to the SE-trending conductor at 20030G. At least three E-W trending linear features can be inferred from the vertical gradient data on this block, as well as two other subtle features that trend ESE.</p> |

8. CONCLUSIONS AND RECOMMENDATIONS

This report provides a very brief description of the survey results and describes the equipment, data processing procedures and logistics of the survey over the Spanish Mountain project area.

There are numerous anomalies in the survey block that are typical of graphitic or massive sulphide responses. The survey was also successful in locating a few moderately weak or broad conductors that may warrant additional work. The various maps included with this report display the magnetic and conductive properties of the survey area. It is recommended that a complete assessment and detailed evaluation of the survey results be carried out, in conjunction with all available geophysical, geological and geochemical information. Particular reference should be made to the multi-parameter data profiles that clearly define the characteristics of the individual anomalies.

The survey has defined two major zones of low resistivity. One zone strikes southeast, along the southwest slope of Spanish Mountain, while the larger, multi-conductor zone dominates the northeastern portion of the property, northeast of tie line 19030. The non-magnetic, highly-conductive characteristics suggest that graphitic units are the most likely causative source. Most of the thin sources exhibit dips towards the northeast.

Some of the magnetic and resistivity patterns have been affected by mining operations and other cultural objects. The estimated depths to some of the deeper units could be erroneous, due to the dense tree canopy in several areas.

Most anomalies in the area are moderately strong and well-defined. A few weak responses have been attributed to conductive overburden or deep weathering. Others coincide with magnetic gradients that may reflect contacts, faults or shears. Such structural breaks are considered to be of particular interest as they may have influenced mineral deposition within the survey area.

The interpreted bedrock conductors and anomalous targets defined by the survey should be subjected to further investigation, using appropriate surface exploration techniques. Anomalies that are currently considered to be of moderately low priority may require upgrading if follow-up results are favourable.

It is also recommended that additional processing of existing geophysical data be considered, in order to extract the maximum amount of information from the survey results.

Current software and imaging techniques often provide valuable information on structure and lithology, which may not be clearly evident on the contour and colour maps. These techniques can yield images that define subtle, but significant, structural details.

Respectfully submitted,

FUGRO AIRBORNE SURVEYS CORP.

Paul A. Smith
Geophysicist

PAS/sdp

R06075DEC.06

APPENDIX A

LIST OF PERSONNEL

The following personnel were involved in the acquisition, processing, interpretation and presentation of data, relating to a DIGHEM^V airborne geophysical survey carried out for Wildrose Resources Ltd. and Skygold Ventures Ltd., near Likely, British Columbia.

| | |
|-------------------|---|
| David Miles | Manager, Helicopter Operations |
| Emily Farquhar | Manager, Data Processing and Interpretation |
| Yuri Mironenko | Senior Geophysical Operator |
| Amit Praharaj | Second Geophysical Operator |
| Chris Sawyer | Field Geophysicist/Crew Leader |
| Al Sweet | Pilot (Questral Helicopters Ltd.) |
| Stephen Harrison | Geophysical Data Processor/Geophysicist |
| Paul A. Smith | Interpretation Geophysicist |
| Lyn Vanderstarren | Drafting Supervisor |
| Susan Pothiah | Word Processing Operator |
| Albina Tonello | Secretary/Expeditor |

The survey consisted of 306 km of coverage, flown from October 14 to October 16, 2006.

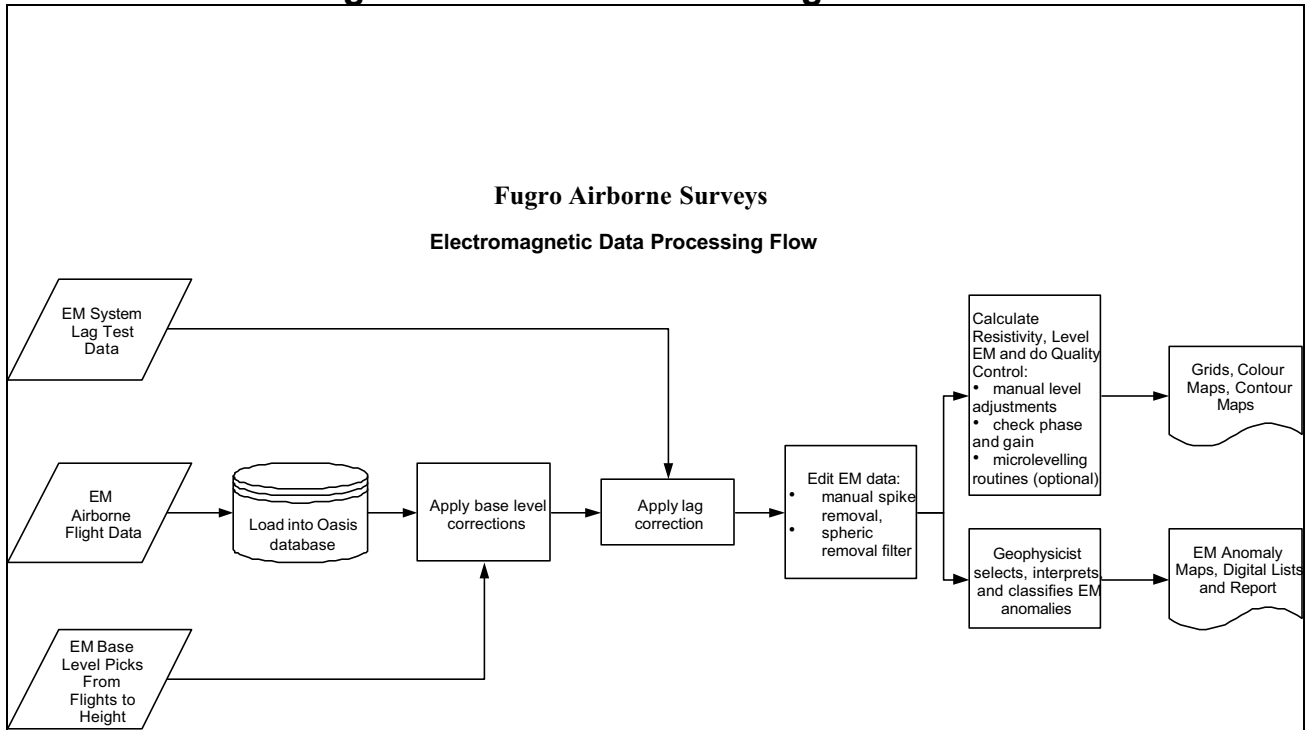
All personnel are employees of Fugro Airborne Surveys, except for the pilot who is an employee of Questral Helicopters Ltd.

APPENDIX B

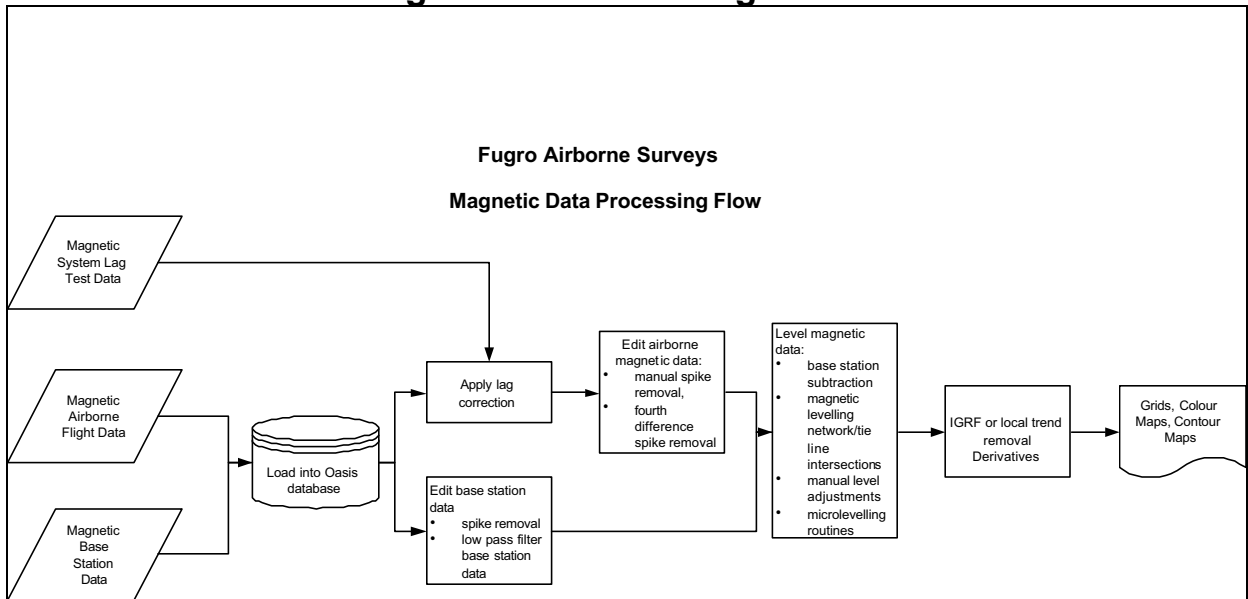
DATA PROCESSING FLOWCHARTS

APPENDIX B

Processing Flow Chart - Electromagnetic Data



Processing Flow Chart - Magnetic Data



APPENDIX C

BACKGROUND INFORMATION

BACKGROUND INFORMATION

Electromagnetics

Fugro electromagnetic responses fall into two general classes, discrete and broad. The discrete class consists of sharp, well-defined anomalies from discrete conductors such as sulphide lenses and steeply dipping sheets of graphite and sulphides. The broad class consists of wide anomalies from conductors having a large horizontal surface such as flatly dipping graphite or sulphide sheets, saline water-saturated sedimentary formations, conductive overburden and rock, kimberlite pipes and geothermal zones. A vertical conductive slab with a width of 200 m would straddle these two classes.

The vertical sheet (half plane) is the most common model used for the analysis of discrete conductors. All anomalies plotted on the geophysical maps are analyzed according to this model. The following section entitled **Discrete Conductor Analysis** describes this model in detail, including the effect of using it on anomalies caused by broad conductors such as conductive overburden.

The conductive earth (half-space) model is suitable for broad conductors. Resistivity contour maps result from the use of this model. A later section entitled **Resistivity Mapping** describes the method further, including the effect of using it on anomalies caused by discrete conductors such as sulphide bodies.

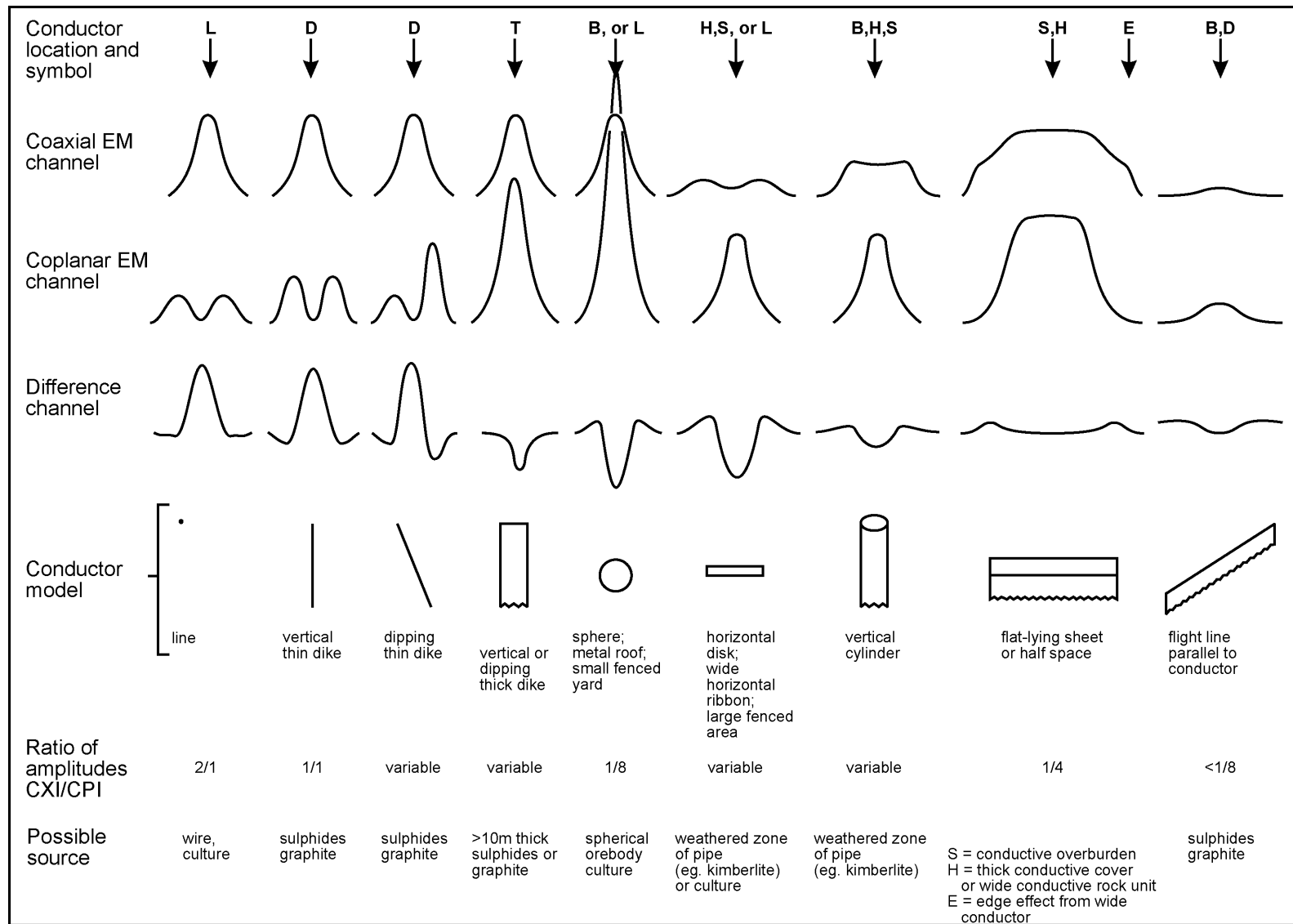
Geometric Interpretation

The geophysical interpreter attempts to determine the geometric shape and dip of the conductor. Figure C-1 shows typical HEM anomaly shapes which are used to guide the geometric interpretation.

Discrete Conductor Analysis

The EM anomalies appearing on the electromagnetic map are analyzed by computer to give the conductance (i.e., conductivity-thickness product) in siemens (mhos) of a vertical sheet model. This is done regardless of the interpreted geometric shape of the conductor. This is not an unreasonable procedure, because the computed conductance increases as the electrical quality of the conductor increases, regardless of its true shape. DIGHEM anomalies are divided into seven grades of conductance, as shown in Table C-1. The conductance in siemens (mhos) is the reciprocal of resistance in ohms.

- Appendix C.2 -



Typical HEM anomaly shapes

Figure C-1

- Appendix C.3 -

The conductance value is a geological parameter because it is a characteristic of the conductor alone. It generally is independent of frequency, flying height or depth of burial, apart from the averaging over a greater portion of the conductor as height increases. Small anomalies from deeply buried strong conductors are not confused with small anomalies from shallow weak conductors because the former will have larger conductance values.

Table C-1. EM Anomaly Grades

| Anomaly Grade | Siemens |
|---------------|----------|
| 7 | > 100 |
| 6 | 50 - 100 |
| 5 | 20 - 50 |
| 4 | 10 - 20 |
| 3 | 5 - 10 |
| 2 | 1 - 5 |
| 1 | < 1 |

Conductive overburden generally produces broad EM responses which may not be shown as anomalies on the geophysical maps. However, patchy conductive overburden in otherwise resistive areas can yield discrete anomalies with a conductance grade (cf. Table C-1) of 1, 2 or even 3 for conducting clays which have resistivities as low as 50 ohm-m. In areas where ground resistivities are below 10 ohm-m, anomalies caused by weathering variations and similar causes can have any conductance grade. The anomaly shapes from the multiple coils often allow such conductors to be recognized, and these are indicated by the letters S, H, and sometimes E on the geophysical maps (see EM legend on maps).

For bedrock conductors, the higher anomaly grades indicate increasingly higher conductances. Examples: the New Inco copper discovery (Noranda, Canada) yielded a grade 5 anomaly, as did the neighbouring copper-zinc Magusi River ore body; Mattabi (copper-zinc, Sturgeon Lake, Canada) and Whistle (nickel, Sudbury, Canada) gave grade 6; and the Montcalm nickel-copper discovery (Timmins, Canada) yielded a grade 7 anomaly. Graphite and sulphides can span all grades but, in any particular survey area, field work may show that the different grades indicate different types of conductors.

Strong conductors (i.e., grades 6 and 7) are characteristic of massive sulphides or graphite. Moderate conductors (grades 4 and 5) typically reflect graphite or sulphides of a less massive character, while weak bedrock conductors (grades 1 to 3) can signify poorly connected graphite or heavily disseminated sulphides. Grades 1 and 2 conductors may not respond to ground EM equipment using frequencies less than 2000 Hz.

The presence of sphalerite or gangue can result in ore deposits having weak to moderate conductances. As an example, the three million ton lead-zinc deposit of Restigouche

- Appendix C.4 -

Mining Corporation near Bathurst, Canada, yielded a well-defined grade 2 conductor. The 10 percent by volume of sphalerite occurs as a coating around the fine grained massive pyrite, thereby inhibiting electrical conduction. Faults, fractures and shear zones may produce anomalies that typically have low conductances (e.g., grades 1 to 3). Conductive rock formations can yield anomalies of any conductance grade. The conductive materials in such rock formations can be salt water, weathered products such as clays, original depositional clays, and carbonaceous material.

For each interpreted electromagnetic anomaly on the geophysical maps, a letter identifier and an interpretive symbol are plotted beside the EM grade symbol. The horizontal rows of dots, under the interpretive symbol, indicate the anomaly amplitude on the flight record. The vertical column of dots, under the anomaly letter, gives the estimated depth. In areas where anomalies are crowded, the letter identifiers, interpretive symbols and dots may be obliterated. The EM grade symbols, however, will always be discernible, and the obliterated information can be obtained from the anomaly listing appended to this report.

The purpose of indicating the anomaly amplitude by dots is to provide an estimate of the reliability of the conductance calculation. Thus, a conductance value obtained from a large ppm anomaly (3 or 4 dots) will tend to be accurate whereas one obtained from a small ppm anomaly (no dots) could be quite inaccurate. The absence of amplitude dots indicates that the anomaly from the coaxial coil-pair is 5 ppm or less on both the in-phase and quadrature channels. Such small anomalies could reflect a weak conductor at the surface or a stronger conductor at depth. The conductance grade and depth estimate illustrates which of these possibilities fits the recorded data best.

The conductance measurement is considered more reliable than the depth estimate. There are a number of factors that can produce an error in the depth estimate, including the averaging of topographic variations by the altimeter, overlying conductive overburden, and the location and attitude of the conductor relative to the flight line. Conductor location and attitude can provide an erroneous depth estimate because the stronger part of the conductor may be deeper or to one side of the flight line, or because it has a shallow dip. A heavy tree cover can also produce errors in depth estimates. This is because the depth estimate is computed as the distance of bird from conductor, minus the altimeter reading. The altimeter can lock onto the top of a dense forest canopy. This situation yields an erroneously large depth estimate but does not affect the conductance estimate.

Dip symbols are used to indicate the direction of dip of conductors. These symbols are used only when the anomaly shapes are unambiguous, which usually requires a fairly resistive environment.

A further interpretation is presented on the EM map by means of the line-to-line correlation of bedrock anomalies, which is based on a comparison of anomaly shapes on adjacent lines. This provides conductor axes that may define the geological structure over portions of the survey area. The absence of conductor axes in an area implies that anomalies could not be correlated from line to line with reasonable confidence.

- Appendix C.5 -

The electromagnetic anomalies are designed to provide a correct impression of conductor quality by means of the conductance grade symbols. The symbols can stand alone with geology when planning a follow-up program. The actual conductance values are printed in the attached anomaly list for those who wish quantitative data. The anomaly ppm and depth are indicated by inconspicuous dots which should not distract from the conductor patterns, while being helpful to those who wish this information. The map provides an interpretation of conductors in terms of length, strike and dip, geometric shape, conductance, depth, and thickness. The accuracy is comparable to an interpretation from a high quality ground EM survey having the same line spacing.

The appended EM anomaly list provides a tabulation of anomalies in ppm, conductance, and depth for the vertical sheet model. No conductance or depth estimates are shown for weak anomalous responses that are not of sufficient amplitude to yield reliable calculations.

Since discrete bodies normally are the targets of EM surveys, local base (or zero) levels are used to compute local anomaly amplitudes. This contrasts with the use of true zero levels which are used to compute true EM amplitudes. Local anomaly amplitudes are shown in the EM anomaly list and these are used to compute the vertical sheet parameters of conductance and depth.

Questionable Anomalies

The EM maps may contain anomalous responses that are displayed as asterisks (*). These responses denote weak anomalies of indeterminate conductance, which may reflect one of the following: a weak conductor near the surface, a strong conductor at depth (e.g., 100 to 120 m below surface) or to one side of the flight line, or aerodynamic noise. Those responses that have the appearance of valid bedrock anomalies on the flight profiles are indicated by appropriate interpretive symbols (see EM legend on maps). The others probably do not warrant further investigation unless their locations are of considerable geological interest.

The Thickness Parameter

A comparison of coaxial and coplanar shapes can provide an indication of the thickness of a steeply dipping conductor. The amplitude of the coplanar anomaly (e.g., CPI channel) increases relative to the coaxial anomaly (e.g., CXI) as the apparent thickness increases, i.e., the thickness in the horizontal plane. (The thickness is equal to the conductor width if the conductor dips at 90 degrees and strikes at right angles to the flight line.) This report refers to a conductor as thin when the thickness is likely to be less than 3 m, and thick when in excess of 10 m. Thick conductors are indicated on the EM map by parentheses "()". For base metal exploration in steeply dipping geology, thick conductors can be high priority targets because many massive sulphide ore bodies are thick. The system cannot

sense the thickness when the strike of the conductor is subparallel to the flight line, when the conductor has a shallow dip, when the anomaly amplitudes are small, or when the resistivity of the environment is below 100 ohm-m.

Resistivity Mapping

Resistivity mapping is useful in areas where broad or flat lying conductive units are of interest. One example of this is the clay alteration which is associated with Carlin-type deposits in the south west United States. The resistivity parameter was able to identify the clay alteration zone over the Cove deposit. The alteration zone appeared as a strong resistivity low on the 900 Hz resistivity parameter. The 7,200 Hz and 56,000 Hz resistivities showed more detail in the covering sediments, and delineated a range front fault. This is typical in many areas of the south west United States, where conductive near surface sediments, which may sometimes be alkaline, attenuate the higher frequencies.

Resistivity mapping has proven successful for locating diatremes in diamond exploration. Weathering products from relatively soft kimberlite pipes produce a resistivity contrast with the unaltered host rock. In many cases weathered kimberlite pipes were associated with thick conductive layers that contrasted with overlying or adjacent relatively thin layers of lake bottom sediments or overburden.

Areas of widespread conductivity are commonly encountered during surveys. These conductive zones may reflect alteration zones, shallow-dipping sulphide or graphite-rich units, saline ground water, or conductive overburden. In such areas, EM amplitude changes can be generated by decreases of only 5 m in survey altitude, as well as by increases in conductivity. The typical flight record in conductive areas is characterized by in-phase and quadrature channels that are continuously active. Local EM peaks reflect either increases in conductivity of the earth or decreases in survey altitude. For such conductive areas, apparent resistivity profiles and contour maps are necessary for the correct interpretation of the airborne data. The advantage of the resistivity parameter is that anomalies caused by altitude changes are virtually eliminated, so the resistivity data reflect only those anomalies caused by conductivity changes. The resistivity analysis also helps the interpreter to differentiate between conductive bedrock and conductive overburden. For example, discrete conductors will generally appear as narrow lows on the contour map and broad conductors (e.g., overburden) will appear as wide lows.

The apparent resistivity is calculated using the pseudo-layer (or buried) half-space model defined by Fraser (1978)⁶. This model consists of a resistive layer overlying a conductive

⁶ Resistivity mapping with an airborne multicoil electromagnetic system: Geophysics, v. 43, p.144-172

- Appendix C.7 -

half-space. The depth channels give the apparent depth below surface of the conductive material. The apparent depth is simply the apparent thickness of the overlying resistive layer. The apparent depth (or thickness) parameter will be positive when the upper layer is more resistive than the underlying material, in which case the apparent depth may be quite close to the true depth.

The apparent depth will be negative when the upper layer is more conductive than the underlying material, and will be zero when a homogeneous half-space exists. The apparent depth parameter must be interpreted cautiously because it will contain any errors that might exist in the measured altitude of the EM bird (e.g., as caused by a dense tree cover). The inputs to the resistivity algorithm are the in-phase and quadrature components of the coplanar coil-pair. The outputs are the apparent resistivity of the conductive half-space (the source) and the sensor-source distance. The flying height is not an input variable, and the output resistivity and sensor-source distance are independent of the flying height when the conductivity of the measured material is sufficient to yield significant in-phase as well as quadrature responses. The apparent depth, discussed above, is simply the sensor-source distance minus the measured altitude or flying height. Consequently, errors in the measured altitude will affect the apparent depth parameter but not the apparent resistivity parameter.

The apparent depth parameter is a useful indicator of simple layering in areas lacking a heavy tree cover. Depth information has been used for permafrost mapping, where positive apparent depths were used as a measure of permafrost thickness. However, little quantitative use has been made of negative apparent depths because the absolute value of the negative depth is not a measure of the thickness of the conductive upper layer and, therefore, is not meaningful physically. Qualitatively, a negative apparent depth estimate usually shows that the EM anomaly is caused by conductive overburden. Consequently, the apparent depth channel can be of significant help in distinguishing between overburden and bedrock conductors.

Interpretation in Conductive Environments

Environments having low background resistivities (e.g., below 30 ohm-m for a 900 Hz system) yield very large responses from the conductive ground. This usually prohibits the recognition of discrete bedrock conductors. However, Fugro data processing techniques produce three parameters that contribute significantly to the recognition of bedrock conductors in conductive environments. These are the in-phase and quadrature difference channels (DIFI and DIFQ, which are available only on systems with "common" frequencies on orthogonal coil pairs), and the resistivity and depth channels (RES and DEP) for each coplanar frequency.

The EM difference channels (DIFI and DIFQ) eliminate most of the responses from conductive ground, leaving responses from bedrock conductors, cultural features (e.g., telephone lines, fences, etc.) and edge effects. Edge effects often occur near the

perimeter of broad conductive zones. This can be a source of geologic noise. While edge effects yield anomalies on the EM difference channels, they do not produce resistivity anomalies. Consequently, the resistivity channel aids in eliminating anomalies due to edge effects. On the other hand, resistivity anomalies will coincide with the most highly conductive sections of conductive ground, and this is another source of geologic noise. The recognition of a bedrock conductor in a conductive environment therefore is based on the anomalous responses of the two difference channels (DIFI and DIFQ) and the resistivity channels (RES). The most favourable situation is where anomalies coincide on all channels.

The DEP channels, which give the apparent depth to the conductive material, also help to determine whether a conductive response arises from surficial material or from a conductive zone in the bedrock. When these channels ride above the zero level on the depth profiles (i.e., depth is negative), it implies that the EM and resistivity profiles are responding primarily to a conductive upper layer, i.e., conductive overburden. If the DEP channels are below the zero level, it indicates that a resistive upper layer exists, and this usually implies the existence of a bedrock conductor. If the low frequency DEP channel is below the zero level and the high frequency DEP is above, this suggests that a bedrock conductor occurs beneath conductive cover.

Reduction of Geologic Noise

Geologic noise refers to unwanted geophysical responses. For purposes of airborne EM surveying, geologic noise refers to EM responses caused by conductive overburden and magnetic permeability. It was mentioned previously that the EM difference channels (i.e., channel DIFI for in-phase and DIFQ for quadrature) tend to eliminate the response of conductive overburden.

Magnetite produces a form of geological noise on the in-phase channels. Rocks containing less than 1% magnetite can yield negative in-phase anomalies caused by magnetic permeability. When magnetite is widely distributed throughout a survey area, the in-phase EM channels may continuously rise and fall, reflecting variations in the magnetite percentage, flying height, and overburden thickness. This can lead to difficulties in recognizing deeply buried bedrock conductors, particularly if conductive overburden also exists. However, the response of broadly distributed magnetite generally vanishes on the in-phase difference channel DIFI. This feature can be a significant aid in the recognition of conductors that occur in rocks containing accessory magnetite.

EM Magnetite Mapping

The information content of HEM data consists of a combination of conductive eddy current responses and magnetic permeability responses. The secondary field resulting from conductive eddy current flow is frequency-dependent and consists of both in-phase and quadrature components, which are positive in sign. On the other hand, the secondary field

resulting from magnetic permeability is independent of frequency and consists of only an in-phase component which is negative in sign. When magnetic permeability manifests itself by decreasing the measured amount of positive in-phase, its presence may be difficult to recognize. However, when it manifests itself by yielding a negative in-phase anomaly (e.g., in the absence of eddy current flow), its presence is assured. In this latter case, the negative component can be used to estimate the percent magnetite content.

A magnetite mapping technique, based on the low frequency coplanar data, can be complementary to magnetometer mapping in certain cases. Compared to magnetometry, it is far less sensitive but is more able to resolve closely spaced magnetite zones, as well as providing an estimate of the amount of magnetite in the rock. The method is sensitive to 1/4% magnetite by weight when the EM sensor is at a height of 30 m above a magnetitic half-space. It can individually resolve steep dipping narrow magnetite-rich bands which are separated by 60 m. Unlike magnetometry, the EM magnetite method is unaffected by remanent magnetism or magnetic latitude.

The EM magnetite mapping technique provides estimates of magnetite content which are usually correct within a factor of 2 when the magnetite is fairly uniformly distributed. EM magnetite maps can be generated when magnetic permeability is evident as negative in-phase responses on the data profiles.

Like magnetometry, the EM magnetite method maps only bedrock features, provided that the overburden is characterized by a general lack of magnetite. This contrasts with resistivity mapping which portrays the combined effect of bedrock and overburden.

The Susceptibility Effect

When the host rock is conductive, the positive conductivity response will usually dominate the secondary field, and the susceptibility effect⁷ will appear as a reduction in the in-phase, rather than as a negative value. The in-phase response will be lower than would be predicted by a model using zero susceptibility. At higher frequencies the in-phase conductivity response also gets larger, so a negative magnetite effect observed on the low frequency might not be observable on the higher frequencies, over the same body. The susceptibility effect is most obvious over discrete magnetite-rich zones, but also occurs over uniform geology such as a homogeneous half-space.

⁷ Magnetic susceptibility and permeability are two measures of the same physical property. Permeability is generally given as relative permeability, μ_r , which is the permeability of the substance divided by the permeability of free space ($4 \pi \times 10^{-7}$). Magnetic susceptibility k is related to permeability by $k = \mu_r - 1$. Susceptibility is a unitless measurement, and is usually reported in units of 10^{-6} . The typical range of susceptibilities is -1 for quartz, 130 for pyrite, and up to 5×10^5 for magnetite, in 10^{-6} units (Telford et al, 1986).

High magnetic susceptibility will affect the calculated apparent resistivity, if only conductivity is considered. Standard apparent resistivity algorithms use a homogeneous half-space model, with zero susceptibility. For these algorithms, the reduced in-phase response will, in most cases, make the apparent resistivity higher than it should be. It is important to note that there is nothing wrong with the data, nor is there anything wrong with the processing algorithms. The apparent difference results from the fact that the simple geological model used in processing does not match the complex geology.

Measuring and Correcting the Magnetite Effect

Theoretically, it is possible to calculate (forward model) the combined effect of electrical conductivity and magnetic susceptibility on an EM response in all environments. The difficulty lies, however, in separating out the susceptibility effect from other geological effects when deriving resistivity and susceptibility from EM data.

Over a homogeneous half-space, there is a precise relationship between in-phase, quadrature, and altitude. These are often resolved as phase angle, amplitude, and altitude. Within a reasonable range, any two of these three parameters can be used to calculate the half space resistivity. If the rock has a positive magnetic susceptibility, the in-phase component will be reduced and this departure can be recognized by comparison to the other parameters.

The algorithm used to calculate apparent susceptibility and apparent resistivity from HEM data, uses a homogeneous half-space geological model. Non half-space geology, such as horizontal layers or dipping sources, can also distort the perfect half-space relationship of the three data parameters. While it may be possible to use more complex models to calculate both rock parameters, this procedure becomes very complex and time-consuming. For basic HEM data processing, it is most practical to stick to the simplest geological model.

Magnetite reversals (reversed in-phase anomalies) have been used for many years to calculate an “FeO” or magnetite response from HEM data (Fraser, 1981). However, this technique could only be applied to data where the in-phase was observed to be negative, which happens when susceptibility is high and conductivity is low.

Applying Susceptibility Corrections

Resistivity calculations done with susceptibility correction may change the apparent resistivity. High-susceptibility conductors, that were previously masked by the susceptibility effect in standard resistivity algorithms, may become evident. In this case the susceptibility corrected apparent resistivity is a better measure of the actual resistivity of the earth. However, other geological variations, such as a deep resistive layer, can also reduce the in-phase by the same amount. In this case, susceptibility correction would not be the best method. Different geological models can apply in different areas of the same

data set. The effects of susceptibility, and other effects that can create a similar response, must be considered when selecting the resistivity algorithm.

Susceptibility from EM vs Magnetic Field Data

The response of the EM system to magnetite may not match that from a magnetometer survey. First, HEM-derived susceptibility is a rock property measurement, like resistivity. Magnetic data show the total magnetic field, a measure of the potential field, not the rock property. Secondly, the shape of an anomaly depends on the shape and direction of the source magnetic field. The electromagnetic field of HEM is much different in shape from the earth's magnetic field. Total field magnetic anomalies are different at different magnetic latitudes; HEM susceptibility anomalies have the same shape regardless of their location on the earth.

In far northern latitudes, where the magnetic field is nearly vertical, the total magnetic field measurement over a thin vertical dike is very similar in shape to the anomaly from the HEM-derived susceptibility (a sharp peak over the body). The same vertical dike at the magnetic equator would yield a negative magnetic anomaly, but the HEM susceptibility anomaly would show a positive susceptibility peak.

Effects of Permeability and Dielectric Permittivity

Resistivity algorithms that assume free-space magnetic permeability and dielectric permittivity, do not yield reliable values in highly magnetic or highly resistive areas. Both magnetic polarization and displacement currents cause a decrease in the in-phase component, often resulting in negative values that yield erroneously high apparent resistivities. The effects of magnetite occur at all frequencies, but are most evident at the lowest frequency. Conversely, the negative effects of dielectric permittivity are most evident at the higher frequencies, in resistive areas.

The table below shows the effects of varying permittivity over a resistive (10,000 ohm-m) half space, at frequencies of 56,000 Hz (DIGHEM^V) and 102,000 Hz (RESOLVE).

Apparent Resistivity Calculations Effects of Permittivity on In-phase/Quadrature/Resistivity

| Freq (Hz) | Coil | Sep (m) | Thres (ppm) | Alt (m) | In Phase | Quad Phase | App Res | App Depth (m) | Permittivity |
|-----------|------|---------|-------------|---------|----------|------------|---------|---------------|--------------|
| 56,000 | CP | 6.3 | 0.1 | 30 | 7.3 | 35.3 | 10118 | -1.0 | 1 Air |
| 56,000 | CP | 6.3 | 0.1 | 30 | 3.6 | 36.6 | 19838 | -13.2 | 5 Quartz |
| 56,000 | CP | 6.3 | 0.1 | 30 | -1.1 | 38.3 | 81832 | -25.7 | 10 Epidote |
| 56,000 | CP | 6.3 | 0.1 | 30 | -10.4 | 42.3 | 76620 | -25.8 | 20 Granite |
| 56,000 | CP | 6.3 | 0.1 | 30 | -19.7 | 46.9 | 71550 | -26.0 | 30 Diabase |

- Appendix C.12 -

| | | | | | | | | | |
|---------|----|------|-----|----|--------|-------|-------|-------|------------|
| 56,000 | CP | 6.3 | 0.1 | 30 | -28.7 | 52.0 | 66787 | -26.1 | 40 Gabbro |
| 102,000 | CP | 7.86 | 0.1 | 30 | 32.5 | 117.2 | 9409 | -0.3 | 1 Air |
| 102,000 | CP | 7.86 | 0.1 | 30 | 11.7 | 127.2 | 25956 | -16.8 | 5 Quartz |
| 102,000 | CP | 7.86 | 0.1 | 30 | -14.0 | 141.6 | 97064 | -26.5 | 10 Epidote |
| 102,000 | CP | 7.86 | 0.1 | 30 | -62.9 | 176.0 | 83995 | -26.8 | 20 Granite |
| 102,000 | CP | 7.86 | 0.1 | 30 | -107.5 | 215.8 | 73320 | -27.0 | 30 Diabase |
| 102,000 | CP | 7.86 | 0.1 | 30 | -147.1 | 259.2 | 64875 | -27.2 | 40 Gabbro |

Methods have been developed (Huang and Fraser, 2000, 2001) to correct apparent resistivities for the effects of permittivity and permeability. The corrected resistivities yield more credible values than if the effects of permittivity and permeability are disregarded.

Recognition of Culture

Cultural responses include all EM anomalies caused by man-made metallic objects. Such anomalies may be caused by inductive coupling or current gathering. The concern of the interpreter is to recognize when an EM response is due to culture. Points of consideration used by the interpreter, when coaxial and coplanar coil-pairs are operated at a common frequency, are as follows:

1. Channels CXPL and CPPL monitor 60 Hz radiation. An anomaly on these channels shows that the conductor is radiating power. Such an indication is normally a guarantee that the conductor is cultural. However, care must be taken to ensure that the conductor is not a geologic body that strikes across a power line, carrying leakage currents.
2. A flight that crosses a "line" (e.g., fence, telephone line, etc.) yields a centre-peaked coaxial anomaly and an m-shaped coplanar anomaly.⁸ When the flight crosses the cultural line at a high angle of intersection, the amplitude ratio of coaxial/coplanar response is 2. Such an EM anomaly can only be caused by a line. The geologic body that yields anomalies most closely resembling a line is the vertically dipping thin dike. Such a body, however, yields an amplitude ratio of 1 rather than 2. Consequently, an m-shaped coplanar anomaly with a CXI/CPI amplitude ratio of 2 is virtually a guarantee that the source is a cultural line.
3. A flight that crosses a sphere or horizontal disk yields centre-peaked coaxial and coplanar anomalies with a CXI/CPI amplitude ratio (i.e., coaxial/coplanar) of 1/8. In the absence of geologic bodies of this geometry, the most likely conductor is a

⁸ See Figure C-1 presented earlier.

- Appendix C.13 -

metal roof or small fenced yard.⁹ Anomalies of this type are virtually certain to be cultural if they occur in an area of culture.

4. A flight that crosses a horizontal rectangular body or wide ribbon yields an m-shaped coaxial anomaly and a centre-peaked coplanar anomaly. In the absence of geologic bodies of this geometry, the most likely conductor is a large fenced area.⁵ Anomalies of this type are virtually certain to be cultural if they occur in an area of culture.
5. EM anomalies that coincide with culture, as seen on the camera film or video display, are usually caused by culture. However, care is taken with such coincidences because a geologic conductor could occur beneath a fence, for example. In this example, the fence would be expected to yield an m-shaped coplanar anomaly as in case #2 above. If, instead, a centre-peaked coplanar anomaly occurred, there would be concern that a thick geologic conductor coincided with the cultural line.
6. The above description of anomaly shapes is valid when the culture is not conductively coupled to the environment. In this case, the anomalies arise from inductive coupling to the EM transmitter. However, when the environment is quite conductive (e.g., less than 100 ohm-m at 900 Hz), the cultural conductor may be conductively coupled to the environment. In this latter case, the anomaly shapes tend to be governed by current gathering. Current gathering can completely distort the anomaly shapes, thereby complicating the identification of cultural anomalies. In such circumstances, the interpreter can only rely on the radiation channels and on the camera film or video records.

Magnetic Responses

The measured total magnetic field provides information on the magnetic properties of the earth materials in the survey area. The information can be used to locate magnetic bodies of direct interest for exploration, and for structural and lithological mapping.

The total magnetic field response reflects the abundance of magnetic material in the source. Magnetite is the most common magnetic mineral. Other minerals such as ilmenite, pyrrhotite, franklinite, chromite, hematite, arsenopyrite, limonite and pyrite are also magnetic, but to a lesser extent than magnetite on average.

⁹ It is a characteristic of EM that geometrically similar anomalies are obtained from: (1) a planar conductor, and (2) a wire which forms a loop having dimensions identical to the perimeter of the equivalent planar conductor.

- Appendix C.14 -

In some geological environments, an EM anomaly with magnetic correlation has a greater likelihood of being produced by sulphides than one which is non-magnetic. However, sulphide ore bodies may be non-magnetic (e.g., the Kidd Creek deposit near Timmins, Canada) as well as magnetic (e.g., the Mattabi deposit near Sturgeon Lake, Canada).

Iron ore deposits will be anomalously magnetic in comparison to surrounding rock due to the concentration of iron minerals such as magnetite, ilmenite and hematite.

Changes in magnetic susceptibility often allow rock units to be differentiated based on the total field magnetic response. Geophysical classifications may differ from geological classifications if various magnetite levels exist within one general geological classification. Geometric considerations of the source such as shape, dip and depth, inclination of the earth's field and remanent magnetization will complicate such an analysis.

In general, mafic lithologies contain more magnetite and are therefore more magnetic than many sediments which tend to be weakly magnetic. Metamorphism and alteration can also increase or decrease the magnetization of a rock unit.

Textural differences on a total field magnetic contour, colour or shadow map due to the frequency of activity of the magnetic parameter resulting from inhomogeneities in the distribution of magnetite within the rock, may define certain lithologies. For example, near surface volcanics may display highly complex contour patterns with little line-to-line correlation.

Rock units may be differentiated based on the plan shapes of their total field magnetic responses. Mafic intrusive plugs can appear as isolated "bulls-eye" anomalies. Granitic intrusives appear as sub-circular zones, and may have contrasting rings due to contact metamorphism. Generally, granitic terrain will lack a pronounced strike direction, although granite gneiss may display strike.

Linear north-south units are theoretically not well-defined on total field magnetic maps in equatorial regions due to the low inclination of the earth's magnetic field. However, most stratigraphic units will have variations in composition along strike that will cause the units to appear as a series of alternating magnetic highs and lows.

Faults and shear zones may be characterized by alteration that causes destruction of magnetite (e.g., weathering) that produces a contrast with surrounding rock. Structural breaks may be filled by magnetite-rich, fracture filling material as is the case with diabase dikes, or by non-magnetic felsic material.

Faulting can also be identified by patterns in the magnetic total field contours or colours. Faults and dikes tend to appear as lineaments and often have strike lengths of several kilometres. Offsets in narrow, magnetic, stratigraphic trends also delineate structure. Sharp contrasts in magnetic lithologies may arise due to large displacements along strike-slip or dip-slip faults.

APPENDIX D

DATA ARCHIVE DESCRIPTION

APPENDIX D

ARCHIVE DESCRIPTION

Reference # : CCD02486
Number of CD's: 1
Archive Date : 2006-DEC-13

This archive contains final data archives and grids of an airborne geophysical survey conducted by FUGRO AIRBORNE SURVEYS CORP. on behalf of Wildrose Resources Ltd. / Skygold Ventures Ltd. during October, 2006 in the Likely area of British Columbia.

Job # 06075

***** Disc 1 of 1 *****

This archive comprises 23 files contained in 4 directories

\GRIDS

Grids in Geosoft float format.

| | |
|-------------------------------|--|
| SpanishMountain_A_dem.grd | - Digital Elevation Model (m) |
| SpanishMountain_A_cvg.grd | - Calculated Vertical Magnetic Gradient (nT/m) |
| SpanishMountain_A_tfmag.grd | - Total Magnetic Field (nT) |
| SpanishMountain_A_res900.grd | - apparent resistivity 900 Hz (ohm·m) |
| SpanishMountain_A_res7200.grd | - apparent resistivity 7200 Hz (ohm·m) |
| SpanishMountain_A_res56k.grd | - apparent resistivity 56K Hz (ohm·m) |
| SpanishMountain_B_dem.grd | - Digital Elevation Model (m) |
| SpanishMountain_B_cvg.grd | - Calculated Vertical Magnetic Gradient (nT/m) |
| SpanishMountain_B_tfmag.grd | - Total Magnetic Field (nT) |
| SpanishMountain_B_res900.grd | - apparent resistivity 900 Hz (ohm·m) |
| SpanishMountain_B_res7200.grd | - apparent resistivity 7200 Hz (ohm·m) |
| SpanishMountain_B_res56k.grd | - apparent resistivity 56K Hz (ohm·m) |

\LINEDATA database in Geosoft ASCII .xyz format

| | |
|-------------------------|--|
| SpanishMountain.txt | - Documentation for data archive file |
| SpanishMountain_A.xyz | - data archive in Geosoft ASCII format |
| SpanishMountain_B.xyz | - data archive in Geosoft ASCII format |
| anSpanishMountain_A.xyz | - anomaly data archive in ASCII format |
| anSpanishMountain_B.xyz | - anomaly data archive in ASCII format |

\PDF map files in Adobe Acrobat 4.0 format

- Appendix D.2 -

| | |
|-----------------------------|--|
| SpanishMountain_em.grd | - Interpreted EM Anomalies |
| SpanishMountain_cvg.grd | - Calculated Vertical Magnetic Gradient (nT/m) |
| SpanishMountain_mag.grd | - Total Magnetic Field (nT) |
| SpanishMountain_res7200.grd | - apparent resistivity 7200 Hz (ohm·m) |
| SpanishMountain_res56k.grd | - apparent resistivity 56K Hz (ohm·m) |

\REPORT report in Adobe Acrobat 4.0 format

r06075DEC.pdf - final report

The coordinate system for all grids and the data archive is projected as follows

| | |
|----------------------------------|-------------|
| Datum | NAD83 |
| Spheroid | GRS80 |
| Projection | UTM Zone 10 |
| Central meridian | 123 West |
| False easting | 500000 |
| False northing | 0 |
| Scale factor | 0.9996 |
| Northern parallel | N/A |
| Base parallel | N/A |
| WGS84 to local conversion method | Molodensky |
| Delta X shift | +0 |
| Delta Y shift | -0 |
| Delta Z shift | -0 |

If you have any problems with this archive please contact

Processing Manager
FUGRO AIRBORNE SURVEYS CORP.
2270 Argentia Road, Unit 2
Mississauga, Ontario
Canada L5N 6A6
Tel (905) 812-0212
Fax (905) 812-1504
E-mail toronto@fugroairborne.com

- Appendix D.3 -

Geosoft ARCHIVE SUMMARY

JOB TITLE:

JOB # :06075
TYPE OF SURVEY :FUGRO DIGHEM EM, MAGNETICS
AREA :Spanish Mountain Project - Blocks A/B, British Columbia
CLIENT :Wildrose Resources Ltd. / Skygold Ventures Ltd.

SURVEY DATA FORMAT: 33 CHANNELS

| # | CHANNAME | TIME | UNITS | DESCRIPTION |
|----|-------------|------|---------|--|
| 1 | x | 0.1 | m | Easting UTME-NAD83 (ZONE-10) |
| 2 | y | 0.1 | m | Northing UTMN-NAD83 (ZONE-10) |
| 3 | fid | 0.1 | | Fiducial Increment |
| 4 | latitude | 0.1 | degrees | Latitude NAD83 |
| 5 | longitude | 0.1 | degrees | Longitude NAD83 |
| 6 | flight | 0.1 | | Flight Number |
| 7 | altbird | 0.1 | m | Bird Height |
| 8 | z_heli | 0.1 | m | Helicopter Height Above Mean Sea Level |
| 9 | dem | 0.1 | m | Digital Elevation Model |
| 10 | diurnal_cor | 0.1 | nt | Diurnal Correction |
| 11 | mag | 0.1 | nt | Total Magnetic Field |
| 12 | CPI900 | 0.1 | ppm | Inphase-Coplanar 881 HZ |
| 13 | CPQ900 | 0.1 | ppm | Quadrature- Coplanar 881 HZ |
| 14 | CXI1000 | 0.1 | ppm | Inphase-Coaxial 1113 HZ |
| 15 | CXQ1000 | 0.1 | ppm | Quadrature- Coaxial 1113 HZ |
| 16 | CXI5500 | 0.1 | ppm | Inphase -Coaxial 5871 HZ |
| 17 | CXQ5500 | 0.1 | ppm | Quadrature -Coaxial 5871 HZ |
| 18 | CPI7200 | 0.1 | ppm | Inphase -Coplanar 7031 HZ |
| 19 | CPQ7200 | 0.1 | ppm | Quadrature -Coplanar 7031 HZ |
| 20 | CPI56K | 0.1 | ppm | Inphase-Coplanar 55,540 HZ |
| 21 | CPQ56K | 0.1 | ppm | Quadrature-Coplanar 55,540 HZ |
| 22 | RES900 | 0.1 | ohm-m | Resistivity - 900 Hz |
| 23 | DEP900 | 0.1 | m | Depth - 900 Hz |
| 24 | RES7200 | 0.1 | ohm-m | Resistivity - 7200 Hz |
| 25 | DEP7200 | 0.1 | m | Depth - 7200 Hz |
| 26 | RES56K | 0.1 | ohm-m | Resistivity - 56,000 Hz |
| 27 | DEP56K | 0.1 | m | Depth - 56,000 Hz |
| 28 | DIFI | 0.1 | | Diff. Based On 5500/7200 Inphase |
| 29 | DIFQ | 0.1 | | Diff. Based On 5500/7200 Quadrature |
| 30 | CPPL | 0.1 | | Coplanar Powerline Monitor |
| 31 | CPSP | 0.1 | | Coplanar Spherics Monitor |
| 32 | CXPL | 0.1 | | Coaxial Powerline Monitor |
| 33 | CXSP | 0.1 | | Coaxial Spheric Monitor |

ISSUE DATE :December 12, 2006
FOR WHOM :Wildrose Resources Ltd. / Skygold Ventures Ltd.

- Appendix D.4 -

BY WHOM :FUGRO AIRBORNE SURVEYS
2270 ARGENTIA ROAD, UNIT 2
MISSISSAUGA, ONTARIO,
CANADA L5N 6A6
TEL. (905) 812-0212
FAX (905) 812-1504

APPENDIX E

EM ANOMALY LIST

EM Anomaly List

| LINE | Fid | Interp | XUTM m | YUTM m | CX 5500 HZ Real Quad ppm ppm | CP 7200 HZ Real Quad ppm ppm | CP 900 HZ Real Quad ppm ppm | Vertical Dike COND DEPTH* siemens m | Mag. Corr NT |
|------------|--------|--------|-----------|-----------|------------------------------------|------------------------------------|-----------------------------------|---|-----------------|
| LINE 10150 | | | FLIGHT 1 | | | | | | |
| D | 4175.2 | B | 602133 | 5828808 | 8.7 2.1 | 35.1 0.4 | 22.8 18.6 | 6.9 56 | 0 |
| E | 4197.1 | B | 602726 | 5829376 | 50.6 7.0 | 388.1 63.2 | 341.4 122.6 | 28.3 15 | 0 |
| F | 4216.4 | H | 603234 | 5829852 | 17.7 3.0 | 130.9 23.0 | 108.2 40.9 | 15.2 34 | 0 |
| G | 4226.4 | B | 603448 | 5830070 | 15.0 4.9 | 124.7 8.9 | 67.9 47.8 | 5.2 30 | 0 |
| H | 4257.5 | H | 603867 | 5830461 | 3.9 2.9 | 33.8 1.7 | 24.9 1.1 | --- --- | 1 |
| LINE 10160 | | | FLIGHT 1 | | | | | | |
| D | 4440.5 | B | 602693 | 5829139 | 96.9 25.7 | 413.0 197.1 | 381.8 99.5 | 13.4 0 | 0 |
| E | 4409.2 | B | 603176 | 5829609 | 18.7 8.4 | 220.6 44.1 | 149.7 74.0 | 3.7 24 | 0 |
| F | 4399.1 | B | 603354 | 5829761 | 41.9 4.9 | 306.0 29.2 | 260.9 85.1 | 34.5 17 | 0 |
| G | 4384.4 | B | 603592 | 5830003 | 19.9 4.4 | 108.0 32.2 | 71.9 49.5 | 10.2 31 | 1 |
| H | 4375.1 | B | 603715 | 5830129 | 16.6 9.5 | 95.4 39.4 | 33.3 39.7 | 2.6 28 | 1 |
| I | 4361.4 | D | 603927 | 5830308 | 21.5 6.4 | 140.4 13.1 | 139.0 33.0 | 6.9 29 | 0 |
| LINE 10171 | | | FLIGHT 3 | | | | | | |
| B | 6072.1 | B | 602568 | 5828807 | 55.4 18.1 | 221.4 52.0 | 139.9 89.0 | 8.2 9 | 0 |
| C | 6079.1 | D | 602766 | 5828993 | 100.0 23.7 | 744.7 211.7 | 561.3 239.7 | 15.9 4 | 0 |
| D | 6081.9 | B | 602840 | 5829064 | 121.4 23.4 | 744.7 142.7 | 561.3 239.7 | 23.1 0 | 0 |
| E | 6102.5 | B | 603316 | 5829524 | 73.2 8.6 | 541.0 51.0 | 412.6 174.5 | 41.2 9 | 0 |
| F | 6108.1 | B | 603450 | 5829648 | 22.4 0.0 | 187.6 0.3 | 215.6 47.4 | --- --- | 0 |
| G | 6122.9 | D | 603697 | 5829898 | 38.5 14.0 | 200.2 73.8 | 81.3 87.0 | 6.3 26 | 0 |
| H | 6132.5 | H | 603824 | 5830009 | 13.7 5.1 | 135.3 44.0 | 67.2 62.1 | 4.3 46 | 0 |
| I | 6146.2 | B | 604023 | 5830205 | 20.8 7.8 | 163.5 47.8 | 99.2 75.4 | 4.9 36 | 1 |
| LINE 10180 | | | FLIGHT 4 | | | | | | |
| D | 4073.0 | E | 602569 | 5828610 | 48.1 13.2 | 310.4 100.6 | 226.6 131.4 | 10.2 24 | 1 |
| E | 4070.0 | D | 602633 | 5828672 | 41.1 0.0 | 309.3 0.0 | 310.3 131.4 | --- --- | 1 |
| F | 4065.8 | D | 602721 | 5828755 | 64.5 17.1 | 389.4 17.9 | 294.8 128.2 | 11.7 21 | 3 |
| G | 4062.3 | B | 602793 | 5828820 | 81.3 22.9 | 510.9 240.2 | 261.1 215.6 | 11.5 12 | 0 |
| H | 4059.9 | D | 602843 | 5828865 | 42.7 48.1 | 510.9 240.2 | 261.1 215.6 | 1.6 5 | 3 |
| I | 4057.7 | B | 602889 | 5828907 | 86.8 48.1 | 646.3 240.2 | 303.6 251.0 | 4.7 0 | 3 |
| J | 4050.3 | H | 603031 | 5829037 | 20.6 6.2 | 78.1 4.7 | 82.2 19.5 | 6.6 19 | 0 |
| K | 4033.5 | B | 603331 | 5829338 | 43.3 13.7 | 514.6 101.9 | 449.1 159.5 | 7.9 17 | 0 |
| L | 4027.8 | D | 603431 | 5829431 | 16.8 4.6 | 188.8 20.0 | 157.2 69.9 | 7.0 30 | 0 |
| M | 4024.6 | B | 603486 | 5829482 | 31.1 1.7 | 235.3 20.0 | 181.2 69.9 | 92.3 36 | 0 |
| N | 4006.8 | H | 603844 | 5829815 | 11.7 1.6 | 80.0 10.2 | 53.4 29.4 | 18.3 46 | 0 |
| O | 4001.5 | H | 603941 | 5829914 | 20.0 4.5 | 108.1 11.6 | 83.1 36.3 | 10.0 32 | 0 |

CX = COAXIAL
CP = COPLANAR

Note: EM values shown above
are local amplitudes

Spanish Mountain Block A

*Estimated Depth may be unreliable because the
stronger part of the conductor may be deeper or
to one side of the flight line, or because of a
shallow dip or magnetite/overburden effects

EM Anomaly List

| | Label | Fid | Interp | XUTM | YUTM | CX | 5500 HZ | CP | 7200 HZ | CP | 900 HZ | Vertical Dike | | Mag. Corr |
|------|--------|-----|--------|----------|---------|-------|---------|--------|---------|--------|--------|---------------|--------|-----------|
| | | | | m | m | Real | Quad | Real | Quad | Real | Quad | COND | DEPTH* | |
| | | | | | | ppm | ppm | ppm | ppm | ppm | ppm | siemens | m | NT |
| LINE | 10180 | | | FLIGHT 4 | | | | | | | | | | |
| P | 3987.1 | | D | 604194 | 5830164 | 15.8 | 1.7 | 60.2 | 10.7 | 18.0 | 29.8 | --- | --- | 0 |
| Q | 3976.6 | | H | 604365 | 5830324 | 6.6 | 5.3 | 23.4 | 23.4 | 21.9 | 10.9 | 1.3 | 47 | 0 |
| LINE | 10190 | | | FLIGHT 4 | | | | | | | | | | |
| F | 4498.6 | | S? | 602622 | 5828444 | 2.0 | 24.2 | 13.2 | 137.6 | 8.8 | 17.2 | 0.1 | 0 | 0 |
| G | 4514.2 | | B | 602959 | 5828770 | 184.1 | 33.1 | 1097.3 | 209.1 | 791.9 | 378.1 | 29.5 | 1 | 0 |
| H | 4517.4 | | B | 603036 | 5828839 | 76.4 | 33.0 | 1097.3 | 209.1 | 791.9 | 378.1 | 6.2 | 0 | 27 |
| I | 4524.5 | | H | 603202 | 5828993 | 37.1 | 0.1 | 352.6 | 43.9 | 295.5 | 42.8 | 999.0 | 22 | 0 |
| J | 4533.5 | | D | 603412 | 5829194 | 89.9 | 3.0 | 577.6 | 95.8 | 396.8 | 128.2 | --- | --- | 0 |
| K | 4537.1 | | B | 603496 | 5829279 | 67.6 | 15.4 | 577.6 | 102.5 | 425.3 | 198.1 | 14.8 | 6 | 0 |
| L | 4550.2 | | B | 603794 | 5829562 | 81.9 | 29.6 | 415.2 | 131.6 | 230.9 | 185.0 | 8.1 | 12 | 0 |
| M | 4567.9 | | H | 604099 | 5829867 | 5.0 | 6.0 | 73.0 | 35.9 | 70.5 | 31.1 | 0.7 | 42 | 3 |
| N | 4577.7 | | B? | 604261 | 5830018 | 11.4 | 8.7 | 27.5 | 22.0 | 1.0 | 8.6 | --- | --- | 0 |
| O | 4588.8 | | H | 604437 | 5830184 | 11.1 | 3.7 | 62.6 | 8.6 | 81.2 | 24.0 | 4.6 | 45 | 0 |
| LINE | 10200 | | | FLIGHT 8 | | | | | | | | | | |
| D | 593.4 | | E | 602797 | 5828410 | 37.3 | 1.3 | 107.1 | 54.2 | 186.0 | 47.3 | --- | --- | 2 |
| E | 586.4 | | D | 602933 | 5828539 | 183.5 | 79.0 | 213.4 | 227.3 | 708.9 | 373.3 | 8.4 | 0 | 1 |
| F | 584.2 | | B | 602972 | 5828577 | 62.9 | 79.0 | 213.4 | 227.3 | 708.9 | 373.3 | 1.6 | 1 | 1 |
| G | 581.3 | | D | 603023 | 5828625 | 22.2 | 4.5 | 213.4 | 76.9 | 708.9 | 373.3 | 12.2 | 33 | 0 |
| H | 574.3 | | B | 603139 | 5828725 | 276.2 | 36.1 | 1722.2 | 281.2 | 1405.0 | 547.9 | 54.2 | 0 | 0 |
| I | 572.8 | | B | 603162 | 5828747 | 307.0 | 36.1 | 1722.2 | 281.2 | 1405.0 | 547.9 | 65.8 | 0 | 8 |
| J | 545.7 | | B | 603567 | 5829126 | 171.0 | 58.1 | 849.0 | 251.3 | 525.9 | 331.3 | 11.4 | 2 | 0 |
| K | 538.7 | | B | 603683 | 5829235 | 9.8 | 0.2 | 317.1 | 17.6 | 309.0 | 77.5 | 289.4 | 60 | 0 |
| L | 534.2 | | E | 603756 | 5829308 | 34.3 | 17.5 | 320.4 | 47.4 | 309.0 | 89.9 | 3.8 | 23 | 0 |
| M | 514.6 | | B? | 604083 | 5829632 | 21.9 | 3.9 | 26.3 | 0.0 | 0.0 | 0.0 | --- | --- | 2 |
| N | 509.7 | | B | 604155 | 5829703 | 13.7 | 4.1 | 133.5 | 28.7 | 113.2 | 40.0 | 6.0 | 35 | 0 |
| O | 502.8 | | B | 604246 | 5829799 | 26.1 | 6.7 | 149.8 | 24.1 | 131.3 | 56.7 | 9.0 | 23 | 2 |
| P | 488.2 | | B | 604421 | 5829974 | 50.3 | 22.7 | 108.8 | 59.0 | 28.2 | 79.4 | 5.1 | 16 | 0 |
| Q | 481.4 | | B | 604497 | 5830050 | 8.4 | 7.2 | 182.3 | 43.3 | 125.0 | 81.2 | 1.3 | 32 | 0 |
| R | 476.3 | | D | 604554 | 5830110 | 35.3 | 11.7 | 59.0 | 18.3 | 47.4 | 10.7 | 7.0 | 18 | 0 |
| S | 465.7 | | D | 604682 | 5830223 | 24.1 | 11.2 | 96.1 | 19.6 | 68.3 | 26.8 | 3.9 | 23 | 1 |
| LINE | 10210 | | | FLIGHT 8 | | | | | | | | | | |
| D | 1013.5 | | B | 603092 | 5828480 | 154.8 | 39.5 | 1105.2 | 260.5 | 764.2 | 384.0 | 16.5 | 4 | 0 |
| E | 1016.0 | | B | 603143 | 5828530 | 98.6 | 34.4 | 1105.2 | 264.6 | 764.2 | 384.0 | 9.1 | 7 | 0 |
| F | 1019.9 | | B | 603222 | 5828604 | 149.5 | 10.7 | 677.4 | 171.3 | 882.8 | 95.2 | 109.0 | 4 | 167 |
| G | 1033.6 | | B? | 603474 | 5828856 | 11.1 | 1.8 | 21.3 | 0.2 | 68.4 | 42.7 | 13.0 | 36 | 0 |

CX = COAXIAL
CP = COPLANAR

Note: EM values shown above
are local amplitudes

*Estimated Depth may be unreliable because the
stronger part of the conductor may be deeper or
to one side of the flight line, or because of a

Spanish Mountain Block A

- 2 - shallow dip or magnetite/overburden effects

EM Anomaly List

| Label | Fid | Interp | XUTM m | YUTM m | CX 5500 HZ Real Quad ppm ppm | CP 7200 HZ Real Quad ppm ppm | CP 900 HZ Real Quad ppm ppm | Vertical Dike COND DEPTH* siemens m | Mag. Corr NT |
|------------|--------|--------|-----------|-----------|------------------------------------|------------------------------------|-----------------------------------|---|-----------------|
| LINE 10210 | | | FLIGHT 8 | | | | | | |
| H | 1043.9 | B | 603696 | 5829067 | 182.6 44.7 | 803.2 123.2 | 615.2 275.5 | 18.6 0 | 0 |
| I | 1051.7 | B | 603891 | 5829255 | 64.6 7.9 | 390.2 40.2 | 278.8 174.9 | 36.7 15 | 0 |
| J | 1073.7 | B | 604284 | 5829621 | 80.5 17.0 | 455.5 101.6 | 336.6 165.6 | 17.6 4 | 3 |
| K | 1080.4 | D | 604394 | 5829727 | 55.7 9.6 | 279.5 47.8 | 174.6 104.1 | 21.0 6 | 0 |
| L | 1085.0 | D | 604463 | 5829795 | 18.5 6.6 | 78.7 1.6 | 56.8 26.4 | 5.1 37 | 0 |
| M | 1097.8 | H | 604687 | 5830006 | 5.9 2.4 | 210.9 50.5 | 159.1 75.1 | 2.9 62 | 0 |
| LINE 10220 | | | FLIGHT 8 | | | | | | |
| D | 1267.9 | D | 602999 | 5828181 | 30.6 1.9 | 85.1 29.5 | 89.4 34.4 | 82.0 20 | 0 |
| E | 1255.0 | B | 603259 | 5828436 | 63.4 6.1 | 395.7 60.0 | 332.7 111.8 | 52.8 15 | 0 |
| F | 1252.0 | D | 603314 | 5828487 | 29.4 0.0 | 395.7 0.2 | 332.7 111.8 | --- --- | 53 |
| G | 1245.2 | B | 603426 | 5828597 | 210.5 37.8 | 1453.4 185.2 | 1242.5 449.9 | 30.8 0 | 1 |
| H | 1237.1 | B | 603560 | 5828723 | 100.0 19.4 | 833.8 208.7 | 479.4 286.9 | 21.4 4 | 0 |
| I | 1233.6 | E | 603619 | 5828777 | 86.4 52.5 | 521.4 208.7 | 56.5 247.5 | 4.2 0 | 0 |
| J | 1226.7 | D | 603739 | 5828888 | 50.8 1.9 | 271.5 10.3 | 297.6 89.2 | 195.8 11 | 0 |
| K | 1219.7 | B | 603876 | 5829014 | 61.9 22.6 | 529.8 106.1 | 419.8 180.9 | 7.3 11 | 0 |
| L | 1211.7 | B | 604046 | 5829180 | 37.7 19.6 | 172.3 72.3 | 101.3 71.8 | 3.9 21 | 0 |
| M | 1203.7 | B | 604218 | 5829346 | 19.2 5.8 | 19.7 7.4 | 65.2 9.2 | 6.5 30 | 1 |
| N | 1197.7 | B | 604337 | 5829462 | 43.1 7.7 | 114.9 31.4 | 117.9 48.9 | 18.3 20 | 0 |
| O | 1189.6 | D | 604487 | 5829605 | 26.1 8.0 | 95.0 46.6 | 22.4 61.2 | 7.1 24 | 2 |
| P | 1184.4 | B? | 604572 | 5829681 | 5.2 1.7 | 2.7 5.8 | 31.2 1.9 | --- --- | 0 |
| Q | 1179.8 | D | 604639 | 5829747 | 35.0 15.2 | 130.6 79.7 | 39.0 66.8 | 4.8 20 | 0 |
| R | 1171.1 | B | 604752 | 5829865 | 43.9 20.5 | 101.8 85.1 | 76.6 56.9 | 4.7 20 | 0 |
| S | 1162.4 | D | 604852 | 5829953 | 23.8 7.9 | 168.3 45.6 | 113.4 58.1 | 6.1 28 | 1 |
| LINE 10230 | | | FLIGHT 8 | | | | | | |
| C | 1886.4 | D | 603109 | 5828056 | 112.9 29.1 | 1003.6 111.5 | 353.2 380.2 | 14.7 4 | 0 |
| D | 1890.0 | B | 603199 | 5828145 | 141.3 39.0 | 1007.3 257.9 | 708.8 380.2 | 14.3 2 | 0 |
| E | 1898.4 | B | 603394 | 5828354 | 7.5 2.3 | 60.8 1.4 | 80.2 43.5 | 4.6 60 | 0 |
| F | 1902.6 | B | 603489 | 5828445 | 56.5 34.0 | 448.8 115.4 | 228.7 170.6 | 3.6 4 | 0 |
| G | 1906.5 | D | 603573 | 5828523 | 76.0 19.1 | 441.4 123.8 | 240.6 170.6 | 13.4 1 | 0 |
| H | 1920.7 | D | 603848 | 5828805 | 62.8 23.5 | 257.2 95.2 | 14.9 94.3 | 7.1 1 | 0 |
| I | 1926.8 | B | 603991 | 5828933 | 39.2 21.7 | 416.0 15.3 | 336.0 122.4 | 3.6 20 | 0 |
| J | 1928.5 | D | 604031 | 5828969 | 39.2 21.7 | 416.0 15.3 | 336.0 122.4 | 3.6 17 | 4 |
| K | 1934.7 | B | 604166 | 5829092 | 79.4 19.4 | 308.8 124.4 | 152.2 141.9 | 14.1 12 | 0 |
| L | 1948.3 | B | 604405 | 5829318 | 12.8 12.0 | 79.5 57.7 | 53.1 59.9 | 1.3 29 | 0 |
| M | 1958.9 | B | 604578 | 5829483 | 13.0 0.8 | 68.9 60.6 | 34.3 37.7 | 62.9 50 | 1 |
| N | 1966.9 | B | 604707 | 5829611 | 0.0 0.0 | 13.7 0.0 | 52.1 0.0 | 179.2 421 | 1 |

CX = COAXIAL
CP = COPLANAR

Note:EM values shown above
are local amplitudes

*Estimated Depth may be unreliable because the
stronger part of the conductor may be deeper or
to one side of the flight line, or because of a

Spanish Mountain Block A

- 3 - shallow dip or magnetite/overburden effects

EM Anomaly List

| | | | | | CX | 5500 HZ | CP | 7200 HZ | CP | 900 HZ | | Vertical Dike | | Mag. Corr | |
|-------|--------|--------|----------|---------|-------|---------|-------|---------|-------|--------|--|---------------|--------|-----------|--|
| Label | Fid | Interp | XUTM | YUTM | Real | Quad | Real | Quad | Real | Quad | | COND | DEPTH* | | |
| | | | m | m | ppm | ppm | ppm | ppm | ppm | ppm | | siemens | m | NT | |
| LINE | 10230 | | FLIGHT 8 | | | | | | | | | | | | |
| O | 1975.3 | B | 604852 | 5829749 | 21.5 | 5.9 | 54.4 | 79.7 | 0.0 | 25.4 | | 7.8 | 35 | 0 | |
| P | 1979.5 | H | 604924 | 5829817 | 4.1 | 6.3 | 95.9 | 36.8 | 89.5 | 38.0 | | 0.5 | 40 | 1 | |
| LINE | 10240 | | FLIGHT 8 | | | | | | | | | | | | |
| A | 2183.6 | D | 601940 | 5826747 | 20.3 | 33.3 | 103.3 | 230.8 | 9.1 | 41.7 | | 0.8 | 7 | 0 | |
| B | 2131.2 | B | 603167 | 5827938 | 136.6 | 21.6 | 631.6 | 129.1 | 452.5 | 233.9 | | 32.3 | 0 | 0 | |
| C | 2129.8 | D | 603200 | 5827968 | 68.7 | 21.6 | 631.6 | 129.1 | 452.5 | 233.9 | | 9.4 | 11 | 0 | |
| D | 2124.6 | B | 603323 | 5828080 | 47.0 | 6.7 | 487.8 | 64.3 | 485.4 | 100.2 | | 26.4 | 10 | 0 | |
| E | 2102.9 | B | 603719 | 5828457 | 91.0 | 22.2 | 525.0 | 81.6 | 365.6 | 229.0 | | 14.8 | 0 | 0 | |
| F | 2089.0 | D | 603955 | 5828708 | 29.4 | 3.1 | 50.9 | 23.5 | 26.1 | 31.8 | | 36.4 | 10 | 0 | |
| G | 2079.6 | B | 604145 | 5828872 | 55.3 | 8.9 | 287.3 | 23.6 | 286.0 | 65.0 | | 23.3 | 20 | 0 | |
| H | 2070.9 | B | 604349 | 5829058 | 41.4 | 10.2 | 142.7 | 38.5 | 158.2 | 42.0 | | 11.2 | 22 | 0 | |
| I | 2067.2 | D | 604431 | 5829135 | 11.6 | 6.3 | 142.7 | 0.0 | 158.2 | 44.6 | | 2.5 | 40 | 0 | |
| J | 2055.3 | B | 604678 | 5829365 | 28.4 | 5.7 | 125.9 | 25.2 | 83.6 | 54.6 | | 13.2 | 26 | 1 | |
| K | 2044.3 | B | 604868 | 5829550 | 13.6 | 1.2 | 51.9 | 23.4 | 33.5 | 30.9 | | 34.5 | 47 | 4 | |
| L | 2041.4 | B | 604913 | 5829593 | 10.3 | 13.0 | 51.9 | 59.0 | 33.5 | 30.9 | | 0.9 | 19 | 0 | |
| M | 2036.2 | B | 604987 | 5829667 | 15.3 | 11.4 | 70.7 | 54.8 | 47.6 | 25.6 | | 1.8 | 31 | 0 | |
| N | 2029.6 | B | 605070 | 5829755 | 17.6 | 26.0 | 114.8 | 106.5 | 32.2 | 52.2 | | 0.9 | 13 | 1 | |
| LINE | 10250 | | FLIGHT 8 | | | | | | | | | | | | |
| B | 2423.5 | D | 603359 | 5827903 | 56.1 | 19.2 | 613.8 | 111.0 | 491.6 | 230.6 | | 7.8 | 10 | 0 | |
| C | 2425.4 | B | 603402 | 5827949 | 100.9 | 14.5 | 613.8 | 120.6 | 491.6 | 230.6 | | 33.6 | 0 | 0 | |
| D | 2434.4 | B | 603622 | 5828168 | 11.7 | 3.6 | 46.9 | 0.1 | 93.0 | 9.8 | | 5.5 | 51 | 0 | |
| E | 2443.2 | H | 603835 | 5828366 | 8.3 | 4.7 | 123.2 | 20.4 | 77.9 | 51.7 | | 2.1 | 35 | 0 | |
| F | 2447.3 | E | 603932 | 5828462 | 21.4 | 6.7 | 122.5 | 20.4 | 60.9 | 46.3 | | --- | --- | 0 | |
| G | 2459.5 | B | 604240 | 5828770 | 44.6 | 4.0 | 294.3 | 23.9 | 257.4 | 85.5 | | 51.4 | 14 | 0 | |
| H | 2470.0 | B | 604487 | 5828983 | 25.5 | 10.2 | 181.1 | 53.8 | 125.4 | 74.4 | | 4.8 | 25 | 0 | |
| I | 2481.6 | B | 604703 | 5829184 | 20.4 | 11.3 | 165.4 | 76.7 | 79.2 | 70.4 | | 2.9 | 27 | 0 | |
| J | 2510.3 | B | 605153 | 5829621 | 34.4 | 10.1 | 243.8 | 102.7 | 127.0 | 88.0 | | 8.2 | 30 | 0 | |
| LINE | 10260 | | FLIGHT 8 | | | | | | | | | | | | |
| B | 2656.3 | B | 603428 | 5827768 | 31.0 | 14.6 | 234.7 | 70.9 | 124.4 | 100.2 | | 4.1 | 13 | 0 | |
| C | 2643.8 | H | 603692 | 5828019 | 0.9 | 0.0 | 27.2 | 8.7 | 54.5 | 2.7 | | --- | --- | 1 | |
| D | 2627.7 | B | 603959 | 5828281 | 25.7 | 8.0 | 237.4 | 25.8 | 204.5 | 88.2 | | 6.8 | 33 | 0 | |
| E | 2604.7 | B | 604377 | 5828675 | 61.7 | 10.4 | 391.2 | 43.5 | 339.5 | 108.0 | | 22.4 | 14 | 0 | |
| F | 2590.9 | B | 604694 | 5828977 | 25.0 | 16.2 | 92.4 | 63.5 | 84.7 | 46.6 | | 2.5 | 24 | 0 | |
| G | 2584.2 | D | 604846 | 5829126 | 24.6 | 12.5 | 144.4 | 57.0 | 67.7 | 55.7 | | 3.5 | 18 | 4 | |
| H | 2560.8 | D | 605313 | 5829547 | 81.7 | 34.0 | 311.3 | 121.5 | 138.6 | 128.6 | | 6.7 | 9 | 3 | |

CX = COAXIAL
CP = COPLANAR

Note:EM values shown above
are local amplitudes

*Estimated Depth may be unreliable because the
stronger part of the conductor may be deeper or
to one side of the flight line, or because of a

Spanish Mountain Block A

- 4 - shallow dip or magnetite/overburden effects

EM Anomaly List

| LINE | Fid | Interp | XUTM m | YUTM m | CX 5500 HZ Real Quad ppm ppm | CP 7200 HZ Real Quad ppm ppm | CP 900 HZ Real Quad ppm ppm | Vertical Dike COND DEPTH* siemens m | Mag. Corr NT |
|------------|--------|--------|-----------|-----------|------------------------------------|------------------------------------|-----------------------------------|---|-----------------|
| LINE 10270 | | | FLIGHT 8 | | | | | | |
| B | 2883.6 | B | 602944 | 5827100 | 23.8 15.3 | 92.2 95.6 | 25.4 44.2 | 2.5 24 | 0 |
| C | 2925.9 | B | 603836 | 5827927 | 8.0 1.5 | 74.6 0.0 | 92.0 13.0 | 9.3 57 | 0 |
| D | 2936.8 | B | 604025 | 5828113 | 232.7 68.5 | 1156.2 260.9 | 851.1 376.2 | 15.4 3 | 1 |
| E | 2943.0 | B | 604129 | 5828231 | 35.9 9.4 | 311.7 108.4 | 192.1 114.5 | 9.8 16 | 0 |
| F | 2954.8 | B | 604342 | 5828441 | 3.7 5.0 | 122.7 0.0 | 156.7 35.1 | 0.6 38 | 0 |
| G | 2964.1 | B | 604524 | 5828630 | 52.6 11.6 | 493.9 63.7 | 417.6 141.5 | 14.3 0 | 1 |
| H | 2967.3 | B | 604594 | 5828701 | 25.4 2.9 | 493.9 24.2 | 417.6 141.5 | 30.1 38 | 0 |
| I | 2985.3 | B | 604930 | 5828990 | 26.7 8.0 | 258.8 43.4 | 226.6 72.0 | 7.3 23 | 2 |
| J | 2992.4 | B | 605047 | 5829103 | 28.3 18.5 | 181.0 69.4 | 134.3 60.8 | 2.6 20 | 1 |
| K | 3000.4 | D | 605154 | 5829210 | 17.1 7.0 | 192.4 56.0 | 87.9 81.5 | 4.0 39 | 0 |
| L | 3016.6 | B | 605419 | 5829443 | 36.5 10.9 | 135.6 58.7 | 18.4 57.3 | 8.2 20 | 1 |
| LINE 10280 | | | FLIGHT 8 | | | | | | |
| B | 3210.2 | H | 603194 | 5827123 | 16.5 8.4 | 140.0 90.5 | 54.0 65.4 | 3.0 33 | 4 |
| LINE 10281 | | | FLIGHT 4 | | | | | | |
| A | 4816.8 | B | 603967 | 5827882 | 54.9 30.8 | 476.7 196.5 | 354.4 159.0 | 4.0 0 | 0 |
| B | 4810.1 | B | 604086 | 5827990 | 141.9 37.5 | 714.9 161.7 | 487.4 274.9 | 15.3 0 | 1 |
| C | 4798.3 | B | 604267 | 5828148 | 166.2 46.9 | 1344.1 260.5 | 1020.6 418.2 | 14.7 4 | 0 |
| D | 4796.2 | B | 604290 | 5828175 | 270.9 72.0 | 1344.1 260.5 | 1020.6 418.2 | 18.8 1 | 0 |
| E | 4783.8 | B | 604470 | 5828344 | 69.4 16.1 | 724.8 157.6 | 568.8 341.1 | 14.5 7 | 0 |
| F | 4778.2 | B | 604568 | 5828435 | 44.8 24.1 | 204.3 107.5 | 76.3 114.5 | 3.9 15 | 0 |
| G | 4769.7 | B | 604730 | 5828598 | 83.3 13.5 | 266.5 20.1 | 261.0 70.6 | 26.3 13 | 0 |
| H | 4761.6 | B | 604907 | 5828768 | 62.5 29.0 | 256.4 112.2 | 93.5 121.7 | 5.3 15 | 0 |
| I | 4755.1 | B | 605056 | 5828912 | 25.9 7.9 | 168.8 19.3 | 192.4 15.9 | 7.0 28 | 3 |
| J | 4744.4 | B | 605281 | 5829125 | 40.1 9.6 | 377.7 62.6 | 262.6 144.3 | 11.5 25 | 3 |
| K | 4733.3 | D | 605485 | 5829322 | 26.5 19.0 | 0.0 30.3 | 0.0 0.0 | 2.3 20 | 1 |
| LINE 10290 | | | FLIGHT 8 | | | | | | |
| A | 3546.2 | B | 603295 | 5827021 | 49.4 17.7 | 268.6 107.5 | 108.0 111.9 | 7.0 14 | 0 |
| B | 3594.0 | B | 604082 | 5827744 | 74.5 28.3 | 286.4 63.0 | 234.9 84.0 | 7.4 8 | 0 |
| C | 3600.3 | D | 604172 | 5827843 | 67.8 25.9 | 353.5 91.4 | 299.9 167.8 | 7.1 4 | 0 |
| D | 3605.5 | B | 604246 | 5827933 | 87.1 5.4 | 549.6 99.5 | 341.2 258.6 | 113.4 0 | 0 |
| E | 3610.3 | B | 604326 | 5828009 | 146.4 27.6 | 783.4 107.8 | 681.8 258.6 | 25.3 0 | 0 |
| F | 3619.5 | B | 604486 | 5828142 | 40.5 6.7 | 97.7 31.5 | 115.9 21.2 | 20.1 14 | 0 |
| G | 3628.0 | B | 604646 | 5828309 | 1.7 3.0 | 72.1 19.2 | 64.9 28.0 | 0.3 44 | 0 |
| H | 3637.4 | B | 604854 | 5828511 | 150.8 36.3 | 717.7 136.4 | 545.0 236.4 | 17.8 6 | 0 |

CX = COAXIAL

CP = COPLANAR

Note: EM values shown above
are local amplitudes

Spanish Mountain Block A

*Estimated Depth may be unreliable because the
stronger part of the conductor may be deeper or
to one side of the flight line, or because of a
shallow dip or magnetite/overburden effects

EM Anomaly List

| Label | Fid | Interp | XUTM m | YUTM m | CX 5500 HZ Real Quad ppm ppm | CP 7200 HZ Real Quad ppm ppm | CP 900 HZ Real Quad ppm ppm | Vertical Dike COND DEPTH* siemens m | Mag. Corr NT |
|------------|--------|--------|-----------|-----------|------------------------------------|------------------------------------|-----------------------------------|---|-----------------|
| LINE 10290 | | | FLIGHT 8 | | | | | | |
| I | 3649.3 | B | 605096 | 5828734 | 44.2 4.5 | 173.1 39.8 | 124.2 60.3 | 43.1 20 | 0 |
| J | 3656.2 | B | 605239 | 5828865 | 41.6 17.6 | 278.4 37.6 | 257.0 70.6 | 5.2 21 | 2 |
| K | 3669.5 | B | 605485 | 5829100 | 17.8 0.4 | 227.8 21.8 | 189.4 91.0 | 283.9 47 | 0 |
| L | 3673.1 | E | 605560 | 5829171 | 39.0 4.3 | 200.6 66.0 | 179.1 72.8 | 36.8 29 | 0 |
| LINE 10300 | | | FLIGHT 8 | | | | | | |
| A | 3874.6 | B | 603282 | 5826793 | 31.1 0.1 | 212.1 28.9 | 113.1 90.7 | --- --- | 1 |
| B | 3872.0 | B | 603347 | 5826858 | 51.5 8.6 | 212.1 28.5 | 113.1 90.7 | 21.6 4 | 0 |
| C | 3827.9 | B | 604165 | 5827633 | 164.9 33.0 | 718.5 124.3 | 567.6 233.7 | 24.0 0 | 0 |
| D | 3821.4 | D | 604271 | 5827739 | 147.9 69.3 | 50.7 288.3 | 153.8 256.7 | 7.0 3 | 0 |
| E | 3815.5 | B | 604365 | 5827838 | 152.4 13.8 | 745.3 270.3 | 647.3 330.8 | 76.5 4 | 45 |
| F | 3811.4 | B | 604438 | 5827907 | 101.9 24.0 | 837.8 172.8 | 645.8 307.5 | 16.1 5 | 0 |
| G | 3804.0 | E | 604571 | 5828028 | 56.0 9.2 | 469.8 33.7 | 424.7 132.0 | 22.6 6 | 2 |
| H | 3793.4 | B | 604747 | 5828197 | 28.4 6.2 | 207.1 46.3 | 131.1 90.8 | 11.7 33 | 0 |
| I | 3779.5 | B | 604972 | 5828416 | 82.5 17.5 | 379.5 68.4 | 302.4 119.8 | 17.5 11 | 0 |
| J | 3763.2 | B | 605273 | 5828698 | 19.3 4.8 | 280.2 61.7 | 216.7 106.7 | 8.6 34 | 0 |
| K | 3757.5 | B | 605364 | 5828784 | 35.0 7.7 | 182.5 30.8 | 154.6 55.4 | 12.6 23 | 2 |
| L | 3749.1 | B | 605497 | 5828901 | 34.7 5.9 | 225.0 22.5 | 231.9 46.4 | 18.2 14 | 0 |
| M | 3734.1 | H | 605725 | 5829121 | 26.4 5.4 | 58.6 17.4 | 0.0 11.5 | 12.5 21 | 0 |
| LINE 10310 | | | FLIGHT 3 | | | | | | |
| A | 3965.7 | S? | 602601 | 5825927 | 17.6 15.7 | 78.3 91.7 | 2.8 19.9 | 1.5 26 | 31 |
| B | 3927.5 | D | 603357 | 5826656 | 16.0 4.0 | 142.7 27.2 | 80.4 65.3 | 7.9 30 | 1 |
| C | 3924.1 | D | 603413 | 5826713 | 30.9 9.7 | 142.7 34.2 | 80.4 65.3 | 7.2 20 | 0 |
| D | 3898.0 | B? | 603851 | 5827147 | 5.3 17.5 | 15.5 30.8 | 3.1 7.9 | --- --- | 39 |
| E | 3876.3 | E | 604209 | 5827468 | 131.3 42.5 | 864.8 164.8 | 657.7 328.7 | 11.1 0 | 0 |
| F | 3873.3 | B | 604256 | 5827519 | 157.2 29.2 | 864.8 179.7 | 657.7 328.7 | 26.5 0 | 0 |
| G | 3865.7 | D | 604387 | 5827649 | 103.8 52.1 | 333.3 103.7 | 121.2 40.5 | 5.7 9 | 5 |
| H | 3859.6 | D | 604488 | 5827746 | 103.4 82.0 | 647.9 336.3 | 293.3 285.9 | 3.2 0 | 0 |
| I | 3857.5 | B | 604523 | 5827780 | 117.1 69.0 | 647.9 336.3 | 293.3 285.9 | 4.8 0 | 0 |
| J | 3844.6 | D | 604739 | 5827981 | 60.2 9.5 | 265.2 19.4 | 256.0 83.4 | 24.7 0 | 0 |
| K | 3834.0 | B | 604928 | 5828166 | 23.1 2.9 | 172.0 9.4 | 146.3 42.1 | 24.6 33 | 0 |
| L | 3825.9 | B | 605069 | 5828298 | 43.7 15.2 | 170.8 33.1 | 126.6 55.7 | 7.0 20 | 0 |
| M | 3819.5 | B | 605193 | 5828413 | 25.2 3.6 | 49.8 16.6 | 28.1 19.7 | 21.1 29 | 0 |
| N | 3812.9 | D | 605346 | 5828552 | 24.8 21.2 | 83.7 57.4 | 0.8 45.9 | 1.8 8 | 0 |
| O | 3805.4 | B | 605507 | 5828709 | 79.1 24.9 | 512.2 101.5 | 434.8 49.9 | 9.8 12 | 0 |
| P | 3800.6 | B | 605605 | 5828801 | 99.1 9.4 | 663.5 85.5 | 524.0 216.3 | 61.9 10 | 0 |
| Q | 3784.5 | D | 605881 | 5829063 | 59.7 32.6 | 212.3 103.3 | 46.3 84.3 | 4.2 14 | 0 |

CX = COAXIAL
CP = COPLANAR

Note:EM values shown above
are local amplitudes

*Estimated Depth may be unreliable because the
stronger part of the conductor may be deeper or
to one side of the flight line, or because of a

Spanish Mountain Block A

- 6 - shallow dip or magnetite/overburden effects

EM Anomaly List

| LINE | Fid | Interp | XUTM m | YUTM m | CX 5500 HZ Real Quad ppm ppm | CP 7200 HZ Real Quad ppm ppm | CP 900 HZ Real Quad ppm ppm | Vertical Dike COND DEPTH* siemens m | Mag. Corr NT |
|------------|--------|--------|-----------|-----------|------------------------------------|------------------------------------|-----------------------------------|---|-----------------|
| LINE 10320 | | | FLIGHT 3 | | | | | | |
| A | 4083.1 | S? | 602774 | 5825888 | 7.1 14.4 | 29.1 90.2 | 1.0 16.5 | --- --- | 0 |
| B | 4108.0 | B? | 603305 | 5826401 | 13.4 8.2 | 50.4 26.4 | 8.5 12.6 | --- --- | 0 |
| C | 4117.1 | B | 603490 | 5826572 | 57.1 10.0 | 301.5 80.2 | 192.1 131.2 | 20.7 15 | 0 |
| D | 4145.7 | S? | 604021 | 5827074 | 1.6 3.9 | 0.5 0.0 | 0.2 0.0 | --- --- | 8 |
| E | 4169.5 | E | 604361 | 5827393 | 150.5 64.7 | 2643.1 443.2 | 2022.7 934.8 | 7.9 0 | 0 |
| F | 4173.7 | B | 604418 | 5827450 | 555.3 110.5 | 2643.1 443.2 | 2022.7 934.8 | 36.5 0 | 1 |
| G | 4184.2 | D | 604539 | 5827582 | 86.4 55.0 | 363.0 193.2 | 160.6 154.8 | 3.9 6 | 0 |
| H | 4193.0 | B | 604654 | 5827692 | 30.3 27.4 | 514.7 108.6 | 261.9 240.7 | 1.8 16 | 0 |
| I | 4198.8 | D | 604727 | 5827767 | 32.8 5.5 | 209.6 12.0 | 280.3 105.4 | 18.4 27 | 0 |
| J | 4204.1 | D | 604797 | 5827835 | 71.2 50.1 | 253.7 147.9 | 299.2 105.4 | 3.2 3 | 0 |
| K | 4210.6 | B | 604895 | 5827928 | 21.7 28.5 | 45.8 113.3 | 7.3 50.6 | 1.1 18 | 0 |
| L | 4220.5 | H | 605073 | 5828099 | 23.0 3.5 | 160.5 2.3 | 206.5 22.5 | 18.6 34 | 0 |
| M | 4227.2 | B | 605206 | 5828219 | 37.8 6.0 | 227.0 23.2 | 195.1 52.5 | 20.7 13 | 0 |
| N | 4231.5 | B | 605290 | 5828300 | 69.8 14.5 | 287.0 56.3 | 227.5 101.2 | 17.2 12 | 0 |
| O | 4244.3 | B | 605566 | 5828549 | 18.0 9.2 | 143.5 47.7 | 92.2 64.7 | 3.1 34 | 0 |
| P | 4250.4 | B | 605688 | 5828672 | 17.1 8.3 | 67.4 71.7 | 82.3 46.1 | 3.3 37 | 0 |
| Q | 4252.8 | B | 605736 | 5828718 | 15.0 0.0 | 67.4 71.7 | 82.3 15.9 | 951.2 54 | 1 |
| R | 4258.7 | H | 605850 | 5828826 | 21.1 11.1 | 172.0 62.2 | 127.7 66.7 | 3.1 27 | 2 |
| LINE 10330 | | | FLIGHT 1 | | | | | | |
| A | 2603.8 | S? | 602858 | 5825756 | 8.6 17.9 | 55.3 129.7 | 2.7 24.2 | 0.5 20 | 0 |
| B | 2578.8 | B? | 603366 | 5826250 | 20.4 13.6 | 24.6 39.8 | 13.2 6.6 | 2.3 16 | 0 |
| C | 2571.0 | B? | 603509 | 5826389 | 25.1 12.5 | 116.5 51.7 | 75.3 56.4 | 3.6 21 | 0 |
| D | 2568.1 | B | 603561 | 5826438 | 32.0 11.1 | 116.5 51.7 | 75.3 56.4 | 6.3 19 | 0 |
| E | 2505.3 | B | 604457 | 5827297 | 23.0 11.0 | 440.5 41.6 | 357.0 173.0 | 3.7 28 | 0 |
| F | 2498.3 | B | 604517 | 5827370 | 40.5 4.5 | 499.0 58.3 | 388.0 152.2 | 36.8 17 | 0 |
| G | 2495.3 | B | 604542 | 5827398 | 37.1 5.1 | 499.0 58.3 | 388.0 152.2 | 26.0 20 | 0 |
| H | 2476.9 | B | 604755 | 5827594 | 28.9 19.2 | 239.6 136.7 | 69.6 105.3 | 2.6 13 | 0 |
| I | 2474.2 | B | 604789 | 5827627 | 2.1 6.0 | 239.6 136.7 | 69.6 105.3 | 0.2 21 | 0 |
| J | 2468.5 | B | 604867 | 5827690 | 58.3 25.7 | 322.4 177.6 | 77.6 137.6 | 5.6 12 | 2 |
| K | 2458.3 | B | 605024 | 5827842 | 21.4 5.0 | 40.3 37.8 | 3.1 21.8 | 9.7 26 | 1 |
| L | 2447.1 | E | 605177 | 5827989 | 27.0 3.3 | 205.3 10.7 | 226.3 34.9 | 27.5 29 | 0 |
| M | 2441.1 | B | 605253 | 5828061 | 40.2 8.8 | 316.0 39.8 | 327.2 66.9 | 13.1 22 | 0 |
| N | 2433.8 | B | 605373 | 5828175 | 15.5 3.6 | 127.3 25.1 | 118.7 28.3 | 8.8 31 | 0 |
| O | 2421.2 | B | 605664 | 5828451 | 8.4 4.4 | 74.3 41.9 | 101.4 16.2 | 2.3 40 | 0 |
| P | 2409.7 | H | 605943 | 5828707 | 11.7 4.4 | 84.2 13.8 | 78.9 28.9 | 4.0 20 | 0 |

CX = COAXIAL
CP = COPLANAR

Note:EM values shown above
are local amplitudes

Spanish Mountain Block A

*Estimated Depth may be unreliable because the
stronger part of the conductor may be deeper or
to one side of the flight line, or because of a
shallow dip or magnetite/overburden effects

EM Anomaly List

| | | | | | CX | 5500 HZ | CP | 7200 HZ | CP | 900 HZ | | Vertical Dike | | Mag. Corr | |
|-------|--------|--------|----------|---------|-------|---------|-------|---------|-------|--------|--|---------------|--------|-----------|--|
| Label | Fid | Interp | XUTM | YUTM | Real | Quad | Real | Quad | Real | Quad | | COND | DEPTH* | | |
| | | | m | m | ppm | ppm | ppm | ppm | ppm | ppm | | siemens | m | NT | |
| LINE | 10340 | | FLIGHT 1 | | | | | | | | | | | | |
| A | 2731.0 | S | 602933 | 5825628 | 12.5 | 22.4 | 107.0 | 169.3 | 3.4 | 36.4 | | 0.6 | 7 | 0 | |
| B | 2756.9 | B? | 603464 | 5826155 | 15.6 | 8.9 | 34.0 | 4.7 | 12.1 | 13.5 | | 2.6 | 8 | 0 | |
| C | 2764.6 | D | 603608 | 5826292 | 32.3 | 0.0 | 144.9 | 37.7 | 129.7 | 72.0 | | 999.0 | 26 | 0 | |
| D | 2768.3 | B | 603676 | 5826353 | 41.6 | 9.3 | 144.9 | 13.4 | 129.7 | 72.0 | | 12.9 | 8 | 0 | |
| E | 2793.1 | S | 604101 | 5826734 | 7.2 | 22.3 | 121.9 | 208.2 | 8.7 | 42.9 | | 0.4 | 0 | 0 | |
| F | 2833.3 | B | 604620 | 5827244 | 60.9 | 9.0 | 297.6 | 29.9 | 344.7 | 86.0 | | 27.4 | 14 | 0 | |
| G | 2842.0 | B | 604725 | 5827347 | 15.6 | 15.0 | 1.5 | 44.1 | 17.5 | 72.4 | | 1.4 | 15 | 0 | |
| H | 2846.8 | B | 604785 | 5827409 | 14.2 | 7.0 | 181.8 | 58.0 | 121.4 | 72.4 | | 3.0 | 34 | 0 | |
| I | 2851.3 | H | 604850 | 5827469 | 36.1 | 32.5 | 174.9 | 58.0 | 71.9 | 0.0 | | 1.9 | 7 | 0 | |
| J | 2861.1 | D | 605001 | 5827619 | 67.4 | 26.8 | 128.5 | 91.9 | 60.6 | 55.8 | | 6.7 | 10 | 0 | |
| K | 2870.4 | B | 605168 | 5827772 | 20.8 | 2.1 | 63.8 | 27.8 | 35.2 | 35.2 | | 33.2 | 38 | 0 | |
| L | 2883.6 | B | 605422 | 5828044 | 59.7 | 14.1 | 288.6 | 58.7 | 240.8 | 75.1 | | 13.5 | 0 | 0 | |
| M | 2888.6 | B | 605521 | 5828142 | 52.5 | 6.8 | 348.2 | 58.7 | 332.1 | 67.2 | | 31.5 | 13 | 0 | |
| N | 2899.1 | B | 605743 | 5828309 | 31.1 | 8.9 | 161.3 | 10.0 | 152.2 | 37.4 | | 8.2 | 20 | 1 | |
| O | 2904.2 | B | 605826 | 5828383 | 4.9 | 3.4 | 13.5 | 11.8 | 10.1 | 8.7 | | 1.3 | 56 | 1 | |
| P | 2917.4 | D | 606026 | 5828576 | 43.9 | 8.0 | 247.1 | 47.7 | 156.1 | 104.2 | | 17.8 | 21 | 0 | |
| LINE | 10350 | | FLIGHT 1 | | | | | | | | | | | | |
| A | 3209.8 | S | 602942 | 5825425 | 11.5 | 24.6 | 90.1 | 164.3 | 5.3 | 34.1 | | 0.5 | 0 | 0 | |
| B | 3192.1 | S? | 603333 | 5825819 | 17.6 | 18.4 | 42.2 | 92.0 | 1.8 | 13.2 | | 1.3 | 6 | 25 | |
| C | 3167.3 | D | 603776 | 5826218 | 49.0 | 14.0 | 184.8 | 68.3 | 89.6 | 82.0 | | 9.6 | 12 | 0 | |
| D | 3142.4 | S? | 604106 | 5826546 | 32.5 | 32.9 | 157.6 | 212.6 | 3.2 | 44.0 | | 1.6 | 9 | 1 | |
| E | 3104.1 | E | 604620 | 5827042 | 43.7 | 24.9 | 248.3 | 73.1 | 25.1 | 115.5 | | 3.6 | 16 | 2 | |
| F | 3097.8 | B | 604681 | 5827104 | 72.5 | 15.5 | 417.8 | 74.7 | 329.9 | 194.2 | | 16.6 | 2 | 0 | |
| G | 3085.6 | B | 604808 | 5827220 | 47.3 | 30.3 | 281.1 | 152.9 | 138.3 | 137.1 | | 3.2 | 3 | 0 | |
| H | 3083.0 | B | 604840 | 5827250 | 37.6 | 30.3 | 281.1 | 152.9 | 138.3 | 137.1 | | 2.2 | 7 | 1 | |
| I | 3074.4 | B | 604964 | 5827371 | 68.8 | 9.9 | 301.6 | 33.9 | 332.2 | 93.5 | | 29.5 | 14 | 0 | |
| J | 3062.6 | B | 605115 | 5827525 | 49.7 | 27.4 | 210.9 | 161.3 | 65.6 | 83.4 | | 3.9 | 6 | 3 | |
| K | 3043.8 | B | 605380 | 5827783 | 13.6 | 1.0 | 68.2 | 29.3 | 64.7 | 22.1 | | 46.9 | 44 | 0 | |
| L | 3028.3 | D | 605634 | 5828012 | 41.8 | 5.1 | 277.2 | 121.3 | 364.6 | 56.4 | | 31.6 | 15 | 0 | |
| M | 3023.1 | B | 605721 | 5828096 | 19.3 | 2.3 | 277.2 | 35.6 | 266.8 | 56.4 | | --- | --- | 0 | |
| N | 3017.2 | B | 605814 | 5828189 | 111.7 | 38.1 | 438.8 | 122.2 | 269.5 | 174.6 | | 9.8 | 11 | 1 | |
| O | 3012.5 | B | 605897 | 5828270 | 39.3 | 8.0 | 186.0 | 13.5 | 189.0 | 46.8 | | 14.6 | 14 | 0 | |
| P | 2999.9 | B | 606115 | 5828465 | 40.1 | 8.8 | 157.4 | 5.5 | 153.3 | 58.4 | | 13.0 | 19 | 0 | |
| Q | 2997.1 | B | 606165 | 5828506 | 31.5 | 3.9 | 157.4 | 24.0 | 153.3 | 58.4 | | 28.2 | 20 | 0 | |
| R | 2988.1 | B | 606312 | 5828638 | 28.4 | 10.0 | 56.2 | 17.0 | 47.0 | 23.3 | | 5.9 | 27 | 0 | |

CX = COAXIAL
CP = COPLANAR

Note: EM values shown above
are local amplitudes

*Estimated Depth may be unreliable because the
stronger part of the conductor may be deeper or
to one side of the flight line, or because of a
shallow dip or magnetite/overburden effects

EM Anomaly List

| Label | Fid | Interp | XUTM m | YUTM m | CX 5500 HZ Real Quad ppm ppm | CP 7200 HZ Real Quad ppm ppm | CP 900 HZ Real Quad ppm ppm | Vertical Dike COND DEPTH* siemens m | Mag. Corr NT |
|-------|--------|--------|-----------|-----------|------------------------------------|------------------------------------|-----------------------------------|---|-----------------|
| LINE | 10360 | | FLIGHT 1 | | | | | | |
| A | 3311.9 | S | 602841 | 5825137 | 13.1 31.1 | 52.8 131.1 | 4.2 27.7 | 0.5 0 | 0 |
| B | 3322.5 | S | 603076 | 5825347 | 4.8 13.4 | 77.8 128.1 | 4.1 31.7 | 0.3 9 | 0 |
| C | 3342.3 | S? | 603472 | 5825732 | 11.6 11.8 | 17.5 58.4 | 2.6 8.6 | 1.2 25 | 0 |
| D | 3366.1 | B | 603890 | 5826146 | 23.3 5.9 | 140.0 43.0 | 74.5 58.5 | 8.8 22 | 0 |
| E | 3373.8 | D | 604015 | 5826248 | 28.5 13.9 | 99.1 30.6 | 73.5 40.6 | 3.8 14 | 0 |
| F | 3391.9 | D | 604258 | 5826474 | 35.6 32.4 | 195.5 188.6 | 11.6 70.1 | 1.9 4 | 0 |
| G | 3397.6 | B | 604341 | 5826552 | 20.1 22.0 | 240.5 153.3 | 35.9 83.5 | 1.3 11 | 0 |
| H | 3403.0 | B | 604424 | 5826629 | 26.3 8.3 | 240.5 134.9 | 35.9 83.5 | 6.8 25 | 0 |
| I | 3422.3 | B | 604713 | 5826903 | 14.6 12.7 | 38.5 104.2 | 6.8 8.7 | 1.5 22 | 0 |
| J | 3436.0 | B | 604919 | 5827120 | 23.4 7.9 | 53.3 30.2 | 51.6 18.6 | 5.9 26 | 0 |
| K | 3443.5 | B | 605059 | 5827264 | 11.7 0.1 | 43.6 47.6 | 68.0 12.5 | 877.3 24 | 0 |
| L | 3451.3 | B | 605226 | 5827406 | 24.4 11.4 | 103.1 61.6 | 36.9 55.4 | 3.8 6 | 0 |
| M | 3455.0 | B | 605308 | 5827480 | 21.5 10.3 | 106.9 62.2 | 36.9 48.7 | 3.6 11 | 0 |
| N | 3464.5 | H | 605512 | 5827681 | 14.2 0.2 | 114.5 18.0 | 97.1 39.7 | 431.2 35 | 0 |
| O | 3471.3 | B | 605653 | 5827823 | 37.9 9.3 | 130.8 54.5 | 64.7 57.8 | 11.0 15 | 0 |
| P | 3475.3 | D | 605741 | 5827907 | 35.0 24.9 | 195.5 123.3 | 105.6 74.6 | 2.5 8 | 0 |
| Q | 3481.1 | H | 605858 | 5828013 | 7.6 4.6 | 104.7 0.0 | 150.9 18.1 | 1.8 34 | 0 |
| R | 3492.1 | H | 606059 | 5828197 | 13.9 0.0 | 149.2 44.6 | 150.3 44.5 | 928.9 46 | 0 |
| S | 3508.7 | H | 606367 | 5828489 | 22.7 9.4 | 124.1 52.9 | 57.4 59.9 | 4.4 23 | 0 |
| LINE | 10370 | | FLIGHT 1 | | | | | | |
| A | 3789.2 | S? | 602972 | 5825047 | 14.2 59.4 | 125.0 339.5 | 6.7 66.2 | 0.3 0 | 0 |
| B | 3786.8 | D | 603034 | 5825108 | 19.7 23.3 | 133.8 339.5 | 6.0 66.2 | 1.2 12 | 0 |
| C | 3752.0 | E | 603926 | 5825942 | 11.5 16.3 | 54.8 48.6 | 7.7 18.8 | --- --- | 0 |
| D | 3742.0 | B | 604094 | 5826119 | 67.8 25.4 | 200.0 62.4 | 92.4 84.7 | 7.3 9 | 0 |
| E | 3732.0 | D | 604222 | 5826245 | 18.3 14.4 | 0.0 36.4 | 20.3 0.0 | 1.8 20 | 0 |
| F | 3722.5 | D | 604325 | 5826348 | 57.6 33.3 | 189.8 123.7 | 30.1 84.3 | 3.9 14 | 1 |
| G | 3674.7 | B | 605017 | 5826995 | 17.9 3.3 | 72.7 43.5 | 22.0 30.9 | 12.9 34 | 0 |
| H | 3660.6 | D | 605163 | 5827119 | 29.4 7.7 | 107.2 34.4 | 61.3 42.0 | 9.2 25 | 0 |
| I | 3638.8 | B | 605372 | 5827356 | 90.3 10.6 | 765.5 100.4 | 626.6 226.6 | 43.6 4 | 1 |
| J | 3636.7 | B | 605405 | 5827382 | 113.4 20.3 | 765.5 110.0 | 626.6 226.6 | 25.1 1 | 0 |
| K | 3618.1 | B | 605678 | 5827635 | 8.4 5.8 | 126.4 68.2 | 82.5 47.0 | 1.6 34 | 0 |
| L | 3613.5 | B | 605738 | 5827694 | 9.7 5.7 | 126.4 17.9 | 76.9 47.0 | 2.1 27 | 0 |
| M | 3601.4 | B | 605850 | 5827795 | 36.6 17.7 | 276.6 86.1 | 215.8 92.0 | 4.2 0 | 0 |
| N | 3592.0 | B | 605987 | 5827930 | 173.3 34.3 | 559.2 234.2 | 402.3 181.3 | 25.0 0 | 0 |
| O | 3586.8 | B | 606063 | 5828009 | 20.3 4.4 | 365.1 46.7 | 402.3 79.0 | 10.8 35 | 0 |
| P | 3582.4 | B | 606129 | 5828072 | 46.0 10.7 | 277.8 46.7 | 255.4 74.9 | 12.6 15 | 0 |

CX = COAXIAL

CP = COPLANAR

Note:EM values shown above
are local amplitudes

Spanish Mountain Block A

*Estimated Depth may be unreliable because the
stronger part of the conductor may be deeper or
to one side of the flight line, or because of a
shallow dip or magnetite/overburden effects

EM Anomaly List

| Label | Fid | Interp | XUTM m | YUTM m | CX 5500 HZ Real ppm | Quad ppm | CP 7200 HZ Real ppm | Quad ppm | CP 900 HZ Real ppm | Quad ppm | Vertical Dike COND siemens | DEPTH* m | Mag. Corr NT |
|------------|--------|--------|-----------|-----------|---------------------------|-------------|---------------------------|-------------|--------------------------|-------------|----------------------------------|-------------|-----------------|
| LINE 10370 | | | FLIGHT 1 | | | | | | | | | | |
| Q | 3566.9 | B | 606390 | 5828320 | 27.1 | 4.9 | 275.8 | 68.6 | 185.4 | 108.2 | 15.5 | 27 | 0 |
| LINE 10380 | | | FLIGHT 3 | | | | | | | | | | |
| A | 3364.2 | S? | 603062 | 5824931 | 17.4 | 66.1 | 113.2 | 301.9 | 7.6 | 59.8 | 0.4 | 0 | 0 |
| B | 3361.5 | B? | 603123 | 5824987 | 14.5 | 17.4 | 113.2 | 301.9 | 7.6 | 59.8 | 1.0 | 14 | 0 |
| C | 3322.8 | D | 604069 | 5825889 | 25.2 | 14.1 | 86.1 | 49.4 | 9.9 | 29.3 | 3.1 | 23 | 0 |
| D | 3316.0 | B | 604193 | 5826007 | 104.5 | 20.4 | 355.2 | 65.4 | 174.6 | 164.3 | 21.5 | 10 | 0 |
| E | 3308.7 | D | 604305 | 5826122 | 42.3 | 20.5 | 63.9 | 14.8 | 32.1 | 22.1 | 4.4 | 15 | 0 |
| F | 3297.5 | D | 604451 | 5826252 | 36.6 | 5.3 | 92.6 | 32.9 | 0.0 | 29.7 | 23.9 | 26 | 1 |
| G | 3290.0 | B | 604545 | 5826342 | 18.8 | 38.9 | 212.7 | 203.3 | 21.9 | 73.1 | 0.7 | 1 | 1 |
| H | 3251.2 | B | 605115 | 5826894 | 35.8 | 6.4 | 280.5 | 65.9 | 139.9 | 130.1 | 17.2 | 25 | 0 |
| I | 3237.6 | B | 605252 | 5827021 | 85.0 | 45.1 | 486.4 | 206.8 | 214.8 | 225.8 | 4.9 | 15 | 0 |
| J | 3212.2 | B | 605510 | 5827284 | 209.0 | 67.8 | 1210.0 | 301.0 | 853.0 | 519.4 | 13.0 | 1 | 0 |
| K | 3184.7 | H | 606060 | 5827781 | 13.0 | 16.2 | 100.8 | 89.0 | 140.4 | 49.8 | 1.0 | 11 | 0 |
| LINE 10390 | | | FLIGHT 3 | | | | | | | | | | |
| B | 3508.1 | S | 603184 | 5824833 | 23.8 | 69.5 | 160.2 | 366.0 | 7.4 | 71.7 | 0.5 | 0 | 0 |
| C | 3517.5 | S? | 603387 | 5825027 | 21.8 | 26.2 | 142.6 | 228.2 | 6.7 | 51.6 | 1.2 | 8 | 2 |
| D | 3563.5 | B | 604339 | 5825938 | 61.5 | 13.0 | 407.9 | 69.6 | 328.1 | 156.6 | 16.0 | 13 | 0 |
| E | 3589.0 | B | 604719 | 5826301 | 18.7 | 22.0 | 215.1 | 231.8 | 30.7 | 87.8 | 1.1 | 15 | 1 |
| F | 3617.0 | D | 605157 | 5826714 | 40.2 | 25.8 | 244.0 | 97.3 | 108.1 | 105.6 | 3.0 | 16 | 0 |
| G | 3620.4 | B | 605207 | 5826770 | 32.4 | 21.0 | 244.0 | 97.3 | 105.7 | 105.6 | 2.8 | 15 | 0 |
| H | 3623.2 | D | 605251 | 5826820 | 31.9 | 4.2 | 170.3 | 48.6 | 105.7 | 84.1 | 26.1 | 16 | 0 |
| I | 3632.5 | B | 605417 | 5826971 | 28.1 | 13.8 | 104.4 | 23.5 | 105.5 | 56.6 | 3.8 | 19 | 0 |
| J | 3646.3 | B | 605691 | 5827256 | 72.3 | 21.6 | 348.1 | 133.6 | 292.0 | 135.1 | 10.3 | 0 | 0 |
| K | 3649.7 | B | 605765 | 5827344 | 54.5 | 6.7 | 348.1 | 0.0 | 292.0 | 135.1 | 34.5 | 22 | 0 |
| L | 3662.2 | B | 606093 | 5827605 | 38.9 | 14.1 | 137.9 | 51.2 | 94.8 | 51.2 | 6.4 | 0 | 1 |
| LINE 10400 | | | FLIGHT 8 | | | | | | | | | | |
| B | 4125.8 | S | 603289 | 5824726 | 30.9 | 88.1 | 191.5 | 429.4 | 8.5 | 84.9 | 0.6 | 0 | 0 |
| C | 4134.5 | S | 603499 | 5824931 | 20.5 | 26.4 | 127.1 | 204.5 | 3.6 | 47.3 | 1.1 | 11 | 0 |
| D | 4179.8 | E | 604467 | 5825853 | 60.8 | 3.8 | 279.1 | 67.8 | 227.3 | 113.7 | 97.9 | 14 | 0 |
| E | 4184.7 | B | 604552 | 5825935 | 31.8 | 0.3 | 279.1 | 0.6 | 227.3 | 77.8 | 999.0 | 29 | 0 |
| F | 4193.9 | D | 604699 | 5826077 | 22.5 | 12.2 | 0.3 | 37.7 | 0.0 | 0.2 | 3.1 | 23 | 0 |
| G | 4199.3 | B | 604788 | 5826147 | 17.7 | 18.1 | 113.2 | 101.4 | 22.0 | 51.9 | 1.3 | 14 | 1 |
| H | 4205.0 | B | 604871 | 5826227 | 24.7 | 24.2 | 113.2 | 153.5 | 22.0 | 51.9 | 1.5 | 15 | 1 |
| I | 4228.3 | D | 605231 | 5826578 | 40.0 | 15.6 | 174.9 | 38.3 | 113.7 | 82.5 | 5.8 | 7 | 0 |
| J | 4233.5 | D | 605305 | 5826651 | 27.5 | 10.2 | 134.0 | 57.9 | 113.7 | 82.5 | 5.5 | 15 | 0 |

CX = COAXIAL
CP = COPLANAR

Note:EM values shown above
are local amplitudes

*Estimated Depth may be unreliable because the
stronger part of the conductor may be deeper or
to one side of the flight line, or because of a

Spanish Mountain Block A

- 10 - shallow dip or magnetite/overburden effects

EM Anomaly List

| Label | Fid | Interp | XUTM m | YUTM m | CX 5500 HZ Real ppm | Quad ppm | CP 7200 HZ Real ppm | Quad ppm | CP 900 HZ Real ppm | Quad ppm | Vertical Dike COND siemens | DEPTH* m | Mag. Corr NT |
|-------|--------|--------|-----------|-----------|---------------------------|-------------|---------------------------|-------------|--------------------------|-------------|----------------------------------|-------------|-----------------|
| LINE | 10400 | | FLIGHT 8 | | | | | | | | | | |
| K | 4235.6 | D | 605334 | 5826680 | 18.1 | 13.3 | 134.0 | 57.9 | 23.3 | 52.4 | 2.0 | 14 | 0 |
| L | 4241.0 | B | 605404 | 5826750 | 34.2 | 21.2 | 109.7 | 48.4 | 26.0 | 40.3 | 3.0 | 19 | 0 |
| M | 4249.2 | B | 605512 | 5826859 | 80.7 | 28.8 | 273.0 | 83.3 | 367.7 | 115.3 | 8.3 | 11 | 0 |
| N | 4258.0 | E | 605651 | 5826983 | 13.1 | 1.1 | 114.4 | 5.3 | 190.6 | 0.0 | 38.0 | 46 | 4 |
| O | 4259.7 | B | 605678 | 5827009 | 24.7 | 0.4 | 114.4 | 55.5 | 190.6 | 0.0 | --- | --- | 4 |
| P | 4273.8 | B | 605909 | 5827237 | 27.9 | 10.5 | 196.3 | 68.0 | 169.4 | 78.6 | 5.4 | 19 | 0 |
| Q | 4277.5 | E | 605972 | 5827305 | 28.4 | 5.4 | 209.9 | 7.4 | 169.4 | 69.7 | 14.4 | 18 | 0 |
| R | 4289.2 | H | 606197 | 5827532 | 36.7 | 14.4 | 248.4 | 73.9 | 187.6 | 99.8 | 5.6 | 5 | 0 |
| LINE | 10410 | | FLIGHT 8 | | | | | | | | | | |
| B | 4514.2 | S? | 603372 | 5824599 | 20.6 | 85.5 | 157.2 | 486.5 | 7.5 | 86.7 | 0.4 | 0 | 82 |
| C | 4506.3 | S | 603559 | 5824782 | 17.4 | 34.8 | 135.4 | 228.7 | 5.1 | 48.9 | 0.7 | 6 | 0 |
| D | 4464.7 | B | 604600 | 5825774 | 53.5 | 8.5 | 278.4 | 81.6 | 167.1 | 120.9 | 23.4 | 19 | 0 |
| E | 4460.2 | D | 604688 | 5825857 | 20.3 | 10.8 | 79.9 | 0.2 | 167.1 | 26.2 | 3.0 | 25 | 0 |
| F | 4448.7 | D | 604879 | 5826031 | 34.9 | 28.8 | 195.4 | 114.6 | 26.4 | 75.4 | 2.1 | 1 | 3 |
| G | 4443.5 | B | 604953 | 5826104 | 60.9 | 35.4 | 251.7 | 189.7 | 26.4 | 81.3 | 3.9 | 7 | 0 |
| H | 4414.8 | B | 605302 | 5826448 | 18.4 | 7.8 | 214.0 | 70.9 | 116.9 | 116.3 | 4.0 | 26 | 0 |
| I | 4407.3 | D | 605395 | 5826546 | 33.9 | 5.9 | 4.8 | 7.7 | 93.0 | 3.0 | 17.7 | 22 | 0 |
| J | 4398.3 | B | 605504 | 5826648 | 25.2 | 13.0 | 90.2 | 61.0 | 19.0 | 39.6 | 3.4 | 26 | 0 |
| K | 4384.0 | B | 605673 | 5826800 | 43.5 | 3.1 | 506.6 | 23.4 | 507.0 | 154.7 | 73.4 | 14 | 0 |
| L | 4378.3 | B | 605755 | 5826888 | 34.2 | 9.3 | 535.6 | 41.9 | 536.2 | 154.7 | 9.2 | 25 | 0 |
| M | 4359.7 | B | 606045 | 5827157 | 42.3 | 11.5 | 262.7 | 59.6 | 193.9 | 99.1 | 9.8 | 19 | 19 |
| LINE | 10420 | | FLIGHT 8 | | | | | | | | | | |
| A | 4636.5 | S | 603575 | 5824572 | 13.9 | 21.7 | 106.0 | 186.3 | 6.0 | 43.5 | 0.8 | 15 | 0 |
| B | 4642.4 | E | 603722 | 5824716 | 15.8 | 12.6 | 96.4 | 100.5 | 2.6 | 29.8 | --- | --- | 0 |
| C | 4679.4 | B? | 604543 | 5825505 | 17.4 | 8.0 | 31.6 | 55.4 | 5.2 | 12.0 | --- | --- | 8 |
| D | 4691.5 | B | 604747 | 5825700 | 59.3 | 0.3 | 289.6 | 40.8 | 303.8 | 130.2 | 999.0 | 27 | 0 |
| E | 4694.5 | B | 604798 | 5825751 | 12.9 | 6.7 | 289.6 | 50.7 | 303.8 | 130.2 | 2.7 | 42 | 0 |
| F | 4697.6 | B | 604853 | 5825804 | 32.0 | 6.5 | 134.5 | 50.7 | 303.8 | 59.6 | 13.6 | 28 | 0 |
| G | 4709.3 | B | 605051 | 5826000 | 25.8 | 18.7 | 130.9 | 70.7 | 21.6 | 43.1 | 2.2 | 8 | 0 |
| H | 4735.5 | B | 605368 | 5826295 | 20.1 | 22.1 | 173.0 | 82.5 | 123.1 | 82.7 | 1.3 | 19 | 0 |
| I | 4745.7 | B | 605502 | 5826413 | 55.7 | 15.9 | 49.3 | 66.2 | 30.8 | 31.7 | 10.0 | 8 | 1 |
| J | 4755.3 | D | 605615 | 5826526 | 17.6 | 17.8 | 27.2 | 30.4 | 0.5 | 9.6 | 1.3 | 18 | 0 |
| K | 4771.5 | B | 605800 | 5826715 | 148.0 | 25.1 | 627.6 | 230.5 | 387.1 | 254.3 | 29.8 | 0 | 3 |
| L | 4776.1 | D | 605858 | 5826780 | 72.2 | 53.9 | 331.7 | 153.6 | 387.1 | 125.5 | 3.0 | 0 | 0 |
| M | 4789.2 | D | 606009 | 5826908 | 12.1 | 23.6 | 47.2 | 70.7 | 19.0 | 7.8 | 0.6 | 7 | 0 |
| N | 4804.0 | B | 606174 | 5827076 | 7.9 | 3.5 | 124.5 | 23.6 | 120.0 | 47.3 | 2.9 | 58 | 3 |

CX = COAXIAL
CP = COPLANAR

Note:EM values shown above
are local amplitudes

*Estimated Depth may be unreliable because the
stronger part of the conductor may be deeper or
to one side of the flight line, or because of a

Spanish Mountain Block A

- 11 - shallow dip or magnetite/overburden effects

EM Anomaly List

| Label | Fid | Interp | XUTM m | YUTM m | CX 5500 HZ Real ppm | Quad ppm | CP 7200 HZ Real ppm | Quad ppm | CP 900 HZ Real ppm | Quad ppm | Vertical Dike COND siemens | DEPTH* m | Mag. Corr NT |
|------------|--------|--------|-----------|-----------|---------------------------|-------------|---------------------------|-------------|--------------------------|-------------|----------------------------------|-------------|-----------------|
| LINE 10420 | | | FLIGHT 8 | | | | | | | | | | |
| O | 4812.7 | B | 606278 | 5827176 | 15.7 | 0.0 | 118.8 | 34.5 | 112.0 | 38.3 | 965.8 | 36 | 0 |
| LINE 10430 | | | FLIGHT 8 | | | | | | | | | | |
| A | 5028.0 | S? | 603687 | 5824486 | 10.0 | 13.4 | 76.5 | 92.0 | 3.5 | 22.3 | --- | --- | 0 |
| B | 4992.4 | D | 604656 | 5825414 | 17.8 | 9.6 | 31.0 | 5.1 | 5.3 | 13.0 | 2.8 | 25 | 20 |
| C | 4982.9 | B | 604895 | 5825653 | 20.4 | 8.5 | 164.4 | 40.8 | 116.2 | 76.5 | 4.2 | 23 | 0 |
| D | 4979.4 | H | 604977 | 5825730 | 5.1 | 0.8 | 164.4 | 0.7 | 116.2 | 76.5 | 10.2 | 69 | 3 |
| E | 4970.8 | S? | 605156 | 5825894 | 19.1 | 10.3 | 70.1 | 78.1 | 15.3 | 17.2 | 2.9 | 13 | 0 |
| F | 4952.9 | E | 605414 | 5826113 | 37.3 | 14.1 | 196.5 | 56.8 | 60.4 | 94.8 | 5.9 | 18 | 0 |
| G | 4948.3 | B | 605467 | 5826158 | 19.5 | 9.6 | 194.9 | 56.8 | 61.8 | 94.5 | 3.3 | 36 | 0 |
| H | 4936.0 | D | 605582 | 5826270 | 24.3 | 14.3 | 6.1 | 17.3 | 3.3 | 3.2 | 2.8 | 23 | 0 |
| I | 4908.0 | B | 605946 | 5826656 | 19.7 | 20.8 | 100.9 | 132.8 | 123.1 | 89.5 | 1.3 | 18 | 12 |
| J | 4903.7 | B | 606016 | 5826727 | 20.3 | 4.3 | 190.6 | 0.0 | 224.9 | 89.5 | 11.2 | 35 | 5 |
| K | 4881.4 | B | 606367 | 5827049 | 17.1 | 6.6 | 280.3 | 50.3 | 206.1 | 94.1 | 4.4 | 40 | 3 |
| L | 4878.8 | B | 606400 | 5827087 | 34.3 | 10.1 | 280.3 | 50.3 | 206.1 | 94.1 | 8.2 | 27 | 0 |
| LINE 10440 | | | FLIGHT 8 | | | | | | | | | | |
| A | 5301.7 | D | 603971 | 5824549 | 36.6 | 42.8 | 69.3 | 148.6 | 2.8 | 28.3 | 1.4 | 4 | 0 |
| B | 5314.1 | B? | 604252 | 5824817 | 2.6 | 0.0 | 7.0 | 11.2 | 1.2 | 1.2 | --- | --- | 0 |
| C | 5333.8 | B? | 604677 | 5825223 | 10.7 | 24.2 | 60.0 | 122.7 | 5.2 | 26.0 | 0.5 | 7 | 0 |
| D | 5347.8 | D | 604916 | 5825444 | 34.9 | 20.3 | 87.1 | 49.3 | 10.1 | 35.9 | 3.2 | 18 | 0 |
| E | 5355.3 | B | 605048 | 5825567 | 33.9 | 3.6 | 254.7 | 44.1 | 227.3 | 121.1 | 36.2 | 27 | 0 |
| F | 5360.8 | B | 605144 | 5825664 | 59.1 | 9.9 | 258.3 | 34.0 | 184.4 | 101.9 | 22.5 | 16 | 0 |
| G | 5387.4 | H | 605564 | 5826067 | 37.0 | 25.9 | 151.6 | 105.0 | 28.2 | 48.4 | 2.6 | 10 | 0 |
| H | 5393.5 | D | 605658 | 5826150 | 37.8 | 8.2 | 59.7 | 33.4 | 28.2 | 20.0 | 13.2 | 16 | 0 |
| I | 5401.4 | D | 605779 | 5826268 | 17.7 | 6.4 | 8.4 | 18.2 | 1.4 | 0.9 | 4.9 | 29 | 0 |
| J | 5425.4 | B | 606174 | 5826653 | 46.5 | 19.8 | 308.3 | 122.1 | 227.1 | 141.4 | 5.4 | 8 | 0 |
| K | 5441.5 | E | 606420 | 5826889 | 15.1 | 4.7 | 120.3 | 22.5 | 112.7 | 54.2 | 5.7 | 36 | 0 |
| L | 5453.3 | B | 606593 | 5827047 | 85.6 | 35.3 | 585.9 | 133.4 | 383.5 | 207.1 | 6.9 | 1 | 0 |
| LINE 10450 | | | FLIGHT 8 | | | | | | | | | | |
| A | 5692.7 | S? | 603860 | 5824237 | 8.3 | 10.6 | 52.0 | 78.1 | 2.9 | 17.7 | --- | --- | 0 |
| B | 5684.3 | E | 604069 | 5824433 | 8.5 | 13.7 | 36.8 | 52.9 | 1.5 | 14.1 | --- | --- | 0 |
| C | 5656.5 | D | 604674 | 5825010 | 20.3 | 25.1 | 55.9 | 75.0 | 1.6 | 16.6 | 1.1 | 19 | 13 |
| D | 5651.3 | D | 604788 | 5825119 | 11.4 | 28.3 | 36.5 | 81.2 | 4.7 | 16.6 | 0.5 | 4 | 22 |
| E | 5636.9 | D | 605071 | 5825401 | 100.1 | 11.7 | 252.4 | 59.3 | 240.0 | 112.8 | 45.6 | 0 | 0 |
| F | 5633.6 | B | 605135 | 5825460 | 40.8 | 6.3 | 307.7 | 26.0 | 265.4 | 122.0 | 22.5 | 19 | 0 |
| G | 5619.4 | B | 605384 | 5825697 | 30.6 | 24.8 | 139.8 | 126.5 | 15.0 | 44.2 | 2.1 | 15 | 0 |

CX = COAXIAL
CP = COPLANAR

Note:EM values shown above
are local amplitudes

*Estimated Depth may be unreliable because the
stronger part of the conductor may be deeper or
to one side of the flight line, or because of a

Spanish Mountain Block A

- 12 - shallow dip or magnetite/overburden effects

EM Anomaly List

| Label | Fid | Interp | XUTM m | YUTM m | CX 5500 HZ Real Quad ppm ppm | CP 7200 HZ Real Quad ppm ppm | CP 900 HZ Real Quad ppm ppm | Vertical Dike COND DEPTH* siemens m | Mag. Corr NT |
|-------|--------|--------|-----------|-----------|------------------------------------|------------------------------------|-----------------------------------|---|-----------------|
| LINE | 10450 | | FLIGHT 8 | | | | | | |
| H | 5603.2 | B | 605622 | 5825929 | 58.8 23.0 | 266.4 149.2 | 82.4 129.6 | 6.6 10 | 0 |
| I | 5598.2 | B | 605691 | 5825996 | 40.2 25.8 | 338.7 149.2 | 133.8 164.9 | 3.0 17 | 0 |
| J | 5584.1 | B | 605874 | 5826160 | 22.2 5.8 | 76.2 63.3 | 17.4 24.8 | 8.4 29 | 0 |
| K | 5566.8 | B | 606087 | 5826358 | 16.1 13.8 | 191.4 75.3 | 41.8 81.3 | 1.6 28 | 0 |
| L | 5549.1 | B | 606282 | 5826549 | 57.0 10.9 | 220.6 108.6 | 240.1 119.4 | 18.2 17 | 1 |
| M | 5528.5 | E | 606556 | 5826822 | 49.9 23.1 | 398.3 107.2 | 196.2 167.5 | 4.9 6 | 0 |
| N | 5521.0 | B | 606671 | 5826915 | 73.1 17.1 | 457.3 115.3 | 356.1 171.7 | 14.7 4 | 0 |
| LINE | 10460 | | FLIGHT 8 | | | | | | |
| A | 5819.2 | D | 604797 | 5824919 | 15.6 24.4 | 45.8 72.8 | 2.6 12.9 | 0.8 10 | 11 |
| B | 5831.9 | D | 605063 | 5825179 | 69.6 60.5 | 227.1 243.9 | 32.1 81.3 | 2.5 7 | 7 |
| C | 5836.2 | B? | 605144 | 5825257 | 6.1 22.6 | 140.8 243.9 | 62.0 52.8 | 0.3 3 | 17 |
| D | 5840.1 | D | 605211 | 5825321 | 123.9 34.3 | 417.1 141.8 | 274.7 170.2 | 13.7 0 | 0 |
| E | 5842.6 | B | 605253 | 5825359 | 52.7 31.4 | 417.1 121.9 | 274.7 170.2 | 3.6 2 | 0 |
| F | 5848.8 | E | 605359 | 5825450 | 45.0 3.3 | 191.7 0.0 | 154.2 85.0 | 71.1 26 | 0 |
| G | 5858.7 | B | 605530 | 5825619 | 30.3 11.7 | 157.5 87.0 | 22.1 51.7 | 5.4 23 | 0 |
| H | 5871.4 | D | 605768 | 5825838 | 106.0 56.0 | 263.5 225.3 | 47.6 93.7 | 5.3 0 | 0 |
| I | 5890.7 | B? | 606058 | 5826117 | 8.0 17.0 | 34.5 61.4 | 2.0 14.3 | --- --- | 0 |
| J | 5917.0 | B | 606450 | 5826493 | 27.2 6.6 | 100.3 21.8 | 139.4 53.4 | 9.9 21 | 0 |
| K | 5942.0 | B | 606738 | 5826788 | 65.4 32.1 | 405.6 148.2 | 235.9 178.5 | 5.0 4 | 0 |
| L | 5946.0 | B | 606802 | 5826853 | 55.8 22.7 | 278.0 69.5 | 202.4 178.5 | 6.1 10 | 0 |
| LINE | 10470 | | FLIGHT 8 | | | | | | |
| A | 6166.0 | S? | 604094 | 5824041 | 10.7 10.2 | 70.6 107.1 | 3.8 25.4 | --- --- | 2 |
| B | 6135.3 | D | 604866 | 5824782 | 11.8 20.0 | 20.3 63.3 | 2.9 13.8 | 0.7 16 | 11 |
| C | 6122.8 | D | 605153 | 5825050 | 67.1 52.1 | 266.4 207.1 | 9.8 96.3 | 2.8 0 | 0 |
| D | 6118.1 | B | 605256 | 5825148 | 121.1 81.1 | 466.0 416.3 | 54.9 389.0 | 4.1 1 | 19 |
| E | 6114.7 | B | 605327 | 5825218 | 184.3 82.0 | 899.5 354.6 | 579.7 389.0 | 8.0 0 | 17 |
| F | 6113.6 | B | 605349 | 5825239 | 184.3 82.0 | 899.5 354.6 | 579.7 389.0 | 8.0 0 | 0 |
| G | 6101.5 | D | 605558 | 5825447 | 30.0 4.8 | 117.9 30.2 | 40.7 50.4 | 19.4 28 | 0 |
| H | 6083.1 | B | 605853 | 5825730 | 220.7 85.9 | 658.3 299.4 | 166.5 271.2 | 10.3 0 | 0 |
| I | 6075.8 | D | 605978 | 5825841 | 24.3 34.5 | 456.6 259.7 | 87.2 175.6 | 1.0 7 | 0 |
| J | 6072.8 | D | 606024 | 5825887 | 102.3 64.7 | 456.6 259.7 | 87.2 175.6 | 4.2 0 | 0 |
| K | 6059.0 | H | 606198 | 5826055 | 8.6 9.5 | 55.4 62.2 | 5.5 24.7 | --- --- | 0 |
| L | 6039.4 | B | 606459 | 5826290 | 30.3 8.7 | 281.0 47.7 | 193.8 138.3 | 8.1 21 | 0 |
| M | 6037.0 | B | 606495 | 5826328 | 51.4 6.4 | 281.0 47.7 | 193.8 138.3 | 33.2 6 | 0 |
| N | 6018.6 | B | 606692 | 5826535 | 19.5 5.2 | 215.6 87.2 | 66.7 99.3 | 7.7 38 | 0 |
| O | 6003.7 | B | 606804 | 5826645 | 39.0 23.6 | 285.6 144.1 | 98.7 117.9 | 3.2 8 | 5 |

CX = COAXIAL
CP = COPLANAR

Note:EM values shown above
are local amplitudes

*Estimated Depth may be unreliable because the
stronger part of the conductor may be deeper or
to one side of the flight line, or because of a

Spanish Mountain Block A

- 13 - shallow dip or magnetite/overburden effects

EM Anomaly List

| | | | | | CX | 5500 HZ | CP | 7200 HZ | CP | 900 HZ | Vertical Dike | | Mag. Corr | |
|-------|--------|--------|----------|---------|-------|---------|--------|---------|--------|--------|---------------|--------|-----------|--|
| Label | Fid | Interp | XUTM | YUTM | Real | Quad | Real | Quad | Real | Quad | COND | DEPTH* | | |
| | | | m | m | ppm | ppm | ppm | ppm | ppm | ppm | siemens | m | NT | |
| LINE | 10480 | | FLIGHT 8 | | | | | | | | | | | |
| A | 6312.8 | S? | 604313 | 5824041 | 9.0 | 10.8 | 134.9 | 183.6 | 6.2 | 45.9 | 0.9 | 24 | 0 | |
| B | 6358.6 | D | 605273 | 5824961 | 70.7 | 64.4 | 368.7 | 292.8 | 8.7 | 128.5 | 2.4 | 4 | 0 | |
| C | 6360.9 | D | 605317 | 5825004 | 52.5 | 69.8 | 368.7 | 292.8 | 64.5 | 128.5 | 1.4 | 5 | 0 | |
| D | 6369.6 | B | 605467 | 5825148 | 173.1 | 61.6 | 1092.6 | 288.7 | 629.9 | 419.7 | 10.7 | 3 | 2 | |
| E | 6371.7 | D | 605502 | 5825181 | 218.2 | 25.6 | 1092.6 | 287.1 | 629.9 | 419.7 | 58.8 | 3 | 2 | |
| F | 6376.8 | B? | 605591 | 5825264 | 31.8 | 34.2 | 325.4 | 301.8 | 53.4 | 104.2 | 1.5 | 9 | 2 | |
| G | 6379.1 | D | 605632 | 5825302 | 61.1 | 41.8 | 327.3 | 301.8 | 42.8 | 106.9 | 3.2 | 10 | 1 | |
| H | 6397.2 | B | 605954 | 5825610 | 202.6 | 39.6 | 1375.6 | 281.2 | 1129.8 | 499.8 | 26.8 | 0 | 0 | |
| I | 6398.8 | B | 605982 | 5825636 | 214.6 | 62.3 | 1375.6 | 281.2 | 1129.8 | 499.8 | 15.3 | 0 | 0 | |
| J | 6406.4 | B | 606103 | 5825748 | 126.5 | 24.0 | 450.0 | 111.0 | 536.9 | 173.0 | 23.9 | 5 | 0 | |
| K | 6414.8 | B | 606224 | 5825862 | 154.3 | 86.7 | 521.2 | 442.8 | 90.3 | 203.5 | 5.6 | 2 | 11 | |
| L | 6425.9 | B | 606382 | 5826013 | 82.8 | 12.2 | 321.8 | 51.8 | 340.9 | 111.3 | 30.5 | 4 | 0 | |
| M | 6436.2 | B | 606538 | 5826168 | 0.8 | 6.1 | 34.9 | 35.0 | 192.5 | 33.5 | --- | --- | 0 | |
| N | 6442.6 | B | 606641 | 5826275 | 46.0 | 2.5 | 166.6 | 29.3 | 214.5 | 27.1 | 108.1 | 6 | 3 | |
| O | 6449.5 | D | 606759 | 5826388 | 22.6 | 7.9 | 29.3 | 36.0 | 52.7 | 17.3 | 5.6 | 29 | 0 | |
| P | 6457.8 | B | 606906 | 5826521 | 47.9 | 19.3 | 168.9 | 36.8 | 72.0 | 75.4 | 5.9 | 13 | 0 | |
| LINE | 10490 | | FLIGHT 3 | | | | | | | | | | | |
| A | 577.3 | S | 603621 | 5823176 | 16.6 | 63.6 | 108.9 | 505.8 | 3.7 | 72.2 | --- | --- | 9 | |
| B | 542.8 | S | 604345 | 5823881 | 45.6 | 85.3 | 346.3 | 553.9 | 10.0 | 118.2 | 1.0 | 0 | 0 | |
| C | 504.1 | D | 605340 | 5824829 | 69.2 | 57.3 | 206.8 | 206.1 | 45.6 | 77.5 | 2.6 | 0 | 2 | |
| D | 502.1 | D | 605397 | 5824883 | 32.2 | 41.9 | 206.8 | 206.1 | 46.3 | 77.5 | 1.2 | 8 | 2 | |
| E | 496.7 | B | 605550 | 5825030 | 172.6 | 21.8 | 545.6 | 124.3 | 398.1 | 256.3 | 48.8 | 0 | 53 | |
| F | 491.0 | D | 605703 | 5825179 | 84.1 | 29.1 | 235.2 | 133.8 | 82.4 | 90.8 | 8.8 | 3 | 0 | |
| G | 474.8 | B | 606057 | 5825510 | 451.5 | 145.9 | 2446.6 | 768.0 | 2017.4 | 1036.9 | 16.9 | 0 | 0 | |
| H | 470.4 | B | 606128 | 5825576 | 228.4 | 30.6 | 2446.6 | 71.9 | 2017.4 | 213.7 | 49.0 | 0 | 0 | |
| I | 462.5 | B | 606235 | 5825674 | 288.9 | 24.9 | 1199.5 | 354.7 | 987.5 | 552.5 | 102.3 | 0 | 3 | |
| J | 458.9 | B | 606282 | 5825718 | 162.1 | 38.5 | 1199.5 | 354.7 | 987.5 | 552.5 | 18.6 | 0 | 0 | |
| K | 447.5 | H | 606444 | 5825870 | 16.7 | 26.5 | 211.4 | 153.8 | 92.3 | 90.9 | 0.8 | 16 | 0 | |
| L | 445.2 | B | 606477 | 5825906 | 24.5 | 6.9 | 98.5 | 13.2 | 92.3 | 40.0 | 7.8 | 28 | 0 | |
| M | 425.8 | B | 606747 | 5826165 | 20.8 | 13.6 | 233.3 | 106.0 | 99.0 | 96.5 | 2.4 | 31 | 0 | |
| N | 416.8 | D | 606881 | 5826297 | 31.6 | 5.0 | 171.7 | 68.2 | 71.7 | 71.6 | 20.0 | 30 | 0 | |
| O | 412.3 | B | 606943 | 5826354 | 32.6 | 12.8 | 171.7 | 68.2 | 71.7 | 71.6 | 5.4 | 22 | 0 | |
| LINE | 10500 | | FLIGHT 3 | | | | | | | | | | | |
| A | 679.1 | S | 603836 | 5823180 | 8.0 | 27.4 | 59.0 | 242.2 | 1.4 | 35.6 | --- | --- | 4 | |
| B | 704.9 | S | 604484 | 5823790 | 34.9 | 65.4 | 236.9 | 361.7 | 8.8 | 78.8 | 0.9 | 0 | 0 | |

CX = COAXIAL

CP = COPLANAR

Note: EM values shown above
are local amplitudes

Spanish Mountain Block A

*Estimated Depth may be unreliable because the
stronger part of the conductor may be deeper or
to one side of the flight line, or because of a
shallow dip or magnetite/overburden effects

EM Anomaly List

| Label | Fid | Interp | XUTM m | YUTM m | CX 5500 HZ Real Quad ppm ppm | CP 7200 HZ Real Quad ppm ppm | CP 900 HZ Real Quad ppm ppm | Vertical Dike COND DEPTH* siemens m | Mag. Corr NT |
|-------|--------|--------|-----------|-----------|------------------------------------|------------------------------------|-----------------------------------|---|-----------------|
| LINE | 10500 | | FLIGHT 3 | | | | | | |
| C | 753.2 | D | 605475 | 5824753 | 72.2 49.8 | 146.9 123.1 | 24.2 39.0 | 3.3 5 | 32 |
| D | 762.4 | B | 605652 | 5824917 | 51.8 44.6 | 148.8 172.0 | 49.8 56.5 | 2.3 3 | 60 |
| E | 764.4 | D | 605689 | 5824948 | 52.5 18.3 | 148.8 172.0 | 28.9 56.5 | 7.4 9 | 0 |
| F | 783.5 | D | 606013 | 5825237 | 61.3 34.1 | 313.1 212.0 | 153.0 170.8 | 4.1 7 | 0 |
| G | 787.5 | B | 606070 | 5825297 | 42.1 36.1 | 313.1 212.0 | 153.0 170.8 | 2.1 12 | 0 |
| H | 797.1 | D | 606193 | 5825421 | 136.3 30.5 | 1230.0 377.3 | 481.2 562.7 | 19.2 7 | 0 |
| I | 800.3 | B | 606235 | 5825461 | 250.5 97.5 | 1230.0 352.6 | 862.5 562.7 | 10.7 0 | 0 |
| J | 805.2 | B? | 606301 | 5825526 | 44.0 23.7 | 242.8 106.9 | 862.5 147.6 | 3.9 13 | 9 |
| K | 807.9 | B | 606336 | 5825564 | 119.0 20.6 | 242.8 106.9 | 494.3 147.6 | 26.9 2 | 8 |
| L | 813.8 | D | 606416 | 5825642 | 37.5 45.9 | 505.0 267.7 | 230.4 226.3 | 1.4 5 | 16 |
| M | 817.3 | E | 606463 | 5825683 | 127.0 61.9 | 505.0 267.7 | 0.0 226.3 | 6.3 0 | 0 |
| N | 825.5 | B | 606564 | 5825772 | 59.2 27.2 | 334.8 32.5 | 432.6 153.3 | 5.3 14 | 0 |
| O | 839.5 | B | 606750 | 5825951 | 29.5 16.8 | 235.4 89.9 | 149.4 87.9 | 3.2 20 | 0 |
| P | 854.2 | B | 606971 | 5826161 | 9.2 2.6 | 225.0 8.6 | 151.1 123.3 | 5.5 53 | 0 |
| Q | 860.3 | E | 607070 | 5826261 | 62.4 18.0 | 299.7 47.8 | 164.3 131.1 | 10.3 19 | 0 |
| LINE | 10510 | | FLIGHT 3 | | | | | | |
| A | 1098.5 | S | 603918 | 5823031 | 6.3 21.1 | 29.0 130.3 | 0.8 21.2 | --- --- | 0 |
| B | 1070.8 | S? | 604545 | 5823645 | 21.1 45.2 | 195.3 299.2 | 6.1 63.3 | 0.7 0 | 0 |
| C | 1069.0 | S? | 604583 | 5823682 | 18.1 54.6 | 195.3 299.2 | 6.1 63.3 | 0.5 0 | 0 |
| D | 1029.6 | B? | 605589 | 5824649 | 15.9 5.1 | 62.9 35.3 | 32.5 25.8 | --- --- | 43 |
| E | 1024.5 | D | 605722 | 5824775 | 35.2 1.3 | 148.7 21.2 | 86.8 60.4 | 186.3 35 | 0 |
| F | 1007.1 | D | 606095 | 5825129 | 77.4 47.9 | 395.5 245.1 | 179.2 191.5 | 3.9 0 | 0 |
| G | 993.1 | B | 606341 | 5825365 | 239.5 89.2 | 900.5 270.3 | 342.9 392.5 | 11.2 0 | 8 |
| H | 986.1 | B | 606453 | 5825469 | 100.9 151.4 | 787.6 950.2 | 61.1 299.7 | 1.6 0 | 0 |
| I | 967.5 | E | 606712 | 5825727 | 26.1 0.2 | 232.1 72.9 | 267.7 88.7 | --- --- | 0 |
| J | 962.6 | B | 606768 | 5825783 | 35.7 4.8 | 277.1 17.8 | 284.9 78.9 | 26.2 28 | 0 |
| K | 957.1 | D | 606832 | 5825841 | 21.5 12.4 | 184.4 147.2 | 104.0 89.6 | 2.8 35 | 0 |
| L | 954.0 | D | 606870 | 5825874 | 31.5 12.3 | 184.4 9.0 | 104.0 89.6 | 5.3 31 | 0 |
| M | 939.8 | D | 607010 | 5825985 | 29.4 22.3 | 353.2 138.7 | 121.6 181.6 | 2.2 25 | 1 |
| N | 933.5 | B | 607077 | 5826053 | 48.9 30.5 | 326.9 151.1 | 330.3 102.6 | 3.3 10 | 0 |
| O | 917.5 | H | 607249 | 5826257 | 2.0 2.5 | 3.9 0.0 | 8.5 0.8 | --- --- | 0 |
| LINE | 10520 | | FLIGHT 3 | | | | | | |
| A | 1225.2 | S | 604706 | 5823590 | 16.2 38.6 | 152.8 268.3 | 5.6 53.5 | 0.6 0 | 0 |
| B | 1248.1 | D | 605161 | 5824022 | 22.7 33.7 | 60.4 42.4 | 2.6 15.5 | 1.0 6 | 76 |
| C | 1254.8 | S? | 605286 | 5824143 | 10.5 13.9 | 80.5 92.4 | 5.2 24.1 | --- --- | 0 |
| D | 1284.0 | D | 605853 | 5824691 | 16.7 2.3 | 154.1 39.1 | 124.9 61.4 | 20.1 47 | 0 |

CX = COAXIAL
CP = COPLANAR

Note:EM values shown above
are local amplitudes

*Estimated Depth may be unreliable because the
stronger part of the conductor may be deeper or
to one side of the flight line, or because of a

Spanish Mountain Block A

- 15 - shallow dip or magnetite/overburden effects

EM Anomaly List

| | | | | | CX | 5500 HZ | CP | 7200 HZ | CP | 900 HZ | | Vertical Dike | | Mag. Corr | |
|-------|--------|--------|----------|---------|-------|---------|-------|---------|-------|--------|-------|---------------|--------|-----------|--|
| Label | Fid | Interp | XUTM | YUTM | Real | Quad | Real | Quad | Real | Quad | | COND | DEPTH* | | |
| | | | m | m | ppm | ppm | ppm | ppm | ppm | ppm | | siemens | m | NT | |
| LINE | 10520 | | FLIGHT 3 | | | | | | | | | | | | |
| E | 1290.7 | B? | 605989 | 5824811 | 12.0 | 4.0 | 54.5 | 22.4 | 30.3 | 6.1 | 4.8 | 48 | | 16 | |
| F | 1303.3 | D | 606239 | 5825051 | 99.7 | 21.9 | 481.1 | 138.5 | 303.5 | 221.0 | 17.8 | 7 | | 0 | |
| G | 1351.2 | B | 607016 | 5825800 | 69.7 | 23.8 | 427.2 | 58.0 | 317.2 | 167.3 | 8.4 | 4 | | 0 | |
| H | 1355.4 | B | 607086 | 5825869 | 32.2 | 8.0 | 427.2 | 54.0 | 317.2 | 167.3 | 10.1 | 28 | | 0 | |
| I | 1362.9 | B | 607221 | 5825992 | 46.0 | 14.9 | 248.6 | 48.0 | 154.8 | 93.6 | 7.8 | 10 | | 0 | |
| LINE | 10530 | | FLIGHT 3 | | | | | | | | | | | | |
| A | 1584.9 | S | 604728 | 5823406 | 15.0 | 26.7 | 78.5 | 201.4 | 2.8 | 33.8 | 0.7 | 9 | | 0 | |
| B | 1564.0 | S? | 605238 | 5823892 | 12.8 | 15.5 | 39.8 | 74.1 | 3.0 | 13.9 | --- | --- | | 99 | |
| C | 1531.6 | H | 606016 | 5824637 | 16.3 | 3.5 | 137.9 | 19.0 | 113.7 | 54.2 | 9.9 | 41 | | 0 | |
| D | 1519.4 | B | 606284 | 5824902 | 69.4 | 25.5 | 795.4 | 239.5 | 588.7 | 344.0 | 7.6 | 2 | | 1 | |
| E | 1517.2 | B | 606329 | 5824945 | 199.1 | 15.2 | 795.4 | 239.5 | 588.7 | 344.0 | 108.1 | 0 | | 1 | |
| F | 1468.1 | E | 607068 | 5825631 | 47.0 | 24.0 | 334.4 | 135.0 | 129.6 | 149.6 | 4.2 | 10 | | 0 | |
| G | 1464.2 | D | 607110 | 5825675 | 25.2 | 16.0 | 334.4 | 135.0 | 191.9 | 149.6 | 2.6 | 23 | | 0 | |
| H | 1453.7 | B | 607223 | 5825786 | 32.9 | 7.5 | 446.9 | 30.7 | 453.4 | 121.4 | 11.5 | 29 | | 0 | |
| I | 1427.2 | D | 607519 | 5826084 | 43.3 | 19.4 | 90.2 | 37.7 | 0.0 | 43.9 | 4.9 | 19 | | 0 | |
| LINE | 10540 | | FLIGHT 3 | | | | | | | | | | | | |
| A | 1869.9 | S | 604599 | 5823073 | 13.7 | 22.3 | 80.0 | 145.7 | 3.5 | 28.1 | 0.7 | 18 | | 19 | |
| B | 1901.5 | D | 605340 | 5823787 | 15.3 | 27.2 | 33.0 | 58.2 | 0.4 | 10.8 | 0.7 | 6 | | 75 | |
| C | 1910.3 | S? | 605507 | 5823941 | 8.9 | 11.6 | 47.8 | 63.4 | 3.7 | 14.7 | --- | --- | | 0 | |
| D | 1941.9 | B | 606190 | 5824600 | 5.9 | 2.6 | 71.5 | 0.1 | 74.1 | 24.1 | 2.6 | 66 | | 0 | |
| E | 1953.2 | D | 606414 | 5824801 | 72.7 | 23.1 | 528.1 | 273.3 | 289.1 | 239.3 | 9.4 | 8 | | 0 | |
| F | 1956.6 | D | 606479 | 5824862 | 106.9 | 46.2 | 528.1 | 270.7 | 326.6 | 239.3 | 7.0 | 8 | | 0 | |
| G | 1993.0 | S? | 607050 | 5825409 | 5.8 | 47.8 | 29.7 | 216.0 | 0.7 | 31.1 | 0.1 | 0 | | 2 | |
| H | 2009.3 | B | 607229 | 5825598 | 60.6 | 25.1 | 468.5 | 49.3 | 324.7 | 208.0 | 6.1 | 12 | | 0 | |
| I | 2015.8 | B | 607315 | 5825679 | 121.8 | 33.6 | 487.3 | 49.9 | 362.0 | 202.1 | 13.7 | 6 | | 0 | |
| J | 2025.0 | D | 607437 | 5825780 | 36.5 | 17.5 | 290.7 | 106.8 | 137.4 | 128.3 | 4.3 | 21 | | 0 | |
| K | 2028.6 | E | 607482 | 5825829 | 46.0 | 20.7 | 290.7 | 106.8 | 137.4 | 128.3 | 5.0 | 17 | | 0 | |
| LINE | 10550 | | FLIGHT 3 | | | | | | | | | | | | |
| A | 2266.3 | S? | 604642 | 5822903 | 7.9 | 11.6 | 61.5 | 108.9 | 1.9 | 24.3 | --- | --- | | 1 | |
| B | 2235.6 | D | 605417 | 5823644 | 12.3 | 22.7 | 23.8 | 37.8 | 0.4 | 4.3 | 0.6 | 2 | | 0 | |
| C | 2201.5 | H | 606266 | 5824453 | 12.4 | 2.9 | 76.1 | 0.0 | 77.8 | 26.7 | 8.3 | 47 | | 0 | |
| D | 2184.4 | B | 606612 | 5824803 | 37.6 | 13.8 | 212.2 | 22.9 | 192.2 | 78.6 | 6.2 | 9 | | 0 | |
| E | 2180.7 | B? | 606675 | 5824867 | 26.3 | 21.4 | 212.2 | 97.9 | 192.2 | 78.6 | 2.0 | 12 | | 0 | |
| F | 2166.9 | H | 606907 | 5825081 | 2.6 | 20.9 | 60.9 | 138.7 | 16.5 | 33.4 | 0.1 | 2 | | 0 | |
| G | 2146.0 | H | 607222 | 5825364 | 8.2 | 4.9 | 22.0 | 20.8 | 7.4 | 10.7 | --- | --- | | 7 | |

CX = COAXIAL
CP = COPLANAR

Note:EM values shown above
are local amplitudes

*Estimated Depth may be unreliable because the
stronger part of the conductor may be deeper or
to one side of the flight line, or because of a

Spanish Mountain Block A

- 16 - shallow dip or magnetite/overburden effects

EM Anomaly List

| Label | Fid | Interp | XUTM m | YUTM m | CX 5500 HZ Real Quad ppm ppm | CP 7200 HZ Real Quad ppm ppm | CP 900 HZ Real Quad ppm ppm | Vertical Dike COND DEPTH* siemens m | Mag. Corr NT |
|------------|--------|--------|-----------|-----------|------------------------------------|------------------------------------|-----------------------------------|---|-----------------|
| LINE 10550 | | | FLIGHT 3 | | | | | | |
| H | 2133.6 | D | 607347 | 5825485 | 58.6 42.0 | 375.4 177.1 | 48.8 164.3 | 3.0 10 | 0 |
| I | 2127.3 | B | 607415 | 5825559 | 49.1 25.4 | 317.2 84.6 | 301.2 156.0 | 4.2 17 | 0 |
| J | 2115.8 | B | 607542 | 5825680 | 32.8 11.3 | 228.8 131.7 | 87.6 88.7 | 6.4 24 | 0 |
| LINE 10560 | | | FLIGHT 3 | | | | | | |
| A | 2408.1 | B? | 604829 | 5822883 | 14.3 12.2 | 35.9 110.4 | 4.5 13.9 | 1.5 26 | 20 |
| B | 2417.0 | S | 605038 | 5823082 | 5.1 27.4 | 41.8 199.4 | 1.5 31.3 | 0.2 0 | 0 |
| C | 2438.2 | B? | 605526 | 5823542 | 9.8 17.3 | 30.3 44.3 | 1.5 10.3 | --- --- | 0 |
| D | 2441.7 | B? | 605594 | 5823605 | 4.2 18.8 | 18.4 44.3 | 1.0 10.3 | 0.2 0 | 76 |
| E | 2476.3 | E | 606338 | 5824323 | 20.1 1.7 | 148.8 12.6 | 119.4 59.9 | 42.7 42 | 0 |
| F | 2478.0 | B | 606375 | 5824360 | 27.3 5.3 | 148.8 17.9 | 119.4 59.9 | 13.8 34 | 0 |
| G | 2483.0 | D | 606484 | 5824466 | 29.6 20.9 | 103.4 94.6 | 0.0 33.5 | 2.4 22 | 4 |
| H | 2501.2 | B | 606890 | 5824842 | 17.6 23.0 | 70.3 82.6 | 54.3 36.1 | 1.0 13 | 0 |
| I | 2506.8 | H | 607001 | 5824955 | 8.4 17.0 | 109.8 162.6 | 44.4 44.4 | 0.5 18 | 0 |
| J | 2528.2 | B | 607340 | 5825289 | 55.6 17.4 | 1206.6 254.7 | 918.6 432.1 | 8.8 20 | 3 |
| K | 2530.7 | B | 607373 | 5825319 | 248.4 29.0 | 1206.6 100.2 | 918.6 246.4 | 62.0 0 | 0 |
| L | 2543.0 | D | 607549 | 5825471 | 66.1 40.4 | 265.1 194.0 | 117.1 129.5 | 3.8 11 | 0 |
| LINE 10570 | | | FLIGHT 3 | | | | | | |
| A | 2737.8 | D | 604970 | 5822814 | 21.7 12.2 | 49.5 71.9 | 4.5 20.7 | 2.9 25 | 0 |
| B | 2709.2 | B? | 605659 | 5823469 | 5.2 10.5 | 18.6 29.5 | 1.8 6.7 | --- --- | 0 |
| C | 2676.3 | D | 606391 | 5824158 | 68.7 7.0 | 202.3 24.6 | 177.3 70.8 | 49.3 10 | 0 |
| D | 2673.0 | B | 606469 | 5824233 | 29.7 3.3 | 202.3 9.8 | 177.3 70.8 | 32.4 29 | 0 |
| E | 2664.4 | H | 606665 | 5824426 | 18.9 12.1 | 101.0 72.7 | 48.7 60.8 | 2.4 27 | 0 |
| F | 2656.4 | B | 606852 | 5824600 | 16.9 8.3 | 42.7 47.3 | 64.2 23.0 | 3.2 33 | 0 |
| G | 2644.1 | H | 607104 | 5824850 | 58.1 52.7 | 465.2 313.6 | 92.4 167.1 | 2.2 2 | 0 |
| H | 2619.8 | B | 607531 | 5825247 | 348.3 80.9 | 2355.5 387.7 | 2083.3 719.2 | 24.8 0 | 0 |
| I | 2605.7 | H | 607701 | 5825416 | 9.1 4.9 | 58.7 47.0 | 47.9 44.2 | 2.3 49 | 0 |
| LINE 10580 | | | FLIGHT 3 | | | | | | |
| A | 2894.7 | S | 604850 | 5822489 | 10.1 32.1 | 71.1 187.4 | 3.7 34.4 | 0.4 0 | 73 |
| B | 2906.9 | D | 605126 | 5822748 | 15.5 8.0 | 22.2 7.1 | 4.6 7.9 | 2.9 39 | 0 |
| C | 2973.4 | E | 606520 | 5824073 | 56.1 5.7 | 280.0 33.8 | 231.2 97.4 | 45.7 21 | 0 |
| D | 2974.7 | B | 606546 | 5824098 | 25.4 5.7 | 280.0 33.8 | 231.2 97.4 | 10.8 36 | 0 |
| E | 2986.8 | B | 606827 | 5824370 | 22.4 3.4 | 66.9 47.2 | 58.5 39.7 | 18.4 30 | 0 |
| F | 2994.9 | B | 607037 | 5824567 | 23.1 0.0 | 252.7 21.6 | 344.7 27.3 | 999.0 44 | 0 |
| G | 3004.6 | B | 607276 | 5824799 | 30.6 20.7 | 313.7 104.0 | 239.7 100.4 | 2.6 10 | 0 |
| H | 3021.6 | B | 607601 | 5825107 | 53.9 15.6 | 706.5 324.5 | 232.6 299.3 | 9.7 12 | 0 |

CX = COAXIAL
CP = COPLANAR

Note:EM values shown above
are local amplitudes

*Estimated Depth may be unreliable because the
stronger part of the conductor may be deeper or
to one side of the flight line, or because of a

Spanish Mountain Block A

- 17 - shallow dip or magnetite/overburden effects

EM Anomaly List

| | | | | | | CX | 5500 HZ | CP | 7200 HZ | CP | 900 HZ | Vertical Dike | | Mag. Corr | |
|-------|--------|--------|----------|---------|--|------|---------|-------|---------|-------|--------|---------------|--------|-----------|--|
| Label | Fid | Interp | XUTM | YUTM | | Real | Quad | Real | Quad | Real | Quad | COND | DEPTH* | | |
| | | | m | m | | ppm | ppm | ppm | ppm | ppm | ppm | siemens | m | NT | |
| LINE | 10580 | | FLIGHT 3 | | | | | | | | | | | | |
| I | 3028.3 | D | 607688 | 5825202 | | 81.9 | 40.7 | 534.0 | 229.7 | 228.0 | 246.2 | 5.3 | 9 | 0 | |
| LINE | 19020 | | FLIGHT 4 | | | | | | | | | | | | |
| B | 527.7 | S | 602060 | 5826832 | | 9.2 | 20.8 | 76.7 | 200.2 | 4.9 | 34.8 | 0.5 | 5 | 0 | |
| LINE | 19030 | | FLIGHT 3 | | | | | | | | | | | | |
| A | 6874.0 | H | 603041 | 5827986 | | 13.1 | 7.8 | 107.5 | 66.5 | 30.6 | 29.1 | 2.3 | 27 | 0 | |
| B | 6824.8 | B? | 604343 | 5826642 | | 48.9 | 43.2 | 279.4 | 207.2 | 48.5 | 104.8 | 2.2 | 3 | 0 | |
| C | 6815.4 | B? | 604603 | 5826367 | | 51.5 | 71.2 | 278.0 | 457.0 | 6.7 | 90.2 | 1.4 | 2 | 0 | |
| D | 6795.2 | H | 605105 | 5825824 | | 11.9 | 17.3 | 60.0 | 58.4 | 42.3 | 21.5 | 0.8 | 15 | 0 | |
| E | 6770.9 | H | 605728 | 5825175 | | 7.0 | 6.7 | 133.2 | 47.8 | 39.1 | 63.3 | 1.0 | 27 | 0 | |
| F | 6755.5 | H | 606114 | 5824774 | | 9.0 | 1.4 | 77.1 | 24.9 | 55.8 | 30.1 | 12.9 | 60 | 0 | |
| LINE | 19040 | | FLIGHT 3 | | | | | | | | | | | | |
| A | 6407.3 | H | 603427 | 5829765 | | 24.5 | 10.3 | 238.7 | 69.3 | 142.7 | 99.0 | 4.4 | 26 | 0 | |
| B | 6427.3 | B | 603907 | 5829279 | | 21.4 | 8.6 | 163.9 | 10.1 | 129.5 | 66.1 | 4.5 | 30 | 0 | |
| C | 6433.0 | B | 604040 | 5829137 | | 57.1 | 14.0 | 232.6 | 83.5 | 186.6 | 93.0 | 12.5 | 11 | 0 | |
| D | 6436.9 | H | 604130 | 5829040 | | 11.9 | 10.3 | 203.2 | 0.0 | 78.9 | 90.4 | 1.4 | 33 | 0 | |
| E | 6456.2 | H | 604580 | 5828573 | | 84.3 | 19.9 | 784.7 | 118.1 | 642.4 | 239.6 | 15.1 | 9 | 0 | |
| F | 6479.9 | H | 605063 | 5828017 | | 11.6 | 2.7 | 130.9 | 22.4 | 123.6 | 26.6 | 7.9 | 47 | 0 | |
| G | 6492.9 | H | 605400 | 5827668 | | 12.2 | 0.0 | 134.1 | 13.1 | 100.5 | 35.2 | 888.0 | 55 | 0 | |
| H | 6508.4 | B | 605800 | 5827278 | | 35.2 | 9.1 | 361.7 | 74.1 | 281.2 | 157.0 | 9.8 | 15 | 0 | |
| I | 6531.1 | H | 606237 | 5826808 | | 11.5 | 10.3 | 47.7 | 85.4 | 55.3 | 18.2 | 1.3 | 33 | 0 | |
| J | 6540.1 | D | 606407 | 5826618 | | 40.8 | 8.9 | 155.4 | 19.4 | 168.8 | 41.0 | 13.3 | 22 | 0 | |
| K | 6542.3 | D | 606446 | 5826573 | | 23.8 | 3.2 | 155.4 | 19.4 | 168.8 | 41.0 | 22.7 | 31 | 0 | |
| L | 6564.6 | B | 606851 | 5826173 | | 20.7 | 8.9 | 307.0 | 90.1 | 162.7 | 148.2 | 4.1 | 32 | 0 | |
| M | 6568.8 | B | 606936 | 5826085 | | 21.2 | 2.5 | 234.3 | 91.5 | 129.1 | 148.2 | 26.2 | 46 | 0 | |
| N | 6571.5 | H | 606986 | 5826035 | | 13.3 | 13.4 | 234.3 | 91.5 | 129.1 | 93.9 | 1.2 | 27 | 0 | |
| O | 6582.6 | E | 607148 | 5825868 | | 36.2 | 8.2 | 239.2 | 56.9 | 259.8 | 101.8 | 12.0 | 29 | 0 | |
| P | 6585.2 | H | 607185 | 5825826 | | 7.2 | 2.5 | 239.2 | 55.0 | 259.8 | 101.8 | 3.9 | 62 | 0 | |
| Q | 6597.9 | B | 607381 | 5825598 | | 16.5 | 1.1 | 143.6 | 13.2 | 306.7 | 96.8 | 60.1 | 36 | 0 | |
| R | 6603.7 | D | 607490 | 5825479 | | 85.7 | 20.3 | 232.4 | 192.2 | 234.8 | 103.5 | 15.2 | 8 | 0 | |
| S | 6607.9 | B | 607571 | 5825402 | | 35.6 | 37.0 | 274.1 | 192.2 | 34.5 | 97.8 | 1.6 | 13 | 0 | |
| T | 6617.2 | B | 607741 | 5825223 | | 39.3 | 19.1 | 201.6 | 122.5 | 98.1 | 95.0 | 4.3 | 21 | 0 | |
| LINE | 30010 | | FLIGHT 1 | | | | | | | | | | | | |
| A | 448.6 | H | 602904 | 5827183 | | 13.6 | 12.3 | 53.5 | 71.2 | 9.8 | 22.8 | 1.4 | 24 | 0 | |
| B | 490.5 | B | 603777 | 5827997 | | 13.4 | 3.3 | 48.4 | 13.4 | 58.6 | 14.1 | 7.6 | 43 | 1 | |

CX = COAXIAL
CP = COPLANAR

Note:EM values shown above
are local amplitudes

*Estimated Depth may be unreliable because the
stronger part of the conductor may be deeper or
to one side of the flight line, or because of a

Spanish Mountain Block A

- 18 - shallow dip or magnetite/overburden effects

EM Anomaly List

| Label | Fid | Interp | XUTM m | YUTM m | CX 5500 HZ Real Quad ppm ppm | CP 7200 HZ Real Quad ppm ppm | CP 900 HZ Real Quad ppm ppm | Vertical Dike COND DEPTH* siemens m | Mag. Corr NT |
|------------|--------|--------|-----------|-----------|------------------------------------|------------------------------------|-----------------------------------|---|-----------------|
| LINE 30010 | | | FLIGHT 1 | | | | | | |
| C | 498.9 | B | 603950 | 5828176 | 10.0 1.9 | 79.1 0.0 | 76.2 27.2 | 10.1 38 | 1 |
| D | 521.9 | B | 604443 | 5828664 | 65.2 9.9 | 348.8 30.0 | 308.3 86.8 | 26.6 0 | 0 |
| E | 531.8 | B | 604692 | 5828876 | 36.0 14.8 | 138.3 67.7 | 26.3 70.3 | 5.2 21 | 0 |
| F | 537.4 | D | 604797 | 5828984 | 64.5 19.0 | 233.2 72.9 | 157.5 86.4 | 10.0 18 | 2 |
| G | 540.8 | D | 604848 | 5829044 | 15.5 0.4 | 233.2 72.9 | 157.5 86.4 | 205.2 47 | 2 |
| H | 543.6 | B | 604891 | 5829089 | 12.4 5.0 | 113.7 30.1 | 137.2 36.3 | 3.7 47 | 3 |
| I | 551.4 | H | 605020 | 5829187 | 14.0 4.9 | 98.2 42.5 | 52.6 39.8 | 4.7 47 | 1 |
| J | 557.7 | H | 605119 | 5829266 | 15.5 4.5 | 159.9 23.5 | 67.9 68.7 | 6.3 37 | 0 |
| K | 574.8 | B | 605349 | 5829503 | 30.9 17.1 | 206.3 95.2 | 85.5 87.2 | 3.3 17 | 1 |
| LINE 30020 | | | FLIGHT 1 | | | | | | |
| A | 773.7 | S? | 602936 | 5826978 | 14.7 6.9 | 96.9 99.0 | 10.8 30.6 | 3.2 28 | 0 |
| B | 765.5 | H | 603119 | 5827155 | 5.1 10.0 | 83.9 77.6 | 30.7 38.9 | 0.4 18 | 3 |
| C | 724.6 | B | 603898 | 5827892 | 11.5 4.4 | 187.4 0.0 | 178.7 35.2 | 3.9 46 | 0 |
| D | 716.8 | B | 604028 | 5828019 | 91.0 12.1 | 591.1 166.4 | 390.8 230.0 | 36.6 1 | 0 |
| E | 703.9 | B | 604235 | 5828207 | 92.4 20.2 | 450.4 92.9 | 362.1 135.0 | 17.4 5 | 0 |
| F | 695.5 | E | 604361 | 5828346 | 29.5 6.6 | 151.6 21.5 | 159.4 49.9 | 11.4 31 | 0 |
| G | 693.1 | H | 604399 | 5828383 | 0.0 1.3 | 151.6 21.5 | 172.5 49.9 | 0.1 9 | 0 |
| H | 683.6 | B | 604556 | 5828528 | 103.0 20.2 | 586.6 84.9 | 474.1 171.8 | 21.2 0 | 0 |
| I | 671.5 | B | 604809 | 5828778 | 17.7 8.8 | 68.6 50.7 | 9.9 49.1 | 3.2 24 | 0 |
| J | 669.1 | D | 604862 | 5828823 | 22.6 12.1 | 68.6 50.7 | 14.8 49.1 | 3.1 26 | 0 |
| K | 663.8 | D | 604979 | 5828927 | 19.2 7.2 | 167.6 7.0 | 179.1 26.9 | 4.8 25 | 0 |
| L | 662.2 | H | 605015 | 5828960 | 36.6 7.4 | 167.6 7.0 | 179.1 25.7 | 14.3 12 | 2 |
| M | 650.7 | B | 605249 | 5829181 | 19.1 4.3 | 176.0 34.0 | 126.7 63.0 | 9.9 31 | 1 |
| N | 639.3 | D | 605446 | 5829379 | 45.8 18.1 | 0.0 35.0 | 0.0 0.0 | 5.9 7 | 1 |
| LINE 30030 | | | FLIGHT 1 | | | | | | |
| A | 892.9 | H | 603260 | 5827084 | 21.9 6.8 | 124.9 69.5 | 48.0 52.8 | 6.5 26 | 4 |
| B | 936.1 | B | 603999 | 5827797 | 16.1 3.5 | 190.7 0.8 | 179.2 55.1 | 9.9 28 | 0 |
| C | 949.3 | B | 604187 | 5827983 | 160.4 33.0 | 1012.3 168.0 | 786.3 354.6 | 22.9 0 | 0 |
| D | 956.6 | B | 604297 | 5828092 | 79.9 22.1 | 576.0 87.9 | 487.3 155.3 | 11.9 9 | 1 |
| E | 972.0 | B | 604547 | 5828311 | 47.1 15.7 | 259.3 89.7 | 177.5 115.0 | 7.6 22 | 0 |
| F | 985.6 | H | 604801 | 5828564 | 79.4 11.8 | 343.5 36.1 | 322.8 98.9 | 29.4 9 | 0 |
| G | 993.4 | H | 604965 | 5828714 | 29.7 7.3 | 109.3 44.5 | 62.6 43.6 | 10.0 26 | 1 |
| H | 1003.1 | B | 605148 | 5828883 | 102.8 27.9 | 397.1 72.1 | 340.5 105.6 | 13.2 5 | 4 |
| I | 1005.5 | B | 605186 | 5828919 | 42.0 8.6 | 397.1 72.1 | 340.5 105.6 | 14.8 21 | 4 |
| J | 1021.2 | B | 605410 | 5829143 | 32.6 13.3 | 305.2 43.3 | 236.5 107.8 | 5.1 21 | 0 |

CX = COAXIAL

CP = COPLANAR

Note:EM values shown above
are local amplitudes

Spanish Mountain Block A

*Estimated Depth may be unreliable because the
stronger part of the conductor may be deeper or
to one side of the flight line, or because of a
shallow dip or magnetite/overburden effects

EM Anomaly List

| LINE | Fid | Interp | XUTM m | YUTM m | CX 5500 HZ Real Quad ppm ppm | CP 7200 HZ Real Quad ppm ppm | CP 900 HZ Real Quad ppm ppm | Vertical Dike COND DEPTH* siemens m | Mag. Corr NT |
|------------|--------|--------|-----------|-----------|------------------------------------|------------------------------------|-----------------------------------|---|-----------------|
| LINE 30040 | | | FLIGHT 1 | | | | | | |
| A | 1219.3 | B | 603306 | 5826908 | 35.0 12.0 | 333.0 91.4 | 150.5 147.3 | 6.6 18 | 0 |
| B | 1160.1 | D | 604104 | 5827678 | 79.0 24.7 | 330.2 71.5 | 214.8 120.4 | 9.9 0 | 0 |
| C | 1153.0 | D | 604216 | 5827791 | 72.3 25.7 | 263.5 141.5 | 135.2 145.1 | 8.0 4 | 0 |
| D | 1147.4 | B | 604306 | 5827877 | 97.3 5.6 | 377.5 156.2 | 190.9 207.4 | 128.5 2 | 0 |
| E | 1142.6 | B | 604389 | 5827958 | 143.9 9.8 | 1225.9 182.6 | 1025.8 369.4 | 115.9 1 | 0 |
| F | 1136.5 | B | 604504 | 5828069 | 66.3 12.3 | 290.0 12.3 | 262.5 90.8 | 19.9 3 | 13 |
| G | 1129.2 | D | 604646 | 5828209 | 41.4 6.9 | 44.3 9.6 | 49.5 24.5 | 19.9 10 | 0 |
| H | 1127.6 | B | 604677 | 5828240 | 16.2 2.3 | 44.3 9.6 | 49.5 24.5 | 18.8 26 | 0 |
| I | 1118.7 | B | 604864 | 5828427 | 55.0 10.5 | 279.2 37.8 | 238.8 77.4 | 17.9 0 | 0 |
| J | 1108.7 | H | 605126 | 5828662 | 61.7 10.3 | 133.1 34.8 | 86.5 52.9 | 23.0 9 | 0 |
| K | 1103.2 | H | 605265 | 5828790 | 39.6 7.9 | 252.8 36.8 | 217.2 69.2 | 15.2 17 | 4 |
| L | 1097.6 | H | 605388 | 5828904 | 14.6 4.0 | 243.2 17.2 | 217.4 59.7 | 6.8 40 | 0 |
| LINE 30050 | | | FLIGHT 1 | | | | | | |
| A | 1472.0 | D | 603014 | 5826440 | 9.7 12.6 | 12.3 20.7 | 2.6 3.6 | --- --- | 0 |
| B | 1488.8 | B? | 603324 | 5826740 | 21.8 3.4 | 125.5 38.5 | 64.0 55.2 | 18.2 29 | 0 |
| C | 1492.5 | B? | 603389 | 5826799 | 21.8 7.1 | 125.5 38.5 | 64.0 55.2 | 6.0 27 | 0 |
| D | 1549.1 | B | 604149 | 5827526 | 134.6 37.8 | 991.2 232.7 | 725.4 393.0 | 13.8 0 | 0 |
| E | 1553.7 | B | 604194 | 5827571 | 128.5 0.0 | 991.2 232.7 | 725.4 393.0 | 999.0 3 | 0 |
| F | 1567.3 | D | 604353 | 5827709 | 101.4 49.1 | 564.8 269.4 | 286.3 278.0 | 5.9 1 | 2 |
| G | 1575.2 | H | 604459 | 5827816 | 13.5 23.5 | 210.0 91.0 | 108.5 87.0 | 0.7 0 | 0 |
| H | 1587.9 | B | 604668 | 5828031 | 62.1 8.4 | 147.5 28.2 | 147.6 45.1 | 31.3 1 | 1 |
| I | 1593.3 | B | 604804 | 5828154 | 32.0 9.2 | 81.8 25.1 | 71.2 31.7 | 8.3 18 | 0 |
| J | 1600.3 | H | 605006 | 5828331 | 23.9 4.6 | 156.9 7.9 | 178.1 20.3 | 13.5 21 | 0 |
| K | 1613.2 | H | 605334 | 5828651 | 15.4 12.0 | 191.4 47.5 | 116.5 79.3 | 1.7 26 | 0 |
| L | 1627.4 | B | 605619 | 5828919 | 52.1 13.2 | 391.2 75.7 | 292.4 148.3 | 11.7 17 | 0 |
| LINE 30060 | | | FLIGHT 1 | | | | | | |
| A | 1869.2 | S | 602659 | 5825885 | 15.9 13.4 | 46.5 57.0 | 1.7 12.4 | 1.6 31 | 35 |
| B | 1837.7 | D | 603337 | 5826531 | 26.1 15.3 | 121.9 75.5 | 76.9 56.5 | 2.9 14 | 0 |
| C | 1833.0 | H | 603418 | 5826612 | 15.3 7.2 | 121.9 22.9 | 75.4 56.5 | 3.3 21 | 0 |
| D | 1771.1 | B | 604347 | 5827499 | 131.4 37.7 | 805.4 74.2 | 697.3 237.4 | 13.2 0 | 0 |
| E | 1764.0 | D | 604471 | 5827608 | 57.1 26.9 | 176.9 137.2 | 11.4 97.8 | 5.0 8 | 1 |
| F | 1759.4 | D | 604543 | 5827687 | 62.3 19.8 | 317.0 138.2 | 214.0 139.0 | 8.9 8 | 0 |
| G | 1747.1 | H | 604732 | 5827889 | 31.6 6.3 | 314.4 42.3 | 261.2 126.6 | 14.1 20 | 2 |
| H | 1726.5 | H | 605122 | 5828243 | 52.2 13.5 | 279.6 40.8 | 232.3 81.4 | 11.3 16 | 0 |
| I | 1720.8 | H | 605244 | 5828358 | 26.5 3.1 | 80.5 18.1 | 33.9 25.0 | 28.6 24 | 0 |

CX = COAXIAL

CP = COPLANAR

Note: EM values shown above
are local amplitudes

Spanish Mountain Block A

*Estimated Depth may be unreliable because the
stronger part of the conductor may be deeper or
to one side of the flight line, or because of a
shallow dip or magnetite/overburden effects

EM Anomaly List

| | | | | | CX 5500 HZ | | CP 7200 HZ | | CP 900 HZ | | Vertical Dike | | Mag. Corr |
|-------|--------|--------|----------|---------|------------|------|------------|-------|-----------|-------|---------------|--------|-----------|
| Label | Fid | Interp | XUTM | YUTM | Real | Quad | Real | Quad | Real | Quad | COND | DEPTH* | |
| | | | | | ppm | ppm | ppm | ppm | ppm | ppm | siemens | m | NT |
| LINE | 30060 | | FLIGHT 1 | | | | | | | | | | |
| J | 1708.0 | D | 605553 | 5828654 | 15.0 | 7.9 | 86.0 | 70.1 | 194.8 | 48.2 | 2.8 | 29 | 0 |
| K | 1703.6 | B | 605654 | 5828749 | 17.4 | 0.0 | 228.4 | 3.9 | 194.8 | 67.3 | 999.0 | 36 | 0 |
| LINE | 30070 | | FLIGHT 1 | | | | | | | | | | |
| A | 2008.4 | D | 603514 | 5826506 | 31.2 | 9.1 | 167.7 | 60.8 | 119.1 | 73.3 | 8.0 | 20 | 0 |
| B | 2057.5 | B | 604378 | 5827309 | 64.3 | 20.9 | 516.4 | 82.8 | 376.5 | 210.7 | 8.7 | 0 | 0 |
| C | 2065.8 | B | 604451 | 5827413 | 100.7 | 10.7 | 593.5 | 82.0 | 461.7 | 188.7 | 52.9 | 3 | 0 |
| D | 2080.8 | D | 604618 | 5827558 | 51.2 | 19.6 | 196.2 | 114.3 | 81.0 | 86.8 | 6.4 | 9 | 0 |
| E | 2087.7 | B | 604716 | 5827653 | 48.8 | 20.5 | 187.1 | 84.9 | 183.2 | 92.1 | 5.6 | 11 | 0 |
| F | 2090.6 | B | 604760 | 5827696 | 2.0 | 17.0 | 187.1 | 51.6 | 183.2 | 92.1 | 0.1 | 0 | 1 |
| G | 2094.9 | E | 604826 | 5827763 | 58.7 | 19.7 | 222.4 | 45.3 | 177.5 | 105.6 | 8.1 | 3 | 0 |
| H | 2102.4 | B | 604968 | 5827910 | 34.9 | 9.3 | 22.7 | 45.1 | 0.0 | 4.7 | 9.4 | 23 | 0 |
| I | 2111.0 | H | 605196 | 5828117 | 23.6 | 4.5 | 139.8 | 1.0 | 209.1 | 4.6 | 13.8 | 23 | 0 |
| J | 2116.9 | H | 605372 | 5828253 | 27.5 | 7.8 | 75.5 | 26.5 | 47.0 | 33.5 | 8.0 | 16 | 0 |
| K | 2126.7 | H | 605607 | 5828487 | 20.7 | 6.0 | 119.8 | 31.7 | 144.4 | 45.1 | 7.1 | 29 | 1 |
| L | 2144.0 | H | 605911 | 5828788 | 22.9 | 4.1 | 215.7 | 16.7 | 198.5 | 72.3 | 15.0 | 34 | 0 |

CX = COAXIAL

CP = COPLANAR

Note: EM values shown above
are local amplitudes

Spanish Mountain Block A

- 21 -

*Estimated Depth may be unreliable because the
stronger part of the conductor may be deeper or
to one side of the flight line, or because of a
shallow dip or magnetite/overburden effects

EM Anomaly List

| | | | | | CX | 5500 HZ | CP | 7200 HZ | CP | 900 HZ | | Vertical Dike | | Mag. Corr | |
|-------|--------|--------|----------|---------|-------|---------|--------|---------|--------|--------|------|---------------|--------|-----------|--|
| Label | Fid | Interp | XUTM | YUTM | Real | Quad | Real | Quad | Real | Quad | | COND | DEPTH* | | |
| | | | m | m | ppm | ppm | ppm | ppm | ppm | ppm | | siemens | m | NT | |
| LINE | 20010 | | FLIGHT 4 | | | | | | | | | | | | |
| A | 3810.5 | B | 603295 | 5828168 | 403.1 | 109.6 | 2153.8 | 342.9 | 1576.4 | 797.0 | 20.8 | 0 | | 0 | |
| B | 3750.4 | H | 604499 | 5827111 | 15.9 | 13.4 | 56.6 | 43.9 | 12.3 | 20.9 | 1.6 | 26 | | 0 | |
| LINE | 20020 | | FLIGHT 4 | | | | | | | | | | | | |
| A | 3604.6 | B | 603390 | 5828208 | 45.0 | 11.6 | 278.1 | 31.1 | 222.8 | 107.8 | 10.7 | 0 | | 0 | |
| B | 3637.3 | B | 604140 | 5827535 | 17.1 | 13.4 | 219.9 | 97.3 | 124.5 | 90.1 | 1.8 | 13 | | 0 | |
| C | 3651.6 | B | 604428 | 5827256 | 23.9 | 8.1 | 246.4 | 43.6 | 156.0 | 122.4 | 5.9 | 32 | | 2 | |
| D | 3657.7 | B | 604564 | 5827138 | 23.2 | 3.7 | 128.3 | 11.1 | 131.8 | 58.6 | 17.4 | 32 | | 0 | |
| LINE | 20030 | | FLIGHT 4 | | | | | | | | | | | | |
| A | 3554.9 | B | 603193 | 5828460 | 155.1 | 42.7 | 833.4 | 190.0 | 532.4 | 274.5 | 14.8 | 1 | | 1 | |
| B | 3547.1 | B | 603388 | 5828289 | 35.0 | 10.8 | 151.0 | 44.5 | 131.9 | 56.0 | 7.7 | 6 | | 1 | |
| C | 3539.4 | B | 603572 | 5828121 | 18.0 | 1.8 | 121.1 | 5.7 | 112.3 | 36.8 | 32.5 | 45 | | 0 | |
| D | 3510.5 | B | 604195 | 5827575 | 113.2 | 41.2 | 686.9 | 326.6 | 921.9 | 488.0 | 9.0 | 4 | | 0 | |
| E | 3504.1 | B | 604336 | 5827439 | 75.6 | 36.7 | 841.3 | 280.0 | 411.4 | 379.3 | 5.3 | 5 | | 0 | |
| F | 3500.8 | B | 604408 | 5827374 | 64.1 | 43.7 | 841.3 | 149.1 | 411.4 | 379.3 | 3.3 | 2 | | 0 | |
| G | 3491.4 | B | 604590 | 5827229 | 36.8 | 6.9 | 111.9 | 0.0 | 126.2 | 32.9 | 16.1 | 29 | | 0 | |
| H | 3485.1 | B | 604701 | 5827128 | 83.7 | 29.9 | 746.3 | 246.2 | 539.0 | 334.2 | 8.4 | 15 | | 0 | |
| LINE | 20040 | | FLIGHT 4 | | | | | | | | | | | | |
| A | 3336.2 | B | 603282 | 5828486 | 89.7 | 18.4 | 609.7 | 62.0 | 534.5 | 128.1 | 18.9 | 4 | | 111 | |
| B | 3352.5 | B | 603654 | 5828165 | 11.9 | 2.9 | 80.4 | 3.9 | 59.1 | 21.9 | 7.4 | 54 | | 0 | |
| C | 3368.2 | B | 604010 | 5827826 | 75.4 | 29.3 | 564.4 | 132.9 | 424.8 | 181.2 | 7.2 | 5 | | 0 | |
| D | 3380.6 | B | 604274 | 5827602 | 80.4 | 26.1 | 432.6 | 124.1 | 295.5 | 173.2 | 9.4 | 13 | | 2 | |
| E | 3385.8 | B | 604385 | 5827507 | 89.1 | 12.4 | 400.5 | 92.6 | 308.8 | 151.4 | 34.0 | 8 | | 0 | |
| F | 3388.3 | B | 604436 | 5827465 | 66.3 | 25.3 | 400.5 | 92.6 | 308.8 | 151.4 | 7.1 | 12 | | 0 | |
| G | 3393.4 | B | 604538 | 5827374 | 45.6 | 4.1 | 291.5 | 16.4 | 269.8 | 63.8 | 51.2 | 17 | | 0 | |
| H | 3400.0 | B | 604682 | 5827230 | 21.1 | 6.3 | 371.6 | 9.6 | 313.8 | 30.8 | 6.8 | 21 | | 0 | |
| I | 3404.4 | E | 604791 | 5827126 | 73.4 | 17.0 | 371.6 | 66.9 | 313.8 | 134.5 | 14.8 | 12 | | 0 | |
| LINE | 20050 | | FLIGHT 4 | | | | | | | | | | | | |
| A | 3292.6 | B | 603306 | 5828564 | 51.6 | 5.8 | 492.0 | 34.9 | 483.0 | 78.9 | 38.4 | 6 | | 0 | |
| B | 3263.7 | B | 603972 | 5827968 | 34.4 | 12.5 | 201.5 | 108.9 | 108.7 | 66.8 | 6.1 | 10 | | 0 | |
| C | 3243.5 | H | 604393 | 5827583 | 12.5 | 9.5 | 89.3 | 73.8 | 98.5 | 23.1 | 1.6 | 36 | | 2 | |
| D | 3235.2 | B | 604555 | 5827442 | 30.6 | 19.1 | 178.7 | 114.2 | 77.1 | 58.9 | 2.8 | 25 | | 2 | |
| E | 3228.7 | D | 604672 | 5827345 | 108.2 | 39.0 | 324.6 | 206.1 | 121.1 | 167.8 | 9.0 | 10 | | 0 | |
| F | 3221.7 | B | 604800 | 5827233 | 53.2 | 8.4 | 296.0 | 46.6 | 247.3 | 104.1 | 23.5 | 10 | | 0 | |

CX = COAXIAL

CP = COPLANAR

Note: EM values shown above
are local amplitudes

Spanish Mountain Block B

*Estimated Depth may be unreliable because the
stronger part of the conductor may be deeper or
to one side of the flight line, or because of a
shallow dip or magnetite/overburden effects

EM Anomaly List

| LINE | Fid | Interp | XUTM m | YUTM m | CX 5500 HZ Real Quad ppm ppm | CP 7200 HZ Real Quad ppm ppm | CP 900 HZ Real Quad ppm ppm | Vertical Dike COND DEPTH* siemens m | Mag. Corr NT |
|------------|--------|--------|-----------|-----------|------------------------------------|------------------------------------|-----------------------------------|---|-----------------|
| LINE 20060 | | | FLIGHT 4 | | | | | | |
| A | 2970.3 | B | 603424 | 5828560 | 119.3 4.7 | 685.2 79.4 | 678.8 191.9 | 244.8 0 | 0 |
| B | 3000.5 | B | 604075 | 5827981 | 146.4 48.8 | 1047.7 303.6 | 639.6 396.3 | 11.1 0 | 0 |
| C | 3003.2 | B | 604133 | 5827933 | 68.9 7.1 | 1047.7 273.3 | 639.6 387.8 | 49.0 11 | 0 |
| D | 3005.7 | B | 604186 | 5827890 | 64.3 9.1 | 641.3 273.3 | 429.5 387.8 | 29.7 14 | 0 |
| E | 3015.4 | D | 604350 | 5827743 | 125.2 17.1 | 631.9 151.4 | 286.1 295.4 | 38.8 9 | 0 |
| F | 3019.1 | D | 604409 | 5827690 | 73.4 25.2 | 631.9 236.1 | 286.1 295.4 | 8.5 11 | 0 |
| G | 3024.2 | D | 604496 | 5827615 | 24.6 12.3 | 570.9 144.5 | 172.3 238.0 | 3.5 23 | 0 |
| H | 3039.4 | B | 604774 | 5827346 | 53.6 23.7 | 328.8 143.3 | 177.9 118.8 | 5.4 10 | 0 |
| I | 3043.2 | B | 604861 | 5827265 | 66.4 11.2 | 279.7 143.3 | 180.4 113.7 | 23.1 0 | 0 |
| LINE 20070 | | | FLIGHT 4 | | | | | | |
| A | 2926.4 | B | 603435 | 5828640 | 189.1 40.9 | 1400.1 199.5 | 1229.1 442.8 | 22.5 1 | 0 |
| B | 2915.0 | B? | 603702 | 5828415 | 16.4 5.8 | 56.6 17.5 | 32.9 29.7 | 4.9 12 | 0 |
| C | 2893.7 | B | 604186 | 5827974 | 159.4 26.4 | 1187.4 290.7 | 1050.7 528.1 | 31.8 7 | 0 |
| D | 2891.4 | B | 604237 | 5827923 | 308.8 94.7 | 1187.4 412.6 | 1050.7 528.1 | 16.0 0 | 0 |
| E | 2887.0 | B | 604338 | 5827833 | 90.4 26.2 | 135.3 121.4 | 77.0 91.1 | 11.5 5 | 14 |
| F | 2883.4 | D | 604419 | 5827764 | 34.9 19.2 | 88.8 41.0 | 77.0 91.1 | 3.5 16 | 1 |
| G | 2876.4 | B | 604565 | 5827636 | 33.5 23.0 | 361.5 114.7 | 202.4 170.7 | 2.6 20 | 2 |
| H | 2862.3 | B | 604838 | 5827399 | 81.1 44.3 | 600.2 221.0 | 469.6 194.8 | 4.7 10 | 0 |
| I | 2860.1 | B | 604881 | 5827363 | 111.7 21.6 | 600.2 221.0 | 469.6 194.8 | 22.3 9 | 0 |
| LINE 20080 | | | FLIGHT 4 | | | | | | |
| A | 2676.0 | B | 603492 | 5828683 | 19.3 2.8 | 156.1 6.8 | 157.6 64.6 | 19.5 13 | 0 |
| B | 2679.1 | B | 603565 | 5828622 | 13.0 9.2 | 146.3 67.7 | 157.6 69.8 | 1.8 13 | 0 |
| C | 2688.1 | B | 603770 | 5828447 | 20.1 4.8 | 59.8 26.4 | 44.1 34.2 | 9.3 46 | 0 |
| D | 2701.1 | B | 604047 | 5828198 | 33.1 15.8 | 284.6 105.9 | 175.0 91.1 | 4.1 13 | 0 |
| E | 2712.6 | B | 604288 | 5827991 | 195.0 52.2 | 1193.2 175.1 | 967.5 432.1 | 16.7 0 | 0 |
| F | 2716.4 | B | 604368 | 5827920 | 112.5 28.3 | 608.3 134.9 | 967.5 383.0 | 15.2 1 | 1 |
| G | 2721.6 | B | 604479 | 5827822 | 51.9 0.5 | 392.4 86.0 | 387.7 37.6 | 999.0 13 | 0 |
| H | 2724.8 | D | 604545 | 5827761 | 66.0 29.4 | 273.3 86.0 | 193.4 94.5 | 5.7 11 | 5 |
| I | 2730.9 | B | 604681 | 5827639 | 40.1 3.8 | 129.0 63.1 | 290.0 114.6 | 46.8 23 | 0 |
| J | 2735.1 | D | 604785 | 5827546 | 42.3 32.3 | 64.9 153.1 | 0.0 70.0 | 2.5 9 | 0 |
| K | 2742.0 | B | 604974 | 5827384 | 88.3 11.4 | 327.7 19.0 | 326.1 123.3 | 37.8 3 | 0 |
| LINE 20090 | | | FLIGHT 4 | | | | | | |
| A | 2632.7 | H | 603534 | 5828765 | 34.4 11.3 | 372.4 61.6 | 260.2 136.6 | 7.0 4 | 0 |
| B | 2606.6 | B | 604091 | 5828259 | 71.9 26.8 | 510.3 238.7 | 274.9 200.0 | 7.5 7 | 0 |

CX = COAXIAL

CP = COPLANAR

Note:EM values shown above
are local amplitudes

Spanish Mountain Block B

*Estimated Depth may be unreliable because the
stronger part of the conductor may be deeper or
to one side of the flight line, or because of a
shallow dip or magnetite/overburden effects

EM Anomaly List

| LINE | Fid | Interp | XUTM m | YUTM m | CX 5500 HZ Real Quad ppm ppm | CP 7200 HZ Real Quad ppm ppm | CP 900 HZ Real Quad ppm ppm | Vertical Dike COND DEPTH* siemens m | Mag. Corr NT |
|------------|--------|--------|-----------|-----------|------------------------------------|------------------------------------|-----------------------------------|---|-----------------|
| LINE 20090 | | | FLIGHT 4 | | | | | | |
| C | 2599.3 | B | 604246 | 5828110 | 123.4 27.2 | 594.7 116.6 | 609.6 141.3 | 18.9 11 | 2 |
| D | 2592.1 | B | 604395 | 5827973 | 138.3 34.2 | 995.5 178.9 | 821.9 309.5 | 16.7 2 | 0 |
| E | 2572.1 | D | 604799 | 5827635 | 57.1 38.6 | 399.2 254.2 | 253.3 199.9 | 3.2 8 | 0 |
| F | 2569.4 | E | 604852 | 5827594 | 96.0 46.0 | 79.8 254.2 | 1.1 35.6 | 5.9 2 | 0 |
| G | 2563.6 | B | 604965 | 5827499 | 31.7 8.8 | 23.6 7.4 | 58.9 10.0 | 8.6 22 | 0 |
| H | 2557.1 | B | 605088 | 5827383 | 22.2 15.7 | 224.9 119.8 | 53.7 92.4 | 2.2 18 | 1 |
| LINE 20100 | | | FLIGHT 4 | | | | | | |
| A | 2417.3 | H | 603564 | 5828817 | 6.2 5.3 | 141.9 63.2 | 101.8 55.9 | 1.1 20 | 0 |
| B | 2421.7 | E | 603669 | 5828735 | 30.1 8.3 | 145.1 63.2 | 12.1 56.2 | 8.6 13 | 0 |
| C | 2449.6 | B | 604292 | 5828187 | 72.6 18.5 | 444.1 67.9 | 338.1 130.8 | 12.9 14 | 0 |
| D | 2453.0 | B | 604364 | 5828119 | 39.8 10.8 | 444.1 67.9 | 338.1 130.8 | 9.6 20 | 9 |
| E | 2460.5 | B | 604527 | 5827968 | 100.3 24.7 | 573.4 120.6 | 434.1 174.5 | 15.1 3 | 2 |
| F | 2468.9 | B | 604684 | 5827838 | 18.3 15.5 | 104.2 80.8 | 137.1 57.9 | 1.7 19 | 1 |
| G | 2474.9 | D | 604789 | 5827747 | 17.8 13.2 | 51.4 43.5 | 223.9 141.7 | 1.9 25 | 0 |
| H | 2477.3 | B | 604829 | 5827708 | 14.6 18.7 | 51.4 163.6 | 223.9 141.7 | 1.0 16 | 0 |
| I | 2480.9 | E | 604889 | 5827648 | 13.0 17.2 | 238.3 163.6 | 0.0 100.6 | 0.9 28 | 2 |
| J | 2491.5 | D | 605099 | 5827464 | 20.3 9.8 | 91.3 35.6 | 74.2 34.8 | 3.5 17 | 1 |
| K | 2497.7 | H | 605236 | 5827356 | 42.1 38.5 | 331.6 175.0 | 71.2 147.3 | 2.0 10 | 0 |
| LINE 20110 | | | FLIGHT 4 | | | | | | |
| A | 2346.9 | B | 604502 | 5828088 | 94.3 15.4 | 606.8 53.5 | 544.9 191.4 | 27.1 6 | 2 |
| B | 2342.2 | B | 604602 | 5827999 | 42.4 11.2 | 73.8 46.4 | 67.6 77.9 | 10.2 17 | 2 |
| C | 2335.8 | B | 604732 | 5827889 | 99.9 43.2 | 648.8 263.8 | 398.0 279.6 | 6.8 10 | 1 |
| D | 2315.6 | B | 605113 | 5827565 | 47.5 21.8 | 208.0 160.1 | 49.0 84.8 | 4.9 15 | 0 |
| LINE 20120 | | | FLIGHT 4 | | | | | | |
| A | 2175.0 | B | 603749 | 5828874 | 23.0 13.3 | 161.3 69.7 | 85.2 66.0 | 2.9 14 | 0 |
| B | 2188.5 | H | 604060 | 5828643 | 3.9 5.0 | 41.9 37.1 | 30.5 19.5 | 0.6 47 | 0 |
| C | 2219.5 | B | 604717 | 5828011 | 127.5 30.8 | 659.2 116.5 | 464.4 265.3 | 16.8 1 | 0 |
| D | 2224.7 | E | 604848 | 5827899 | 94.6 26.5 | 427.2 81.5 | 294.7 180.8 | 12.3 2 | 0 |
| E | 2238.7 | B | 605218 | 5827568 | 51.2 32.6 | 156.1 111.1 | 7.7 54.3 | 3.3 7 | 1 |
| LINE 20130 | | | FLIGHT 4 | | | | | | |
| A | 2128.5 | B | 603763 | 5828959 | 76.4 17.0 | 609.4 128.9 | 510.7 219.5 | 15.9 7 | 1 |
| B | 2099.5 | B | 604406 | 5828386 | 36.7 13.8 | 383.9 50.5 | 326.3 172.6 | 5.9 24 | 0 |
| C | 2077.7 | B | 604873 | 5827973 | 25.2 10.4 | 110.3 43.1 | 72.3 50.7 | 4.6 35 | 0 |
| D | 2064.8 | B | 605158 | 5827734 | 12.4 3.9 | 88.2 0.2 | 49.7 44.6 | 5.2 41 | 0 |

CX = COAXIAL
CP = COPLANAR

Note: EM values shown above
are local amplitudes

*Estimated Depth may be unreliable because the
stronger part of the conductor may be deeper or
to one side of the flight line, or because of a

Spanish Mountain Block B

- 3 - shallow dip or magnetite/overburden effects

EM Anomaly List

| | Label | Fid | Interp | XUTM | YUTM | CX 5500 HZ | | CP 7200 HZ | | CP 900 HZ | | Vertical Dike | | Mag. Corr | |
|------|--------|-----|--------|----------|---------|------------|------|------------|-------|-----------|-------|---------------|--------|-----------|--|
| | | | | | | Real | Quad | Real | Quad | Real | Quad | COND | DEPTH* | | |
| | | | | m | m | ppm | ppm | ppm | ppm | ppm | ppm | siemens | m | NT | |
| LINE | 20140 | | | FLIGHT 4 | | | | | | | | | | | |
| A | 1911.3 | B | | 603868 | 5828972 | 41.8 | 17.8 | 276.8 | 94.0 | 212.5 | 115.0 | 5.2 | 9 | 0 | |
| B | 1917.6 | B | | 604042 | 5828826 | 40.7 | 10.3 | 223.6 | 69.0 | 109.0 | 92.3 | 10.8 | 25 | 0 | |
| C | 1932.6 | H | | 604426 | 5828489 | 10.4 | 2.3 | 69.7 | 7.7 | 70.3 | 9.1 | 8.2 | 55 | 0 | |
| D | 1940.7 | B | | 604632 | 5828296 | 18.1 | 3.4 | 216.4 | 25.6 | 204.1 | 53.0 | 12.8 | 20 | 0 | |
| E | 1950.2 | H | | 604864 | 5828070 | 1.0 | 2.8 | 19.4 | 3.4 | 35.0 | 10.7 | 0.2 | 44 | 0 | |
| F | 1964.2 | H | | 605272 | 5827713 | 3.1 | 0.6 | 50.7 | 7.0 | 34.6 | 21.3 | 6.1 | 95 | 0 | |
| LINE | 20150 | | | FLIGHT 4 | | | | | | | | | | | |
| A | 1867.8 | H | | 603904 | 5829046 | 30.6 | 7.0 | 262.6 | 37.6 | 207.9 | 86.8 | 11.3 | 29 | 1 | |
| B | 1854.1 | H | | 604239 | 5828747 | 10.0 | 3.6 | 134.1 | 23.2 | 109.0 | 39.3 | 4.0 | 49 | 0 | |
| C | 1845.5 | H | | 604438 | 5828564 | 33.0 | 2.6 | 286.1 | 19.1 | 276.0 | 60.2 | 55.5 | 20 | 0 | |
| D | 1823.5 | H | | 604944 | 5828110 | 5.4 | 0.3 | 57.4 | 0.5 | 64.9 | 13.9 | 60.4 | 79 | 0 | |
| E | 1808.3 | E | | 605291 | 5827808 | 4.0 | 9.1 | 55.7 | 17.8 | 28.7 | 23.9 | 0.4 | 21 | 0 | |
| F | 1801.6 | H | | 605441 | 5827672 | 6.5 | 5.3 | 119.3 | 1.2 | 103.9 | 34.3 | 1.2 | 42 | 0 | |
| G | 1799.2 | B? | | 605494 | 5827625 | 22.9 | 9.8 | 119.3 | 18.5 | 103.9 | 34.3 | 4.3 | 25 | 0 | |
| LINE | 20160 | | | FLIGHT 4 | | | | | | | | | | | |
| A | 1681.4 | H | | 604177 | 5828914 | 33.9 | 10.1 | 408.0 | 99.7 | 278.4 | 163.3 | 8.0 | 17 | 0 | |
| B | 1697.0 | H | | 604571 | 5828564 | 64.3 | 18.1 | 576.9 | 73.4 | 489.9 | 168.5 | 10.7 | 11 | 0 | |
| C | 1723.3 | H | | 605205 | 5827982 | 6.3 | 1.8 | 105.7 | 2.4 | 122.2 | 3.7 | 4.7 | 64 | 0 | |
| D | 1735.7 | H | | 605555 | 5827681 | 8.5 | 5.4 | 150.6 | 41.6 | 123.9 | 56.2 | 1.8 | 51 | 0 | |
| LINE | 20170 | | | FLIGHT 4 | | | | | | | | | | | |
| A | 1620.0 | H | | 604049 | 5829116 | 42.7 | 14.3 | 247.6 | 93.5 | 129.2 | 107.3 | 7.3 | 16 | 0 | |
| B | 1597.8 | H | | 604559 | 5828655 | 42.9 | 12.8 | 453.1 | 69.0 | 350.4 | 147.3 | 8.6 | 14 | 2 | |
| C | 1589.6 | H | | 604748 | 5828484 | 61.1 | 14.8 | 796.8 | 140.9 | 598.1 | 276.4 | 13.1 | 22 | 0 | |
| D | 1579.3 | B | | 604977 | 5828286 | 19.9 | 4.7 | 142.4 | 31.0 | 85.9 | 65.6 | 9.4 | 36 | 4 | |
| E | 1564.0 | H | | 605274 | 5828020 | 18.8 | 5.6 | 283.2 | 10.3 | 328.3 | 83.1 | 6.6 | 39 | 0 | |
| F | 1547.6 | H | | 605620 | 5827713 | 21.9 | 5.9 | 171.9 | 27.4 | 145.8 | 57.6 | 7.9 | 32 | 0 | |

CX = COAXIAL

CP = COPLANAR

Note:EM values shown above
are local amplitudes

Spanish Mountain Block B

*Estimated Depth may be unreliable because the
stronger part of the conductor may be deeper or
to one side of the flight line, or because of a
shallow dip or magnetite/overburden effects

APPENDIX F

GLOSSARY

APPENDIX F

GLOSSARY OF AIRBORNE GEOPHYSICAL TERMS

Note: The definitions given in this glossary refer to the common terminology as used in airborne geophysics.

altitude attenuation: the absorption of gamma rays by the atmosphere between the earth and the detector. The number of gamma rays detected by a system decreases as the altitude increases.

apparent- : the *physical parameters* of the earth measured by a geophysical system are normally expressed as apparent, as in “apparent *resistivity*”. This means that the measurement is limited by assumptions made about the geology in calculating the response measured by the geophysical system. Apparent resistivity calculated with *HEM*, for example, generally assumes that the earth is a *homogeneous half-space* – not layered.

amplitude: The strength of the total electromagnetic field. In *frequency domain* it is most often the sum of the squares of *in-phase* and *quadrature* components. In multi-component electromagnetic surveys it is generally the sum of the squares of all three directional components.

analytic signal: The total amplitude of all the directions of magnetic *gradient*. Calculated as the sum of the squares.

anisotropy: Having different *physical parameters* in different directions. This can be caused by layering or fabric in the geology. Note that a unit can be anisotropic, but still *homogeneous*.

anomaly: A localized change in the geophysical data characteristic of a discrete source, such as a conductive or magnetic body: something locally different from the *background*.

B-field: In time-domain *electromagnetic* surveys, the magnetic field component of the (electromagnetic) *field*. This can be measured directly, although more commonly it is calculated by integrating the time rate of change of the magnetic field dB/dt , as measured with a receiver coil.

background: The “normal” response in the geophysical data – that response observed over most of the survey area. *Anomalies* are usually measured relative to the background. In airborne gamma-ray spectrometric surveys the term defines the *cosmic*, radon, and aircraft responses in the absence of a signal from the ground.

base-level: The measured values in a geophysical system in the absence of any outside signal. All geophysical data are measured relative to the system base level.

- Appendix F.2 -

base frequency: The frequency of the pulse repetition for a **time-domain electromagnetic** system. Measured between subsequent positive pulses.

bird: A common name for the pod towed beneath or behind an aircraft, carrying the geophysical sensor array.

bucking: The process of removing the strong **signal** from the **primary field** at the **receiver** from the data, to measure the **secondary field**. It can be done electronically or mathematically. This is done in **frequency-domain EM**, and to measure **on-time** in **time-domain EM**.

calibration coil: A wire coil of known size and dipole moment, which is used to generate a field of known **amplitude** and **phase** in the receiver, for system calibration. Calibration coils can be external, or internal to the system. Internal coils may be called Q-coils.

coaxial coils: [CX] Coaxial coils in an HEM system are in the vertical plane, with their axes horizontal and collinear in the flight direction. These are most sensitive to vertical conductive objects in the ground, such as thin, steeply dipping conductors perpendicular to the flight direction. Coaxial coils generally give the sharpest anomalies over localized conductors. (See also **coplanar coils**)

coil: A multi-turn wire loop used to transmit or detect electromagnetic fields. Time varying **electromagnetic** fields through a coil induce a voltage proportional to the strength of the field and the rate of change over time.

compensation: Correction of airborne geophysical data for the changing effect of the aircraft. This process is generally used to correct data in **fixed-wing time-domain electromagnetic** surveys (where the transmitter is on the aircraft and the receiver is moving), and magnetic surveys (where the sensor is on the aircraft, turning in the earth's magnetic field).

component: In **frequency domain electromagnetic** surveys this is one of the two **phase** measurements – **in-phase or quadrature**. In “multi-component” electromagnetic surveys it is also used to define the measurement in one geometric direction (vertical, horizontal in-line and horizontal transverse – the Z, X and Y components).

Compton scattering: gamma ray photons will bounce off electrons as they pass through the earth and atmosphere, reducing their energy and then being detected by **radiometric** sensors at lower energy levels. See also **stripping**.

conductance: See **conductivity thickness**

conductivity: [σ] The facility with which the earth or a geological formation conducts electricity. Conductivity is usually measured in milli-Siemens per metre (mS/m). It is the reciprocal of **resistivity**.

conductivity-depth imaging: see **conductivity-depth transform**.

conductivity-depth transform: A process for converting electromagnetic measurements to an approximation of the conductivity distribution vertically in the earth, assuming a **layered earth**. (Macnae and Lamontagne, 1987; Wolfgram and Karlik, 1995)

conductivity thickness: [σt] The product of the **conductivity**, and thickness of a large, tabular body. (It is also called the “conductivity-thickness product”) In electromagnetic geophysics, the response of a thin plate-like conductor is proportional to the conductivity multiplied by thickness. For example a 10 metre thickness of 20 Siemens/m mineralization will be equivalent to 5 metres of 40 S/m; both have 200 S conductivity thickness. Sometimes referred to as conductance.

conductor: Used to describe anything in the ground more conductive than the surrounding geology. Conductors are most often clays or graphite, or hopefully some type of mineralization, but may also be man-made objects, such as fences or pipelines.

coplanar coils: [CP] In HEM, the coplanar coils lie in the horizontal plane with their axes vertical, and parallel. These coils are most sensitive to massive conductive bodies, horizontal layers, and the **halfspace**.

cosmic ray: High energy sub-atomic particles from outer space that collide with the earth’s atmosphere to produce a shower of gamma rays (and other particles) at high energies.

counts (per second): The number of **gamma-rays** detected by a gamma-ray **spectrometer**. The rate depends on the geology, but also on the size and sensitivity of the detector.

culture: A term commonly used to denote any man-made object that creates a geophysical anomaly. Includes, but not limited to, power lines, pipelines, fences, and buildings.

current channelling: See current gathering.

current gathering: The tendency of electrical currents in the ground to channel into a conductive formation. This is particularly noticeable at higher frequencies or early time channels when the formation is long and parallel to the direction of current flow. This tends to enhance anomalies relative to inductive currents (see also **induction**). Also known as current channelling.

daughter products: The radioactive natural sources of gamma-rays decay from the original “parent” element (commonly potassium, uranium, and thorium) to one or more lower-energy “daughter” elements. Some of these lower energy elements are also

- Appendix F.4 -

radioactive and decay further. **Gamma-ray spectrometry** surveys may measure the gamma rays given off by the original element or by the decay of the daughter products.

dB/dt : As the **secondary electromagnetic field** changes with time, the magnetic field [**B**] component induces a voltage in the receiving **coil**, which is proportional to the rate of change of the magnetic field over time.

decay: In **time-domain electromagnetic** theory, the weakening over time of the **eddy currents** in the ground, and hence the **secondary field** after the **primary field** electromagnetic pulse is turned off. In **gamma-ray spectrometry**, the radioactive breakdown of an element, generally potassium, uranium, thorium, or one of their **daughter** products.

decay constant: see time constant.

decay series: In **gamma-ray spectrometry**, a series of progressively lower energy **daughter products** produced by the radioactive breakdown of uranium or thorium.

depth of exploration: The maximum depth at which the geophysical system can detect the target. The depth of exploration depends very strongly on the type and size of the target, the contrast of the target with the surrounding geology, the homogeneity of the surrounding geology, and the type of geophysical system. One measure of the maximum depth of exploration for an electromagnetic system is the depth at which it can detect the strongest conductive target – generally a highly conductive horizontal layer.

differential resistivity: A process of transforming **apparent resistivity** to an approximation of layer resistivity at each depth. The method uses multi-frequency HEM data and approximates the effect of shallow layer **conductance** determined from higher frequencies to estimate the deeper conductivities (Huang and Fraser, 1996)

dipole moment: [NIA] For a transmitter, the product of the area of a **coil**, the number of turns of wire, and the current flowing in the coil. At a distance significantly larger than the size of the coil, the magnetic field from a coil will be the same if the dipole moment product is the same. For a receiver coil, this is the product of the area and the number of turns. The sensitivity to a magnetic field (assuming the source is far away) will be the same if the dipole moment is the same.

diurnal: The daily variation in a natural field, normally used to describe the natural fluctuations (over hours and days) of the earth's magnetic field.

dielectric permittivity: [ϵ] The capacity of a material to store electrical charge, this is most often measured as the relative permittivity [ϵ_r], or ratio of the material dielectric to that of free space. The effect of high permittivity may be seen in HEM data at high frequencies over highly resistive geology as a reduced or negative **in-phase**, and higher **quadrature** data.

- Appendix F.5 -

drape: To fly a survey following the terrain contours, maintaining a constant altitude above the local ground surface. Also applied to re-processing data collected at varying altitudes above ground to simulate a survey flown at constant altitude.

drift: Long-time variations in the base-level or calibration of an instrument.

eddy currents: The electrical currents induced in the ground, or other conductors, by a time-varying **electromagnetic field** (usually the **primary field**). Eddy currents are also induced in the aircraft's metal frame and skin; a source of **noise** in EM surveys.

electromagnetic: [EM] Comprised of a time-varying electrical and magnetic field. Radio waves are common electromagnetic fields. In geophysics, an electromagnetic system is one which transmits a time-varying **primary field** to induce **eddy currents** in the ground, and then measures the **secondary field** emitted by those eddy currents.

energy window: A broad spectrum of **gamma-ray** energies measured by a spectrometric survey. The energy of each gamma-ray is measured and divided up into numerous discrete energy levels, called windows.

equivalent (thorium or uranium): The amount of radioelement calculated to be present, based on the gamma-rays measured from a **daughter** element. This assumes that the **decay series** is in equilibrium – progressing normally.

exposure rate: in radiometric surveys, a calculation of the total exposure rate due to gamma rays at the ground surface. It is used as a measurement of the concentration of all the **radioelements** at the surface. See also: **natural exposure rate**.

fiducial, or fid: Timing mark on a survey record. Originally these were timing marks on a profile or film; now the term is generally used to describe 1-second interval timing records in digital data, and on maps or profiles.

Figure of Merit: (FOM) A sum of the 12 distinct magnetic noise variations measured by each of four flight directions, and executing three aircraft attitude variations (yaw, pitch, and roll) for each direction. The flight directions are generally parallel and perpendicular to planned survey flight directions. The FOM is used as a measure of the **manoeuvre noise** before and after **compensation**.

fixed-wing: Aircraft with wings, as opposed to “rotary wing” helicopters.

footprint: This is a measure of the area of sensitivity under the aircraft of an airborne geophysical system. The footprint of an **electromagnetic** system is dependent on the altitude of the system, the orientation of the transmitter and receiver and the separation between the receiver and transmitter, and the conductivity of the ground. The footprint of

- Appendix F.6 -

a **gamma-ray spectrometer** depends mostly on the altitude. For all geophysical systems, the footprint also depends on the strength of the contrasting **anomaly**.

frequency domain: An **electromagnetic** system which transmits a **primary field** that oscillates smoothly over time (sinusoidal), inducing a similarly varying electrical current in the ground. These systems generally measure the changes in the **amplitude** and **phase** of the **secondary field** from the ground at different frequencies by measuring the **in-phase** and **quadrature** phase components. See also **time-domain**.

full-stream data: Data collected and recorded continuously at the highest possible sampling rate. Normal data are stacked (see **stacking**) over some time interval before recording.

gamma-ray: A very high-energy photon, emitted from the nucleus of an atom as it undergoes a change in energy levels.

gamma-ray spectrometry: Measurement of the number and energy of natural (and sometimes man-made) gamma-rays across a range of photon energies.

gradient: In magnetic surveys, the gradient is the change of the magnetic field over a distance, either vertically or horizontally in either of two directions. Gradient data is often measured, or calculated from the total magnetic field data because it changes more quickly over distance than the **total magnetic field**, and so may provide a more precise measure of the location of a source. See also **analytic signal**.

ground effect: The response from the earth. A common calibration procedure in many geophysical surveys is to fly to altitude high enough to be beyond any measurable response from the ground, and there establish **base levels** or **backgrounds**.

half-space: A mathematical model used to describe the earth – as infinite in width, length, and depth below the surface. The most common halfspace models are **homogeneous** and **layered earth**.

heading error: A slight change in the magnetic field measured when flying in opposite directions.

HEM: Helicopter ElectroMagnetic, This designation is most commonly used for helicopter-borne, **frequency-domain** electromagnetic systems. At present, the transmitter and receivers are normally mounted in a **bird** carried on a sling line beneath the helicopter.

herringbone pattern: A pattern created in geophysical data by an asymmetric system, where the **anomaly** may be extended to either side of the source, in the direction of flight. Appears like fish bones, or like the teeth of a comb, extending either side of centre, each tooth an alternate flight line.

- Appendix F.7 -

homogeneous: This is a geological unit that has the same **physical parameters** throughout its volume. This unit will create the same response to an HEM system anywhere, and the HEM system will measure the same apparent **resistivity** anywhere. The response may change with system direction (see **anisotropy**).

HTEM: Helicopter Time-domain ElectroMagnetic, This designation is used for the new generation of helicopter-borne, **time-domain** electromagnetic systems.

in-phase: the component of the measured **secondary field** that has the same phase as the transmitter and the **primary field**. The in-phase component is stronger than the **quadrature** phase over relatively higher **conductivity**.

induction: Any time-varying electromagnetic field will induce (cause) electrical currents to flow in any object with non-zero **conductivity**. (see **eddy currents**)

induction number: also called the “response parameter”, this number combines many of the most significant parameters affecting the **EM** response into one parameter against which to compare responses. For a **layered earth** the response parameter is $\mu\omega\sigma h^2$ and for a large, flat, **conductor** it is $\mu\omega\sigma t h$, where μ is the **magnetic permeability**, ω is the angular **frequency**, σ is the **conductivity**, t is the thickness (for the flat conductor) and h is the height of the system above the conductor.

inductive limit: When the frequency of an EM system is very high, or the **conductivity** of the target is very high, the response measured will be entirely **in-phase** with no **quadrature** (**phase** angle =0). The in-phase response will remain constant with further increase in conductivity or frequency. The system can no longer detect changes in conductivity of the target.

infinite: In geophysical terms, an “infinite” dimension is one much greater than the **footprint** of the system, so that the system does not detect changes at the edges of the object.

International Geomagnetic Reference Field: [IGRF] An approximation of the smooth magnetic field of the earth, in the absence of variations due to local geology. Once the IGRF is subtracted from the measured magnetic total field data, any remaining variations are assumed to be due to local geology. The IGRF also predicts the slow changes of the field up to five years in the future.

inversion, or inverse modeling: A process of converting geophysical data to an earth model, which compares theoretical models of the response of the earth to the data measured, and refines the model until the response closely fits the measured data (Huang and Palacky, 1991)

- Appendix F.8 -

layered earth: A common geophysical model which assumes that the earth is horizontally layered – the **physical parameters** are constant to **infinite** distance horizontally, but change vertically.

magnetic permeability: [μ] This is defined as the ratio of magnetic induction to the inducing magnetic field. The relative magnetic permeability [μ_r] is often quoted, which is the ratio of the rock permeability to the permeability of free space. In geology and geophysics, the **magnetic susceptibility** is more commonly used to describe rocks.

magnetic susceptibility: [k] A measure of the degree to which a body is magnetized. In SI units this is related to relative **magnetic permeability** by $k = \mu_r - 1$, and is a dimensionless unit. For most geological material, susceptibility is influenced primarily by the percentage of magnetite. It is most often quoted in units of 10^{-6} . In HEM data this is most often apparent as a negative **in-phase** component over high susceptibility, high **resistivity** geology such as diabase dikes.

manoeuvre noise: variations in the magnetic field measured caused by changes in the relative positions of the magnetic sensor and magnetic objects or electrical currents in the aircraft. This type of noise is generally corrected by magnetic **compensation**.

model: Geophysical theory and applications generally have to assume that the geology of the earth has a form that can be easily defined mathematically, called the model. For example steeply dipping **conductors** are generally modeled as being **infinite** in horizontal and depth extent, and very thin. The earth is generally modeled as horizontally layered, each layer infinite in extent and uniform in characteristic. These models make the mathematics to describe the response of the (normally very complex) earth practical. As theory advances, and computers become more powerful, the useful models can become more complex.

natural exposure rate: in radiometric surveys, a calculation of the total exposure rate due to natural-source gamma rays at the ground surface. It is used as a measurement of the concentration of all the natural **radioelements** at the surface. See also: **exposure rate**.

noise: That part of a geophysical measurement that the user does not want. Typically this includes electronic interference from the system, the atmosphere (**sferics**), and man-made sources. This can be a subjective judgment, as it may include the response from geology other than the target of interest. Commonly the term is used to refer to high frequency (short period) interference. See also **drift**.

Occam's inversion: an **inversion** process that matches the measured **electromagnetic** data to a theoretical model of many, thin layers with constant thickness and varying resistivity (Constable et al, 1987).

off-time: In a **time-domain electromagnetic** survey, the time after the end of the **primary field pulse**, and before the start of the next pulse.

- Appendix F.9 -

on-time: In a *time-domain electromagnetic* survey, the time during the *primary field pulse*.

overburden: In engineering and mineral exploration terms, this most often means the soil on top of the unweathered bedrock. It may be sand, glacial till, or weathered rock.

Phase, phase angle: The angular difference in time between a measured sinusoidal electromagnetic field and a reference – normally the primary field. The phase is calculated from $\tan^{-1}(\text{in-phase} / \text{quadrature})$.

physical parameters: These are the characteristics of a geological unit. For electromagnetic surveys, the important parameters are *conductivity*, *magnetic permeability* (or *susceptibility*) and *dielectric permittivity*; for magnetic surveys the parameter is magnetic susceptibility, and for gamma ray spectrometric surveys it is the concentration of the major radioactive elements: potassium, uranium, and thorium.

permittivity: see *dielectric permittivity*.

permeability: see *magnetic permeability*.

primary field: the EM field emitted by a transmitter. This field induces *eddy currents* in (energizes) the conductors in the ground, which then create their own *secondary fields*.

pulse: In time-domain EM surveys, the short period of intense *primary* field transmission. Most measurements (the *off-time*) are measured after the pulse. *On-time* measurements may be made during the pulse.

quadrature: that component of the measured *secondary field* that is phase-shifted 90° from the *primary field*. The quadrature component tends to be stronger than the *in-phase* over relatively weaker *conductivity*.

Q-coils: see *calibration coil*.

radioelements: This normally refers to the common, naturally-occurring radioactive elements: potassium (K), uranium (U), and thorium (Th). It can also refer to man-made radioelements, most often cobalt (Co) and cesium (Cs)

radiometric: Commonly used to refer to *gamma ray* spectrometry.

radon: A radioactive daughter product of uranium and thorium, radon is a gas which can leak into the atmosphere, adding to the non-geological background of a gamma-ray spectrometric survey.

- Appendix F.10 -

receiver: the **signal** detector of a geophysical system. This term is most often used in active geophysical systems – systems that transmit some kind of signal. In airborne **electromagnetic** surveys it is most often a **coil**. (see also, **transmitter**)

resistivity: [ρ] The strength with which the earth or a geological formation resists the flow of electricity, typically the flow induced by the **primary field** of the electromagnetic transmitter. Normally expressed in ohm-metres, it is the reciprocal of **conductivity**.

resistivity-depth transforms: similar to **conductivity depth transforms**, but the calculated **conductivity** has been converted to **resistivity**.

resistivity section: an approximate vertical section of the resistivity of the layers in the earth. The resistivities can be derived from the **apparent resistivity**, the **differential resistivities**, **resistivity-depth transforms**, or **inversions**.

Response parameter: another name for the **induction number**.

secondary field: The field created by conductors in the ground, as a result of electrical currents induced by the **primary field** from the **electromagnetic** transmitter. Airborne **electromagnetic** systems are designed to create and measure a secondary field.

Sengpiel section: a **resistivity section** derived using the **apparent resistivity** and an approximation of the depth of maximum sensitivity for each frequency.

sferic: Lightning, or the **electromagnetic** signal from lightning, it is an abbreviation of “atmospheric discharge”. These appear to magnetic and electromagnetic sensors as sharp “spikes” in the data. Under some conditions lightning storms can be detected from hundreds of kilometres away. (see **noise**)

signal: That component of a measurement that the user wants to see – the response from the targets, from the earth, etc. (See also **noise**)

skin depth: A measure of the depth of penetration of an electromagnetic field into a material. It is defined as the depth at which the primary field decreases to 1/e of the field at the surface. It is calculated by approximately $503 \times \sqrt{(\text{resistivity}/\text{frequency})}$. Note that depth of penetration is greater at higher **resistivity** and/or lower **frequency**.

spectrometry: Measurement across a range of energies, where **amplitude** and energy are defined for each measurement. In gamma-ray spectrometry, the number of gamma rays are measured for each energy **window**, to define the **spectrum**.

spectrum: In **gamma ray spectrometry**, the continuous range of energy over which gamma rays are measured. In **time-domain electromagnetic** surveys, the spectrum is the energy of the **pulse** distributed across an equivalent, continuous range of frequencies.

spheric: see *sferic*.

stacking: Summing repeat measurements over time to enhance the repeating *signal*, and minimize the random *noise*.

stripping: Estimation and correction for the gamma ray photons of higher and lower energy that are observed in a particular *energy window*. See also *Compton scattering*.

susceptibility: See *magnetic susceptibility*.

tau: [τ] Often used as a name for the *time constant*.

TDEM: *time domain electromagnetic*.

thin sheet: A standard model for electromagnetic geophysical theory. It is usually defined as a thin, flat-lying conductive sheet, *infinite* in both horizontal directions. (see also *vertical plate*)

tie-line: A survey line flown across most of the *traverse lines*, generally perpendicular to them, to assist in measuring *drift* and *diurnal* variation. In the short time required to fly a tie-line it is assumed that the drift and/or diurnal will be minimal, or at least changing at a constant rate.

time constant: The time required for an *electromagnetic* field to decay to a value of 1/e of the original value. In *time-domain* electromagnetic data, the time constant is proportional to the size and *conductance* of a tabular conductive body. Also called the decay constant.

Time channel: In *time-domain electromagnetic* surveys the decaying *secondary field* is measured over a period of time, and the divided up into a series of consecutive discrete measurements over that time.

time-domain: *Electromagnetic* system which transmits a pulsed, or stepped *electromagnetic* field. These systems induce an electrical current (*eddy current*) in the ground that persists after the *primary field* is turned off, and measure the change over time of the *secondary field* created as the currents *decay*. See also *frequency-domain*.

total energy envelope: The sum of the squares of the three *components* of the *time-domain electromagnetic secondary field*. Equivalent to the *amplitude* of the secondary field.

transient: Time-varying. Usually used to describe a very short period pulse of *electromagnetic* field.

- Appendix F.12 -

transmitter: The source of the **signal** to be measured in a geophysical survey. In airborne **EM** it is most often a **coil** carrying a time-varying electrical current, transmitting the **primary field**. (see also **receiver**)

traverse line: A normal geophysical survey line. Normally parallel traverse lines are flown across the property in spacing of 50 m to 500 m, and generally perpendicular to the target geology.

vertical plate: A standard model for electromagnetic geophysical theory. It is usually defined as thin conductive sheet, **infinite** in horizontal dimension and depth extent. (see also **thin sheet**)

waveform: The shape of the **electromagnetic pulse** from a **time-domain** electromagnetic transmitter.

window: A discrete portion of a **gamma-ray spectrum** or **time-domain electromagnetic decay**. The continuous energy spectrum or **full-stream** data are grouped into windows to reduce the number of samples, and reduce **noise**.

Version 1.5, November 29, 2005
Greg Hodges,
Chief Geophysicist
Fugro Airborne Surveys, Toronto

Common Symbols and Acronyms

| | |
|-------------------------|---|
| k | Magnetic susceptibility |
| ε | Dielectric permittivity |
| μ, μ_r | Magnetic permeability, relative permeability |
| ρ, ρ_a | Resistivity, apparent resistivity |
| σ, σ_a | Conductivity, apparent conductivity |
| σt | Conductivity thickness |
| τ | Tau, or time constant |
| Ωm | ohm-metres, units of resistivity |
| AGS | Airborne gamma ray spectrometry. |
| CDT | Conductivity-depth transform, conductivity-depth imaging (Macnae and Lamontagne, 1987; Wolfgram and Karlik, 1995) |
| CPI, CPQ | Coplanar in-phase, quadrature |
| CPS | Counts per second |
| CTP | Conductivity thickness product |
| CXI, CXQ | Coaxial, in-phase, quadrature |
| FOM | Figure of Merit |
| fT | femtoteslas, normal unit for measurement of B-Field |
| EM | Electromagnetic |
| keV | kilo electron volts – a measure of gamma-ray energy |
| MeV | mega electron volts – a measure of gamma-ray energy 1MeV = 1000keV |
| NIA | dipole moment: turns x current x Area |
| nT | nanotesla, a measure of the strength of a magnetic field |
| nG/h | nanoGreys/hour – gamma ray dose rate at ground level |
| ppm | parts per million – a measure of secondary field or noise relative to the primary or radioelement concentration. |
| pT/s | picoteslas per second: Units of decay of secondary field, dB/dt |
| S | siemens – a unit of conductance |
| x: | the horizontal component of an EM field parallel to the direction of flight. |
| y: | the horizontal component of an EM field perpendicular to the direction of flight. |
| z: | the vertical component of an EM field. |

References:

Constable, S.C., Parker, R.L., And Constable, C.G., 1987, Occam's inversion: a practical algorithm for generating smooth models from electromagnetic sounding data: *Geophysics*, 52, 289-300

Huang, H. and Fraser, D.C, 1996. The differential parameter method for multifrequency airborne resistivity mapping. *Geophysics*, 55, 1327-1337

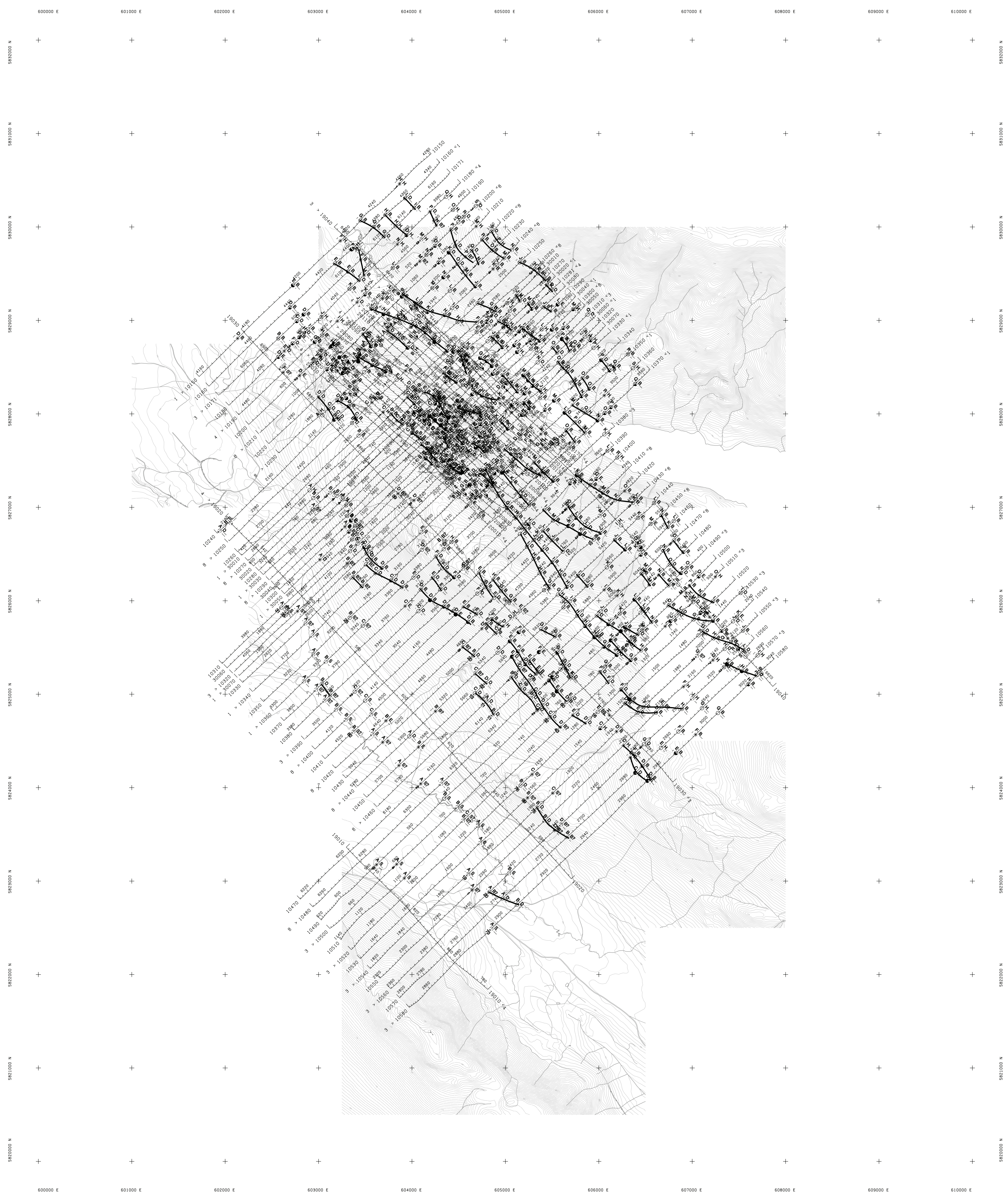
Huang, H. and Palacky, G.J., 1991, Damped least-squares inversion of time-domain airborne EM data based on singular value decomposition: *Geophysical Prospecting*, v.39, 827-844

Macnae, J. and Lamontagne, Y., 1987, Imaging quasi-layered conductive structures by simple processing of transient electromagnetic data: *Geophysics*, v52, 4, 545-554.

Sengpiel, K.P. 1988, Approximate inversion of airborne EM data from a multi-layered ground. *Geophysical Prospecting*, 36, 446-459

Wolfgram, P. and Karlik, G., 1995, Conductivity-depth transform of GEOTEM data: *Exploration Geophysics*, 26, 179-185.

Yin, C. and Fraser, D.C. (2002), The effect of the electrical anisotropy on the responses of helicopter-borne frequency domain electromagnetic systems, Submitted to *Geophysical Prospecting*



TECHNICAL SUMMARY

Navigation Differentially-corrected GPS
Data reduction grid interval 15 metres
Terrain clearance Helicopter 57 m
Electromagnetic sensor 30 m
Magnetometer 30 m
Data sampling interval 0.1 second
Magnetometer / sensitivity Cesium / 0.01 nT
Electromagnetic system DIGHEM[®]

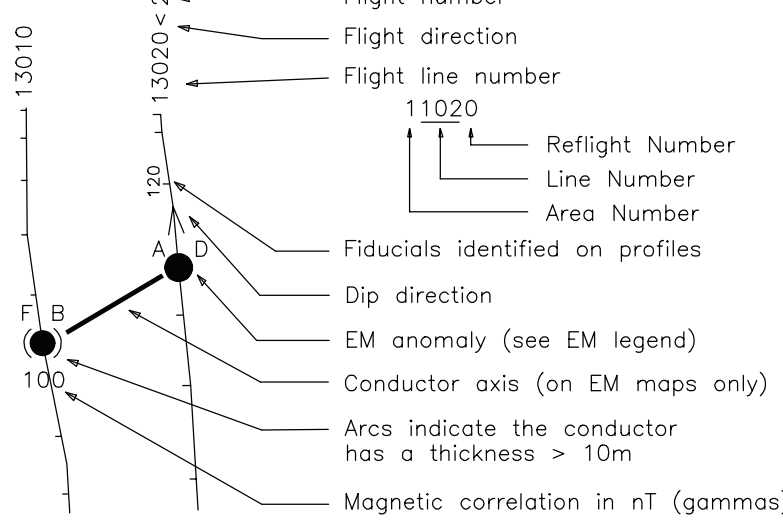
| Frequency | Sensitivity | Coil Orientation |
|-----------|-------------|---------------------|
| 1000 Hz | .06 ppm | Vertical coaxial |
| 5500 Hz | .12 ppm | Vertical coaxial |
| 900 Hz | .12 ppm | Horizontal coplanar |
| 7200 Hz | .24 ppm | Horizontal coplanar |
| 56000 Hz | .60 ppm | Horizontal coplanar |

ELECTROMAGNETIC ANOMALIES

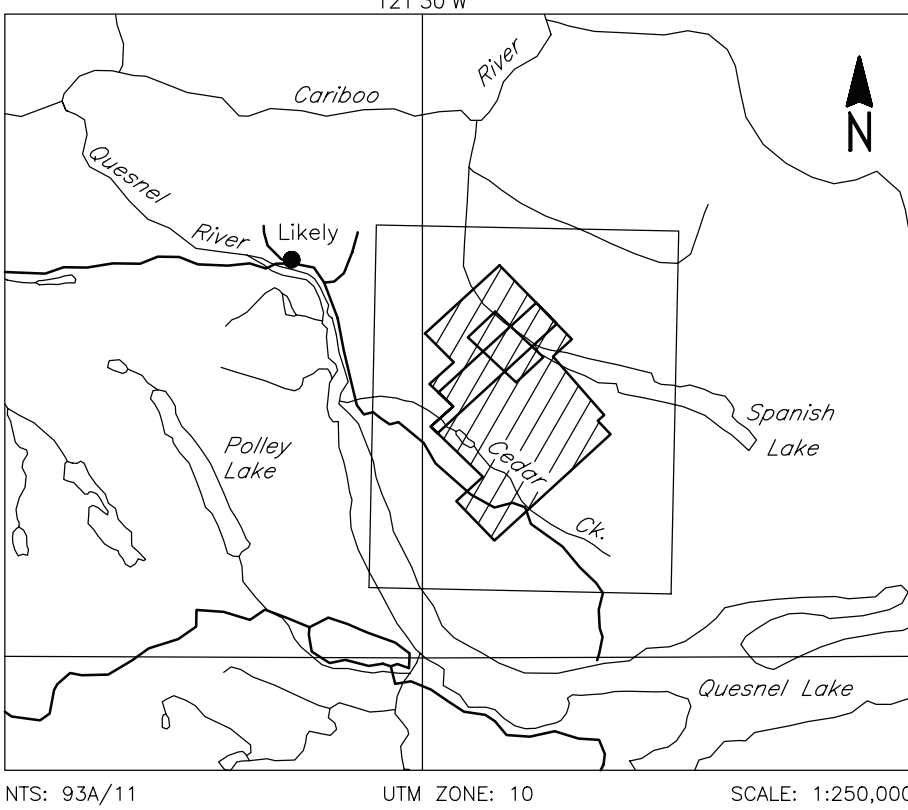
| Grade | Anomaly | Conductance |
|-------|---------|----------------------|
| 7 | ● | >100 siemens |
| 6 | ● | 50-100 siemens |
| 5 | ● | 20-50 siemens |
| 4 | ● | 10-20 siemens |
| 3 | ● | 5-10 siemens |
| 2 | ○ | 1-5 siemens |
| 1 | ○ | < 1 siemens |
| - | * | Questionable anomaly |

| Interpretive symbol | Conductor ("model") |
|---------------------|---|
| B | Bedrock conductor |
| D | Narrow bedrock conductor ("thin dike") |
| S | Conductive cover ("horizontal thin sheet") |
| H | Broad conductive rock unit, deep conductive weathering, thick conductive cover ("half space") |
| E | Edge of broad conductor ("edge of half space") |
| L | Culture, e.g. power line, metal building or fence |

FLIGHT LINES WITH EM ANOMALIES



LOCATION MAP

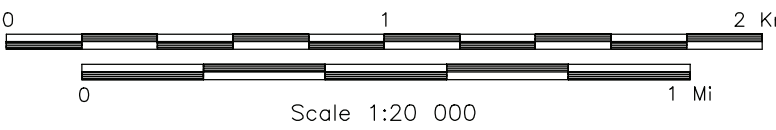


WILDROSE RESOURCES LTD./
SKYGOLD VENTURES LTD.
SPANISH MOUNTAIN PROJECT, B.C.

ELECTROMAGNETIC ANOMALIES

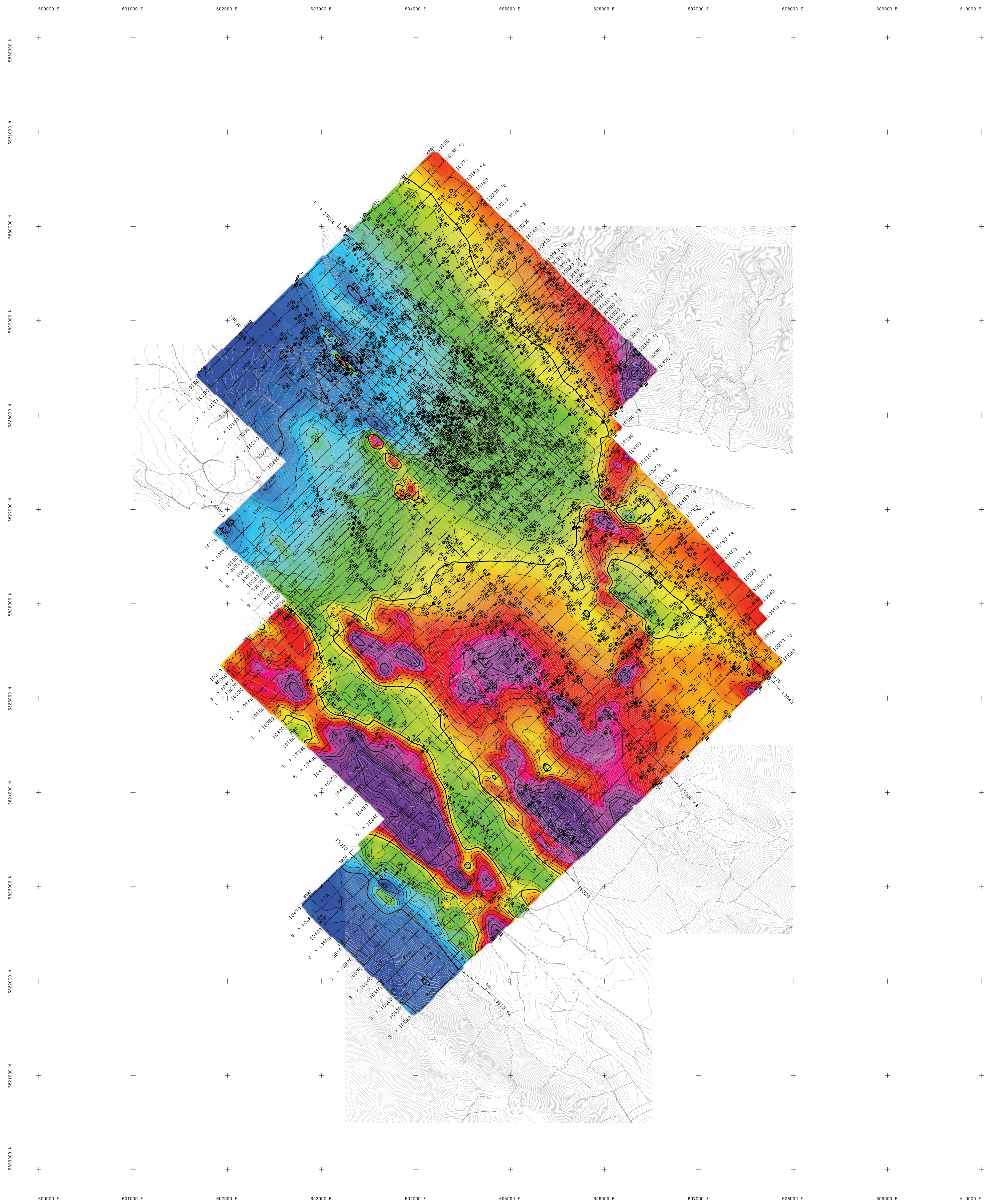
| | | |
|----------------------------------|-------------|---------------|
| FUGRO DIGHEM [®] SURVEY | NTS: 93A/11 | GEOPHYSICIST: |
| DATE: OCTOBER, 2006 | JOB: 06075 | SHEET: 1 |

Fugro Airborne Surveys



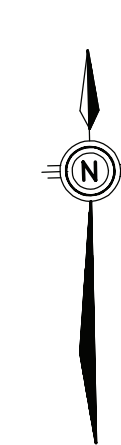
FUGRO AIRBORNE SURVEYS













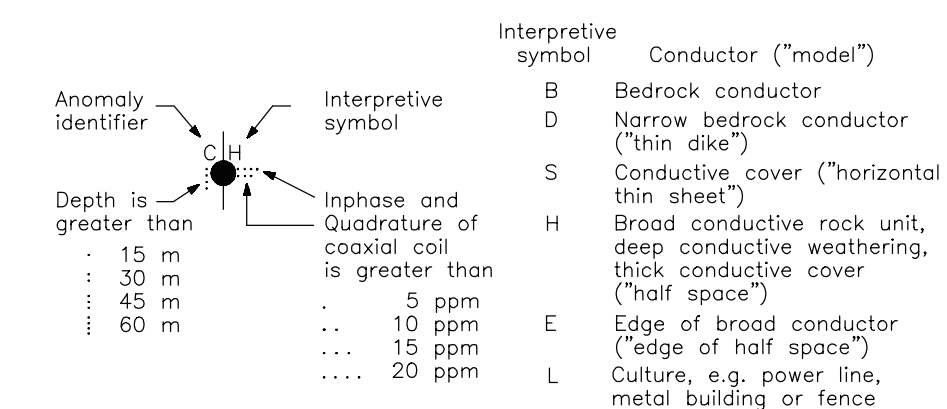
TECHNICAL SUMMARY

| | |
|------------------------------|------------------------------|
| Navigation | Differentially-corrected GPS |
| Data reduction grid interval | 5 m |
| Terrain clearance | Helicopter 57 m |
| | Electromagnetic sensor 30 m |
| | Magnetometer 30 m |
| Data sampling interval | 0.1 second |
| Magnetometer / sensitivity | Cesium / 0.01 nT |
| Electromagnetic system | DIGHEM* |

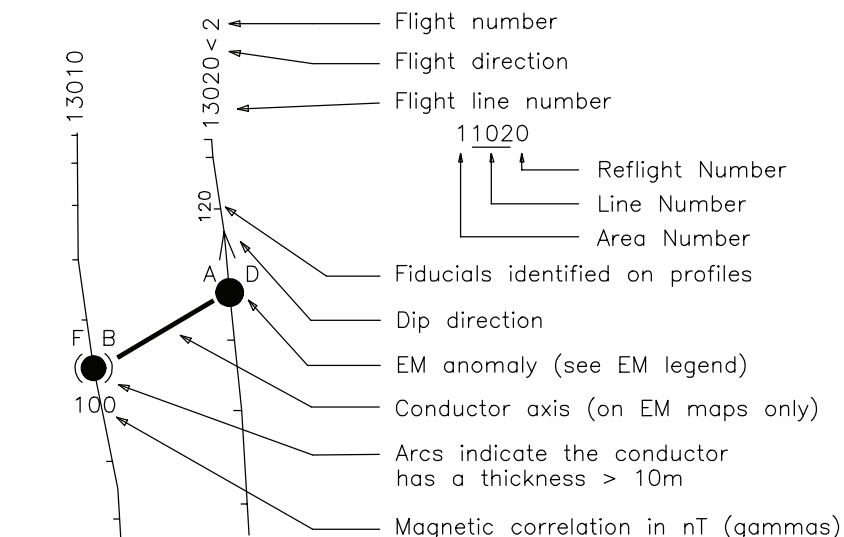


ELECTROMAGNETIC ANOMALIES

| Grade | Anomaly | Conductance |
|-------|---|----------------------|
| 7 |  | >100 siemens |
| 6 |  | 50–100 siemens |
| 5 |  | 20–50 siemens |
| 4 |  | 10–20 siemens |
| 3 |  | 5–10 siemens |
| 2 |  | 1–5 siemens |
| 1 |  | < 1 siemens |
| – |  | Questionable anomaly |



FLIGHT LINES WITH EM ANOMALIES

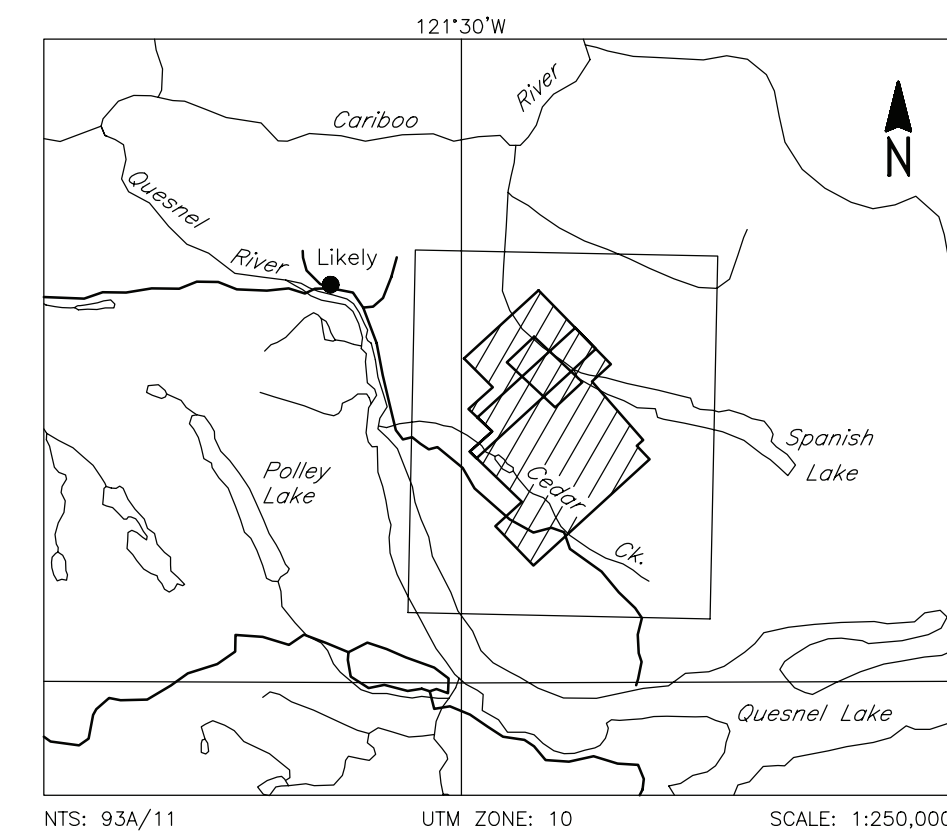


TOTAL MAGNETIC FIELD CONTOURS



Magnetic inclination within the survey area: 73 degrees N
Magnetic declination within the survey area: 19 degrees E

LOCATION MAP

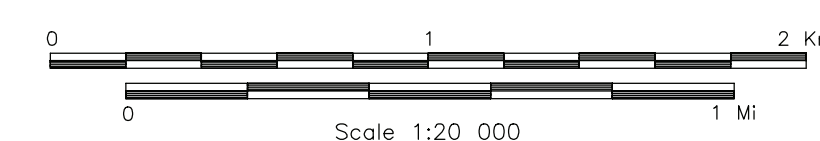


WILDROSE RESOURCES LTD./
SKYGOLD VENTURES LTD.
SPANISH MOUNTAIN PROJECT, B.C.

TOTAL MAGNETIC FIELD

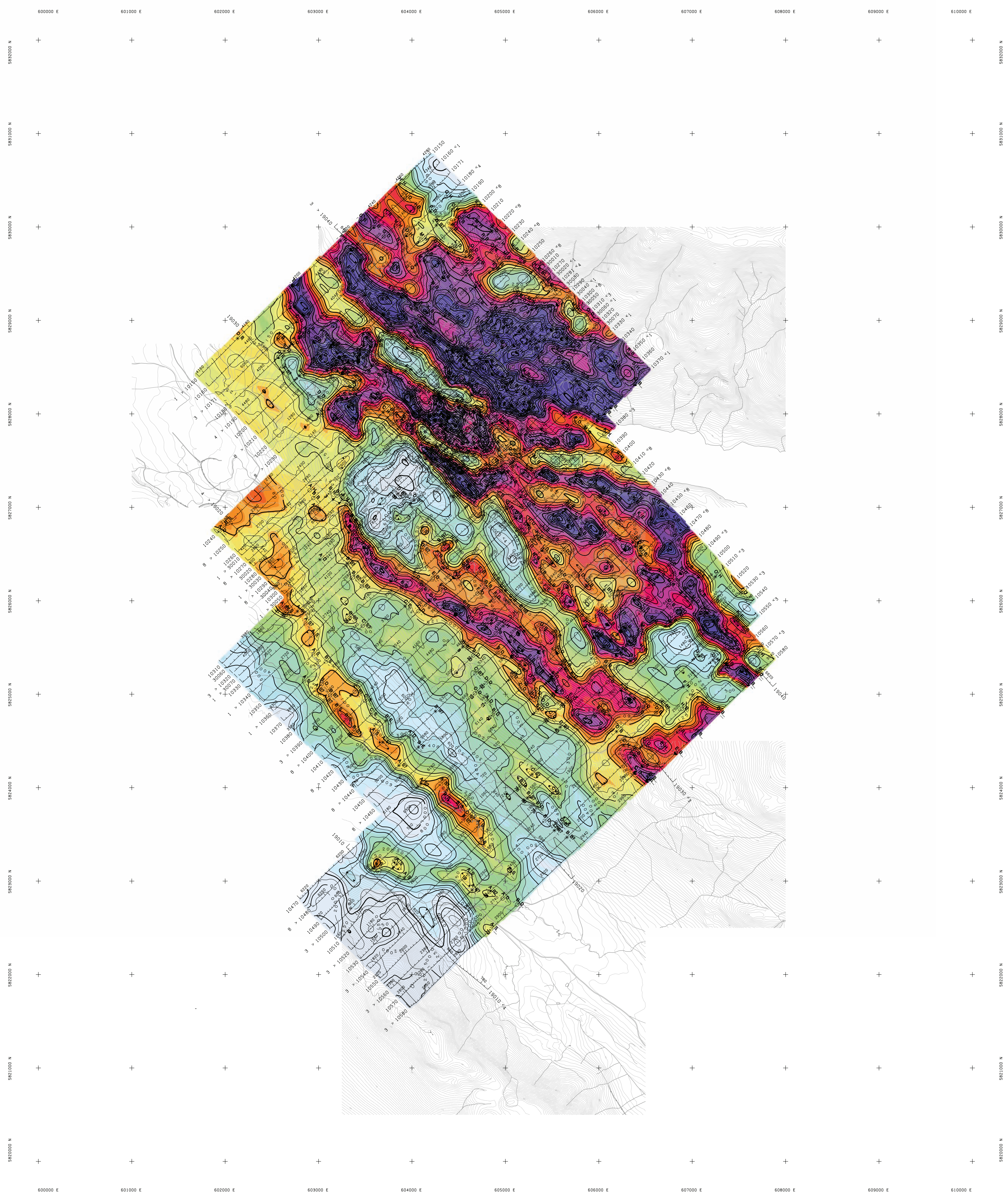
| | | |
|----------------------|-------------|--------------|
| FUGRO DIGHEM* SURVEY | NTS: 93A/11 | GEOPHYSICIST |
| DATE: OCTOBER, 2006 | JOB: 06075 | SHEET: 1 |

Fugro Airborne Surveys



FUGRO AIRBORNE SURVEYS





TECHNICAL SUMMARY

Navigation Differentially-corrected GPS
Data reduction grid interval 15 metres
Terrain clearance Helicopter 57 m
Electromagnetic sensor 30 m
Magnetometer 30 m
Data sampling interval 0.1 second
Magnetometer / sensitivity Cesium / 0.01 nT
Electromagnetic system DIGHEM[®]

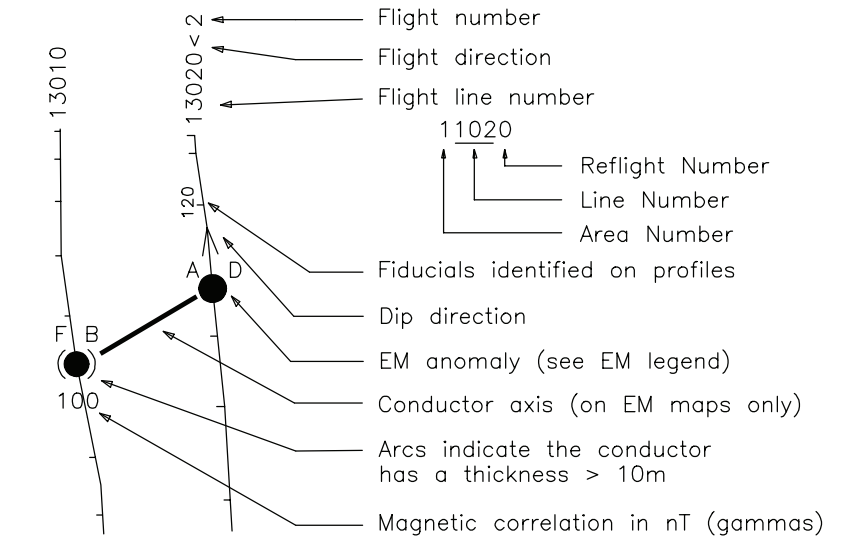
| Frequency | Sensitivity | Coil Orientation |
|-----------|-------------|---------------------|
| 1000 Hz | .06 ppm | Vertical coaxial |
| 5500 Hz | .12 ppm | Vertical coaxial |
| 900 Hz | .12 ppm | Horizontal coplanar |
| 7200 Hz | .24 ppm | Horizontal coplanar |
| 56000 Hz | .60 ppm | Horizontal coplanar |

ELECTROMAGNETIC ANOMALIES

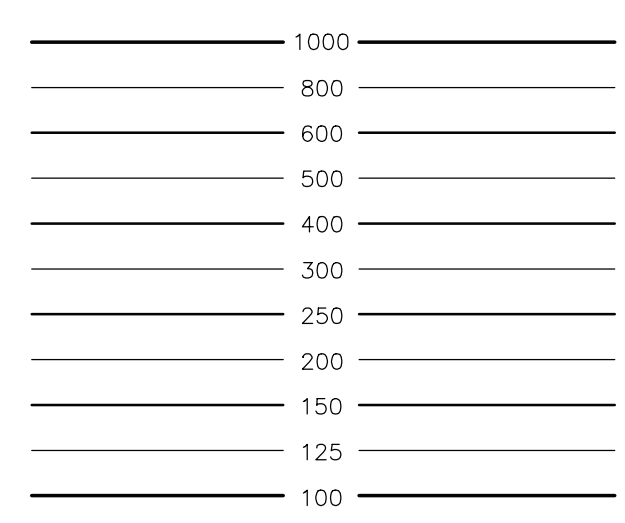
| Grade | Anomaly | Conductance |
|-------|---------|----------------------|
| 7 | ● | >100 siemens |
| 6 | ● | 50-100 siemens |
| 5 | ● | 20-50 siemens |
| 4 | ● | 10-20 siemens |
| 3 | ● | 5-10 siemens |
| 2 | ● | 1-5 siemens |
| 1 | ● | <1 siemens |
| - | * | Questionable anomaly |

| Interpretive symbol | Conductor ("model") |
|---------------------|---|
| B | Bedrock conductor |
| D | Narrow bedrock conductor ("thin dike") |
| S | Conductive cover ("horizontal thin sheet") |
| H | Broad conductive rock unit, deep conductive weathering, thick conductive cover ("half space") |
| E | Edge of broad conductor ("edge of half space") |
| L | Culture, e.g. power line, metal building or fence |

FLIGHT LINES WITH EM ANOMALIES

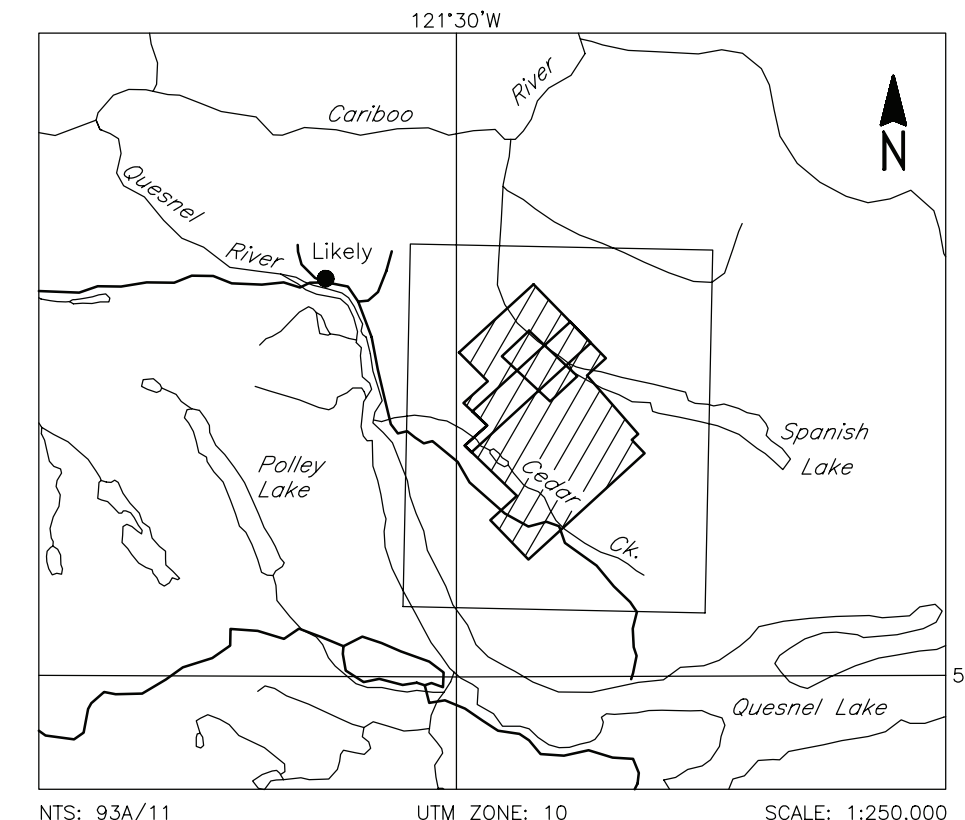


RESISTIVITY CONTOURS



Contours in ohm-m at 10 intervals per decade.
Apparent resistivity calculated using a pseudo-layer half-space model (Fraser 1978).

LOCATION MAP

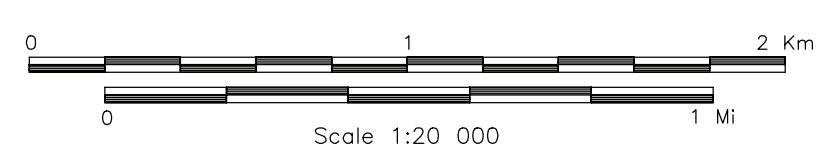


**WILDROSE RESOURCES LTD./
SKYGOLD VENTURES LTD.
SPANISH MOUNTAIN PROJECT, B.C.**

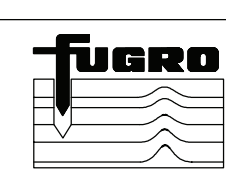
**APPARENT RESISTIVITY
56,000 Hz COPLANAR**

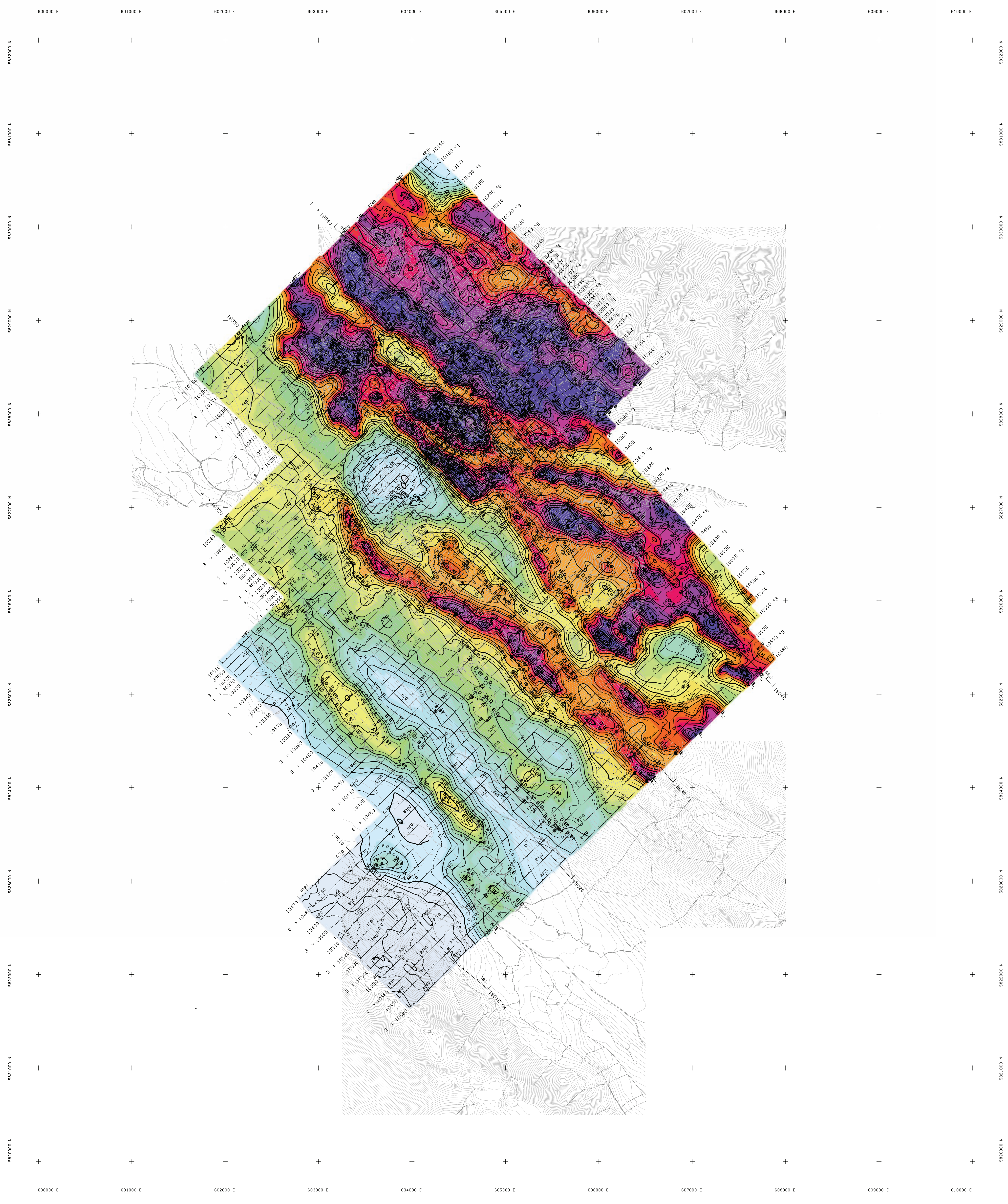
| | | |
|----------------------------------|-------------|---------------|
| FUGRO DIGHEM [®] SURVEY | NTS: 93A/11 | GEOPHYSICIST: |
| DATE: OCTOBER, 2006 | JOB: 06075 | SHEET: 1 |

Fugro Airborne Surveys



FUGRO AIRBORNE SURVEYS





TECHNICAL SUMMARY

Navigation Differentially-corrected GPS
Data reduction grid interval 15 metres
Terrain clearance Helicopter 57 m
Electromagnetic sensor 30 m
Magnetometer 30 m
Data sampling interval 0.1 second
Magnetometer / sensitivity Cesium / 0.01 nT
Electromagnetic system DIGHEM[®]

| ohm-m | Frequency | Sensitivity | Coil Orientation |
|-------|-----------|-------------|---------------------|
| 1005 | 1000 Hz | .06 ppm | Vertical coaxial |
| 662 | 5500 Hz | .12 ppm | Vertical coaxial |
| 479 | 900 Hz | .12 ppm | Horizontal coplanar |
| 351 | 7200 Hz | .24 ppm | Horizontal coplanar |
| 274 | 56000 Hz | .60 ppm | Horizontal coplanar |

ELECTROMAGNETIC ANOMALIES

| Grade | Anomaly | Conductance |
|-------|---------|----------------------|
| 7 | ● | >100 siemens |
| 6 | ● | 50-100 siemens |
| 5 | ● | 20-50 siemens |
| 4 | ● | 10-20 siemens |
| 3 | ● | 5-10 siemens |
| 2 | ● | 1-5 siemens |
| 1 | ● | < 1 siemens |
| - | * | Questionable anomaly |

Interpretive symbol: B Bedrock conductor, D Narrow bedrock conductor ("thin dike"), S Conductive cover ("horizontal thin sheet"), H Broad conductive rock unit, deep conductive weathering, thick conductive cover ("half space"), E Edge of broad conductor ("edge of half space"), L Culture, e.g. power line, metal building or fence.

FLIGHT LINES WITH EM ANOMALIES

Flight number, Flight direction, Flight line number, Reflight Number, Line Number, Area Number, Fiducials identified on profiles, Dip direction, EM anomaly (see EM legend), Conductor axis (on EM maps only), Arcs indicate the conductor has a thickness > 10m, Magnetic correlation in nT (gammas).

RESISTIVITY CONTOURS

Contours in ohm-m at 10 intervals per decade. Apparent resistivity calculated using a pseudo-layer half-space model (Fraser 1978).

| |
|------|
| 1000 |
| 800 |
| 600 |
| 500 |
| 400 |
| 300 |
| 250 |
| 200 |
| 150 |
| 125 |
| 100 |

LOCATION MAP

Map showing the project area in British Columbia, Canada. Key features include Cariboo River, Quesnel River, Polley Lake, Spanish Lake, and Quesnel Lake. The project area is outlined in a rectangle. Coordinates: NTS: 93A/11, UTM ZONE: 10, NAD83, SCALE: 1:250,000.

WILDROSE RESOURCES LTD./ SKYGOLD VENTURES LTD. SPANISH MOUNTAIN PROJECT, B.C.

APPARENT RESISTIVITY 7200 Hz COPLANAR

| | | |
|----------------------------------|-------------|---------------|
| FUGRO DIGHEM [®] SURVEY | NTS: 93A/11 | GEOPHYSICIST: |
| DATE: OCTOBER, 2006 | JOB: 06075 | SHEET: 1 |

Fugro Airborne Surveys

Scale 1:20 000

FUGRO AIRBORNE SURVEYS